Ecological Monographs

Article

Patterns of wind dispersal within a forest canopy: An epiphyte perspective

Marie Hoensbroech[1], Juliano Sarmento Cabral[2], Gerhard Zotz[1,3]

1: Institute of Biology and Environmental Sciences, Carl von Ossietzky Universität Oldenburg, Ammerländer Heerstr. 114–118, 26129 Oldenburg, Germany

2: Ecological Modelling, Bonner Institute for Organismal Biology — Department of Plant Biodiversity, Universität Bonn, Venusbergweg 22, 53115 Bonn, Germany

3: Smithsonian Tropical Research Institute, Box 0843-03092, Panama, Republic of Panama

Correspondence: Marie Hoensbroech; email: marie.hoensbroech@uni-oldenburg.de

Open Research Statement: Data and code supporting this study, including novel code generated during the study, are provided as private-for-peer review at https://figshare.com/s/4d7c0a1b9894dad136c1 and will be archived on the Smithsonian Research Data Repository upon acceptance. This study also used publicly available datasets. These datasets are listed below and are cited in the manuscript where appropriate and listed in the Reference List:

Mendieta-Leiva et al. (2021), https://doi.org/10.5281/zenodo.5645775;

Paton (2019a), https://doi.org/10.25573/data.10042640.v25;

Paton (2019b), https://doi.org/10.25573/data.10042658.v23;

Paton (2019c), https://doi.org/10.25573/data.10042688.v23;

Paton (2019d), https://doi.org/10.25573/data.10042718.v23;

Paton (2019e), https://doi.org/10.25573/data.10042694.v23;
Paton (2019f), https://doi.org/10.25573/data.10042679.v23;
Paton (2020), https://doi.org/10.25573/data.11799309.v6;
Ramos et al. (2024), https://doi.org/10.25573/data.24954204.v1;
and Vasquez et al. (2024), https://doi.org/10.60635/C33W2K.
Additional data used in this study were shared privately by the original data owners and are not publicly available: Janner et al. (in preparation), and data underlying Zotz and Schultz (2008). These privately shared datasets are cited in the manuscript where relevant, and complete references, where available, are provided in the Reference List. Access to these data may be requested from the original data owners, subject to their permission and any applicable restrictions.

Keywords: anemometry; apparent wind; deposition process; dispersal limitation; dispersal model; long-distance dispersal (LDD); patchy distribution; terminal velocity; trajectory model; tree sway; updrafts; vertical stratification

Abstract

Plant dispersal theory has largely been developed from a terrestrial perspective, in which interception by vegetation is considered a loss, and success is defined by arrival at suitable ground-level habitat. True epiphytes—non-parasitic plants structurally dependent on a host throughout their lives—represent a striking reversal of this framework: their diaspores must be intercepted by suitable aboveground substrates to disperse successfully. Although dispersal is frequently assumed to underlie the spatially patchy distributions common in epiphyte communities, it remains poorly understood. Here, we quantify airflow along tree vertical profiles in a tropical lowland forest and incorporate these measurements into a mechanistic dispersal model to investigate how airflow, vegetation density, diaspore terminal velocity, and release height jointly shape dispersal within a forest. We examine how these factors influence interception by vegetation—particularly bark, a prerequisite for epiphyte establishment—and promote long-distance dispersal. We further introduce a quantitative metric of dispersal limitation that integrates dispersal success, dispersal distance, and fecundity. Our results reveal aerodynamic stratification within the forest canopy, with weak mean vertical airflow but pronounced turbulence between the upper and lower crowns. This trunk zone may operate as a strong yet permeable filter: although occasional updrafts enable escape above the canopy, most diaspores released in the understorey remain confined within it. Only a fraction is intercepted by bark, typically within 5 m vertically and 15 m horizontally from the release point. This results in strong per-diaspore dispersal limitation and may contribute to spatially patchy epiphyte distributions. However, the degree of dispersal limitation is context-dependent and, when accounting for the high fecundity of many epiphytes, may be less severe than commonly assumed, with post-dispersal demographic filters ultimately shaping distribution patterns. More

broadly, our findings highlight a gap in within-forest dispersal theory and underscore the importance of local canopy structure and airflow in shaping diaspore movement in complex, stratified environments. Our model is transferable to other systems—from understorey and invasive plant species to pollen, fungal spores, and ballooning arthropods—and can improve our understanding of connectivity and gene flow within and among forests, informing conservation strategies that enhance dispersal pathways.

Introduction

"*Tossing crowns and creaking trunks, and the occasional crash of a falling tree, attest to the strength of the wind aloft, but only an occasional weak gust is felt near the ground.*"–
John J. Finnigan (2000)

Plant dispersal theory has long been grounded in a terrestrial perspective, in which **diaspores** (see Table 1 for a glossary of bolded terms) move away from a parent plant to land, ideally, in a suitable ground-level habitat at some distance (Nathan et al., 2002; Nathan, Katul et al., 2011; Tackenberg et al., 2003). Within this framework, atmospheric processes such as turbulence and updrafts are interpreted primarily as modifiers of transport distance, occasionally generating **long-distance dispersal** (LDD) events that support colonisation, gene flow, and range dynamics (Bohrer et al., 2008; Heydel et al., 2014; Mondragón et al., 2015; Soons & Ozinga, 2005). Implicit in this view is a key assumption: vegetation encountered along the dispersal trajectory represents a barrier, limiting dispersal distances or preventing diaspores from reaching their intended destination on the ground (Bohrer et al., 2008; Pounden et al., 2008). Epiphytes fundamentally challenge this assumption: **successful dispersal** does not occur when diaspores avoid vegetation, but when they encounter it.

For epiphytes—non-parasitic plants relying on hosts to complete their life cycle above ground (Zotz, 2016)—soil contact can be detrimental, at least in the wild (e.g., Benzing, 1990; Spicer & Ortega, 2023). Therefore, they face a fundamental challenge during dispersal: their diaspores must not land on the "inhospitable ground" (Benzing, 1990) but instead reach suitable host surfaces where germination and establishment are possible (García-Franco & Rico-Gray, 1988; Zotz, Hietz & Einzmann, 2021). Such **safe sites** (*sensu* Harper et al., 1961) must also occur

within a species' **vertical niche**, across a forest height gradient characterised by steep variation in temperature, moisture, light, and wind regimes. Because dispersal success depends on reaching suitable positions within this vertically structured environment, epiphytes provide an ideal system for examining how dispersal operates within such habitats.

Epiphytes are a defining component of tropical vegetation, contributing up to 50% of local plant diversity (Kelly et al., 2004). Orchids and bromeliads are the most species-rich vascular epiphytic families, but at least 77 other plant families contain epiphytic members, together comprising approximately 31,000 species—roughly 10% of all vascular plant species (Zotz, Weigelt, et al., 2021). When considering only wind-dispersed vascular plants, they make up an even larger share (> 20% globally and ~40–60% in the tropics). Beyond their diversity, epiphytes play key roles in interaction networks, nutrient and water cycling, structural complexity, and habitat provisioning for arboreal fauna (e.g., Ladino et al., 2019; Spicer & Woods, 2022; Thomsen et al., 2018). Despite this ecological importance, they, and specifically their dispersal, remain comparatively understudied (e.g., Spicer & Woods, 2022).

Current dispersal frameworks do not adequately capture the processes governing dispersal within such vertically structured environments. In particular, existing dispersal models (e.g., Bohrer et al., 2008; Heydel et al., 2014; Tackenberg, 2003; Tackenberg et al., 2003) provide limited insight into epiphyte, let alone within-canopy, dispersal. This is striking given that wind dispersal is among the best-studied dispersal types (Cousens et al., 2008), except possibly in tropical forests (Augspurger, 2024). For instance, many models neglect substrate interception altogether (Heydel et al., 2014; Wright et al., 2008; Lee & Yoon, 2025) or consider it only on horizontal surfaces (e.g., Bohrer et al., 2008), despite the central importance of interception on vertical (bark) surfaces for epiphytes—and for limiting dispersal distances in general. Furthermore, dispersal

models are typically based on idealised wind functions or wind measurements from fixed structures such as meteorological towers (Kruijt et al., 2000; Rudnicki et al., 2001), whereas diaspores are released and transported within a dynamic canopy, where they experience **apparent wind** (as opposed to **actual wind**; see Appendix 1: Figure S1 for a conceptual diagram) shaped by local turbulence and tree or branch sway. Empirical measurements of such conditions are rare (Einzmann et al., 2022), and their implications for dispersal remain largely unexplored (Cousens et al., 2008; Murray, 1986; Niklas, 1992; Salisbury, 1942).

In addition, existing dispersal models often initiate dispersal from a **release height** corresponding to the lower part of a plant bearing the diaspores (Greene & Johnson, 1996; Nathan, Horvitz, et al., 2011). In forests, where dispersal studies have largely focused on trees, such assumptions effectively exclude everything below the high crowns (see Appendix 1: Figure S2 for the forest zones we refer to)—sometimes more than two-thirds of the forest height gradient, thereby neglecting wind-dispersed species occurring far below them (though there are exceptions, see e.g., Nathan et al., 2002; Norros et al., 2014). This might reflect the prevailing view that dispersal success is low in forest understories, where very low wind speeds are assumed to limit dispersal (Finnigan, 2000; Schimper, 1888), leading to the expectation that wind dispersal is rare in understorey plants—epiphytic (Kelly, 1985; Vieira & Izar, 1999) or not (Muller-Landau et al., 2008; Roth, 1986). Yet wind-dispersed species can be abundant throughout the understorey and across the full forest height gradient (van der Pijl, 1982; Mendieta-Leiva et al., 2021; see also Appendix 1: Figure S3).

Most epiphytes are wind-dispersed (Madison, 1977; Zotz, 2016). Their diaspores, as other wind-dispersed diaspores, are adapted to very faint winds, being either tiny and extremely light—like the dust seeds of orchids—or plumed with specialised structures such as coma hairs in

tillandsioid diaspores (Schimper, 1888; Benzing, 1990; Chilpa-Galván et al., 2018). Information on **terminal velocity**—the constant speed at which an object falls in still air—is available for only a tiny number of epiphyte species (Bennett, 1988; Chilpa-Galván et al., 2018; Zotz et al., 2016), but available estimates suggest that these traits allow uplift in winds as low as 0.1–0.5 m s^{-1}.

Updrafts are considered important in wind-dispersed (terrestrial) plants, both for **abscission** and LDD (Greene & Quesada, 2011; Heydel et al., 2014; Horn et al., 2012; Tackenberg, 2003; Tackenberg et al., 2003). For epiphytes, however, the role of updrafts may be more fundamental. Because suitable habitat occurs above ground, diaspores that simply descend under gravity risk leaving the species-specific vertical niche, or epiphytic niche altogether. Updrafts allow epiphyte diaspores to remain within, or re-enter, suitable strata after failed interception. Without them, forests might gradually lose epiphytes from upper strata to the ground. Therefore, successful dispersal, **effective dispersal**, and the evolutionary persistence of epiphyte populations are all expected to depend strongly on updrafts.

Most of the few studies on epiphyte dispersal relied on indirect methods, such as nearest-neighbour analyses or colonisation and gene flow rates (e.g., Einzmann & Zotz, 2017a; Gandawijaja & Arditti, 1983; Taylor & Burns, 2015; Zotz & Vollrath, 2003). Only a handful of studies have empirically assessed dispersal distances in epiphytes (e.g., Ackerman et al., 1996; Bennett, 1988; Cascante-Marín et al., 2008, 2009; Mondragón & Calvo-Irabién, 2006), and, together, they reveal a striking paradox. On the one hand, the low terminal velocities of epiphyte diaspores suggest a high potential for transport by updrafts (Schimper, 1908), and thus for LDD (Arditti & Ghani, 2000; Barrington, 1993; Givnish et al., 2016). Indeed, epiphytic orchid species were among the first plants to colonise the islands of Krakatau following the volcanic eruption

(Partomihardjo, 2003). Their high colonisation rates, together with their evolutionary history—colonising and subsequently radiating in distant continents—further support this view (Givnish et al., 2014, 2016; Kessler, 2002; Mendieta-Leiva et al., 2022).

On the other hand, such LDD events are considered exceptional (Givnish et al., 2016; Trapnell et al., 2013). In fact, epiphytes are frequently described as dispersal-limited, often because of their highly clumped (patchy) distributions (Kelly et al., 2004; Nieder & Zotz, 1998). In epiphytes, these patchy distributions may indicate that diaspores often remain near the mother plant, move primarily along branches or stems within the same tree, colonise at best neighbouring trees, and only rarely reach more distant sites (Schimper, 1908; Torres et al., 2018; Zotz & Vollrath, 2003). Accordingly, previous modelling approaches have assumed low dispersal ability, for example through strongly downward-biased dispersal kernels (Petter et al., 2021). However, patchiness alone is weak evidence for **dispersal limitation** unless underlying environmental filters can be excluded, a problem that reflects the broader inconsistent and often implicit use of dispersal limitation (and similar terminology) in plant ecology (Münzbergová & Herben, 2005). Whether patchy distributions in epiphytes actually arise from dispersal limitation is rarely tested explicitly (but see Cascante-Marín et al., 2008, 2009; Mondragón & Calvo-Irabién, 2006).

In contrast, the pronounced **vertical stratification** often observed in epiphytes—where individuals of a species occupy distinct height ranges (Pittendrigh, 1948; Wagner et al., 2013)—is typically attributed to post-dispersal filtering. This distribution pattern primarily reflects the steep microclimatic gradients along the vertical axis (Krömer et al., 2007; Petter et al., 2021; Wagner et al., 2013; Zotz & Hietz, 2001), but could also result from variation in substrate characteristics, including mycorrhizal associations, availability, and substrate age (Francisco et al., 2021; Dislich & Mantovani, 2016; Ruiz-Cordova et al., 2014). This creates a conceptual

asymmetry: while patchy distributions are commonly interpreted as evidence of dispersal limitation, the potential role of dispersal in shaping vertical stratification is rarely considered. Consequently, whether—and how—dispersal contributes to either of these patterns remains an open and surprisingly underexplored question.

This study addresses this gap by explicitly linking vertical airflow dynamics to dispersal outcomes. We quantify vertical wind dynamics directly where epiphytes experience them—along stems and branches across the forest height gradient—and incorporate these measurements into a mechanistic dispersal model for within-forest canopy dispersal (*EpiDisp 1.0*) to simulate diaspore trajectories across a range of terminal velocities and release heights. Specifically, we ask (i) how vertical airflow is structured across forest strata and environmental conditions, (ii) whether lower terminal velocity and higher release height increase dispersal success and escape from the canopy within this stratified forest, and (iii) whether these same conditions, coupled with dispersal distances and fecundity, decrease the degree of dispersal limitation and thereby contribute to spatially patchy and vertically stratified epiphyte communities. Overall, our model represents a pivotal step in quantifying wind dispersal within forests, with relevance extending beyond epiphytes to other wind-dispersed organisms in vertically structured habitats.

Materials and Methods

Study site

The Smithsonian Tropical Research Institute's (STRI) canopy access crane, established in 1997 (9.28° N, 79.97° W), and the associated field station are located within the San Lorenzo National Park, near the Caribbean coast of Panama (Wright et al., 2003). The crane allows access to all layers within a 1 ha permanent plot of this mature lowland tropical moist forest (Figure 1). The

local climate is characterised by a dry season, from approximately mid-December to April, and a wet season, from approximately May to mid-December (Paton, 2020). Mean monthly rainfall increases from below 100 mm in the dry season to around 350 mm in the wet season; mean relative humidity increases from a low of 87% in February to a high of 96% in November; average daily maxima in air temperature, though relatively stable, increase from ca. 26 °C in the dry season to around 29 °C during the wet season (Paton, 2020). Wind also shows marked seasonal differences. Typically, the predominantly northerly winds of the dry season peak at a monthly average of 3.2 m s^{-1} and a daily maximum of 8 m s^{-1} in February; the predominantly north-westerly winds of the wet season drop to a monthly average of 1 m s^{-1} and a daily maximum of 5 m s^{-1} in October (Paton, 2020).

The closed canopy of forest is between 25 and 35 meters high (Figure 1, also see Appendix 1: Figure S2 for the forest zones we refer to). A repeated census of epiphyte community dynamics at the site has determined a trend of increasing vascular epiphyte abundance from 2002 to 2012, an abundance of nearly 14,000 individuals within a 0.4 ha subplot, and a richness totalling just over 100 species (belonging to 61 genera and 13 families; Mendieta-Leiva et al., 2022).

Though no study explicitly investigated epiphyte phenology at this particular site, studies from Central Panama suggest that many of the wind-dispersed epiphytic (Croat, 1978) and non-epiphytic species (Augspurger & Franson, 1988) release their mature diaspores towards the end of the dry season and the early wet season, when conditions promoting dispersal and successful establishment coincide (Maurer et al., 2013). For this reason, our field work was conducted at the transition from the dry to the wet season.

Terminology

Dispersal is the movement of a diaspore through space (and time, but most epiphytic diaspores will not disperse through time via dormancy). In this study, we consider it successful when the abscised diaspore settles on a suitable substrate (bark). Whether the dispersal is effective (Cousens et al., 2008), depends on whether the site it settles on is a safe site, i.e., whether conditions are suitable for subsequent germination and establishment. Assessing this was beyond the scope of this study, but was assumed, based on prior studies, to fall within a 5–10 m range around the release height (Wagner et al., 2013; Zotz, 2016; Zotz & Schultz, 2008). This area can also be described as a species' vertical nich**e**, meaning the range of heights within the forest where the local microclimate permits epiphyte germination, establishment, and persistence (Krömer et al., 2007; Wagner et al., 2013; Zotz & Hietz, 2001).

The dispersal vector—the external force that mediates diaspore movement (Cousens et al., 2008)—of this study is wind. Wind comes in different forms and can be disassembled into different components like a mathematical vector, i.e., magnitude (speed, in m s^{-1}) and direction (in degrees). The direction of horizontal wind usually refers to its origin: a northerly wind comes from the North. Conversely, in the vertical plane, an updraft will indeed flow upward and a downdraft downward.

This study differentiates between horizontal and vertical winds as well as horizontal and vertical gusts. Winds are defined as the mean airflow and the circular mean direction measured over a specified time interval in either a horizontal or a vertical plane. The minimum time interval over which the mean was calculated is 1 minute, the maximum 5 minutes. Gusts are defined as a sudden and brief increase in wind speed and are reported as the maximum speeds measured in

the same time interval over which the mean is calculated. However, for specific analyses, their continuous occurrence in shorter time intervals (3 to 10 seconds) will be treated independently.

Updrafts and downdrafts (simply, upward or downward moving air), **ejections** and **sweeps** (see glossary), as well as vertical turbulence (vertically oriented irregular airflow) are common terms to denote different kinds of upward and downward moving air. We will only use these terms when drawing from literature that uses these terms. For our purposes, we will use the terms **up/down-gusts** for maximum and **up/down-winds** for mean air movement in a specified time period. The term **airflow** will comprise both winds and gusts, and the term **wind dynamics** will refer to greater spatial or temporal scales, including both winds and gusts.

All environmental parameters, including temperature, humidity, and wind typically vary along the gradient from forest floor to upper canopy. In the literature, the term “vertical” is often added to specify gradients that are perpendicular to the ground. The *vertical* wind gradient might then refer to the *horizontal* wind at different heights above the ground. In this study, the term forest gradient will imply a vertical gradient, but the terms *vertical* and *horizontal* will be exclusively reserved for denoting the direction of wind. Thus, the *vertical* wind gradient will indeed be the gradient of *vertical* wind at different heights above the forest floor.

Additionally, we distinguish between **release** and abscission. Release refers to the height at which a diaspore is first exposed to the environment, either through the opening of the seed pod or the start of the simulation. Abscission, in contrast, refers to the point at which the diaspore detaches from the seed pod and dispersal begins.

Data collection

Our first aim was to assess wind dynamics across the forest height gradient. The trees, in which vertical airflow was measured (Figure 1), were chosen primarily based on accessibility, while also ensuring that trees of different heights, architectures, and species were included in the sampling. In 15 out of 16 cases, the trees were accessed with the canopy crane, and once through a rope access system. The first replicate was the crane itself, which was securely accessed by climbing its mast. Hereafter, these seventeen replicates will be referred to as vertical profiles.

Field work began on March 8, 2023, and lasted eight weeks (until May 4). Two-dimensional ultrasonic anemometers (HOBO Ultrasonic Wind Speed and Direction Smart Sensor S-WCG-M003, Onset Computer Corporation, Bourne, MA, USA) were installed at various heights and distances along the stems of trees. Where possible, this encompassed the entire forest height gradient from trunk base to upper crown. Often, however, this was not possible as densely growing vegetation prevented access to some parts of the tree. This was particularly often the case from 10–15 m downwards. Then, anemometers were placed where access was possible.

Per vertical profile, four different heights were sampled (once only three). Per height, we installed two anemometers: one near the stem (the “in” position, 0.35 m distance from stem) and one further out (the “out” position, 1.35 m distance from stem). This aimed to investigate whether there are differences in air movement close to the stem and slightly further out. The anemometers were screwed to an aluminium frame, which was strapped to the stem at different points to keep it in a horizontal position (Appendix 1: Figure S4). Importantly, because our focus was on vertical airflow, the anemometers were installed horizontally (even when the tree or branch was growing at an angle). Typically, these anemometers are installed vertically, but prior

trials showed that horizontal installation does not influence the measurements (Westphal & Zotz, unpublished). Consequently, instead of aligning the anemometers to the True North using a Northing tool, as is standard practice, they were aligned to face upward (Appendix 1: Figure S5).

One logger (HOBO H21-USB Micro Station Data Logger, Onset Computer Corporation, Bourne, MA, USA) per height and per two anemometers was strapped directly onto the stem (Appendix 1: Figure S4). The first three replicates were set to logging intervals of 4, 10, and 5 seconds, and thereafter all replicates logged at three second intervals, the maximum resolution of these anemometers. Within their measurement range (0 to 41.2 m s^{-1}), they measure at a resolution of 0.33 m s^{-1}—which also corresponds to the minimum non-zero speed they can accurately measure (measurement threshold)—and with an accuracy of ±0.8 m s^{-1} or ±4% of the reading, whichever is greater. The anemometers take a reading once every three seconds and then report wind speed (m s^{-1}) as the mean speed calculated over a specified logging interval; gust speed (m s^{-1}) as the maximum 3-second wind speed in that same interval; and wind direction (in degrees) as the unit-vector averaged direction of that interval.

At each attachment point, we measured height (meters above ground) using a 50 m measuring tape, facing direction (the cardinal direction, in degrees, toward which the anemometer set is oriented) using a handheld compass, and stem diameter (cm) using a diameter tape. We recorded the total height of the tree (using the same 50 m measuring tape) and its GPS position (using a Garmin eTrex 30, Garmin Ltd., Olathe, Kansas, USA). The trees were identified to species level. All plant names follow Plants of the World Online (POWO; 2026).

As there may be minor measuring differences between individual anemometers, their positions and heights were varied at random. During the process of randomisation and reading out data

from the preceding replicate—which was done at the forest floor or at the research station 500 m away from the crane site, using the free software HOBOware (Onset Computer Corporation, 2022)—the solar-powered anemometers were placed in the sun to recharge their batteries.

During the 59 days of fieldwork, 124 different height × position combinations were assessed, with differing numbers of replicates among combinations. This amounted to approximately 11,000 hours of wind measurements in total, with most sampling effort concentrated at intermediate heights (Appendix 1: Figure S6). We sampled 17 vertical profiles, the canopy access crane itself and nine different tree species: four times a *Brosimum utile* (Kunth) Oken, three times *Socratea exorrhiza* (Mart) H. Wendl. and *Virola fosteri* D. Santam., and once a *Cordia bicolor* A. DC., *Dussia atropurpurea* N. Zamora, R.T. Penn. & C.H. Stirt., *Guatteria lucens* Standl., *Humiriastrum diguense* (Cuatrec.) Cuatrec., *Lonchocarpus heptaphyllus* (Poir.) DC., and a *Pera arborea* Mutis. Except for *S. exorrhiza* and *C. bicolor*, which only reached the mid-canopy, trees were approximately average forest height (ca. 30 m at San Lorenzo) or emergent, i.e., part of the high-crown zone (Appendix 1: Figure S2). Most trees had numerous (hemi-) epiphytes except *Virola* trees, which had very few or none. Rain was registered on eleven days. For an interactive map of the field site with detailed information on the vertical profiles, including imagery, refer to our shinyApp (Appendix 2).

Lidar and topographic data, as well as aerial imagery of the forest plot recorded in May 2023, were obtained from Vasquez et al. (2024). We also used subsets of the long-term climate dataset for sites across Panama hosted by the Smithsonian Tropical Research Institute (STRI; Paton, 2019a–f, 2020). At San Lorenzo, among other devices, a temperature sensor and a cup anemometer are installed near the top of the crane. They log minimum, mean, and maximum temperature, as well as mean and maximum wind speed, and mean wind direction for every 15-

minute interval. However, due to a failure in the anemometer during the sampling period, no wind data were available for San Lorenzo. The nearest functional meteorological station was the Galeta tower site ca. 15 km distance from the San Lorenzo crane.

We modelled the long-term relationship between Galeta and San Lorenzo (14 years of data; Paton 2019a–d) using simple linear regression to assess whether it is justified to impute the missing data. Because the relationships between wind and gust speeds at Lorenzo and Galeta was moderately strong and significant ($R = 0.5$ for wind and $R = 0.53$ for gusts; $p < 0.01$ for both), we replaced the missing data for San Lorenzo using the fitted data of the model.

To relate any obtained patterns of wind dynamics to the dispersal of epiphyte diaspores, we sourced data on the terminal velocity of epiphyte diaspores from primary literature (Bennett, 1988; Mondragón & Calvo-Irabién, 2006; Zotz et al., 2016). Additionally, we measured the falling velocity of three *Tillandsia* species in a custom-built apparatus at the University of Oldenburg, Germany (see Zotz et al., 2016 for specifications).

Data analysis

Lidar data and aerial imagery

Using CloudCompare (2023), only the relevant geographical section of the lidar data (Vasquez et al., 2024) was extracted and transformed to the LAS file type. Using ArcGIS Pro (Esri Inc., 2024), we overlaid the aerial imagery of the San Lorenzo plot with the GPS data of the 17 vertical profiles for post-referencing. In all cases of emergent trees, we were able to locate the crown of the trees in which wind dynamics were assessed using the imagery. Where applicable, we adjusted the GPS positions to match the middle of the crowns. In the case of non-emergent

trees, which did not appear in the aerial imagery, the measured GPS positions were used. We then traced the outline of the tree crowns to calculate crown area. Subsequently, the point locations of trees and the polygons of the crowns were extracted.

The lidar point cloud, point locations and polygons were imported to R (ver. 4.5.2; R Core Team, 2023) and processed, analysed, and visualised using the libraries lidR (Roussel et al., 2020), tidyverse (Wickham et al., 2019), raster (Hijmans, 2025), sf (Pebesma, 2018), sp (Bivand et al., 2013), and terra (Hijmans, 2025). We generated a 2D image of the canopy from the lidar surface (shown in Figure 1). With the crown polygons, we extracted a subset of lidar points that show only the locations of the 17 vertical profiles. We used the anemometers' x, y, and z coordinates to mark their measuring positions in the full point cloud as well as the subset. These can be viewed interactively in our shinyApp (Appendix 2).

Using the leafR library (Almeida et al., 2021), we derived **leaf area density (*LAD*)** profiles across the full forest height gradient, averaged a) across the entire plot (i.e., mean *LAD* per height), b) across all vertical profiles, and c) for each profile individually. However, because this method does not distinguish between leaves and wood (or other structures), these estimates are more appropriately interpreted as **plant area density *(PAD)*** rather than true leaf area density. Further, plant or leaf area densities are often criticised for omitting vertical surface components (Olivas et al., 2013), which are formed mainly by tree trunks and provide important attachment surfaces for epiphytes. We therefore refer to the lidar-derived estimates as *horizontal* plant area density (PAD_h), representing the horizontal plant surface area per unit volume.

To account for this limitation, we estimated a second component, namely the vertical plant area density (PAD_v), from stem surfaces. Specifically, we used diameter at breast height (dbh;

374 measured at 1.3 m above ground) and stem diameter data collected at higher positions along the
375 stem from previous censuses (Janner & Fernández-Lucero, work in progress; Ramos et al., 2024)
376 alongside our own stem diameter measurements at sensor heights.

377 We interpolated missing diameters at 1 m height intervals using simple linear regression. For
378 each 1 m stem segment, we calculated vertical surface areas as $2\pi rh$ (where r = stem radius [m]
379 and height h = 1 m) and divided this by the corresponding stem volume (m^3), $\pi r^2 h$, and the
380 crown surface area (m^2) to obtain PAD_v beneath the crown. To reflect our assumption that
381 epiphyte diaspores are most likely to attach only to the side of the stem facing their release point,
382 we multiplied this surface area by 0.5, thereby ignoring redistribution to the opposite side of the
383 stem by turbulent airflows. This yielded a local estimate of PAD_v for the airspace beneath that
384 crown. For a plot-level estimate, we averaged stem diameters within each 1 m height class across
385 all trees. We then converted these mean diameters to stem surface area, scaled them by the
386 number of trees in the plot, and divided by plot area (1 ha), following our previous
387 implementation.

388 In both approaches, the resulting PAD_v profiles were matched to the lidar-derived horizontal
389 plant area density profile (PAD_h) at 1 m vertical resolution. Thus, total plant area density was
390 defined as the sum of the (lidar-derived) horizontal and the (stem diameter-derived) vertical
391 components of plant area density ($PAD = PAD_h + PAD_v$). Hereafter, we use PAD to refer to this
392 combined measure.

393 ***Wind dynamics***

394 To answer our first question, how vertical airflow is structured across forest strata and
395 environmental conditions, the measurement data were imported into R for all subsequent

analyses and combined with site characteristics (e.g., anemometer height, *PAD*, stem diameter etc.). Because the data were not normally distributed (according to Shapiro-Wilk tests, histograms, and qqplots), showed high skewness, high kurtosis, and non-homogenous variances, and had uneven sample sizes among height categories (Appendix 1: Figure S6), we used non-parametric tests. Specifically, we used Kruskal-Wallis (KW) tests followed by Dunn's post hoc tests with Bonferroni correction, implemented with the rstatix library (Kassambara, 2025). Outliers, i.e., points exceeding 1.5 times the interquartile range, were not removed from the data as gusts—the maximum wind speeds in a specified time interval—represent, by definition, extreme values.

To investigate wind dynamics across vertical profiles we pooled the replicates into 5-meter height categories, starting from 0–5 m and ending at 30–35 m, where the highest anemometers were installed. To justify pooling, we assessed the contribution of height to the total variance within each replicate and across all replicates together. Specifically, we calculated the ratio of intra-height variance to inter-height variance, and because inter-height variance exceeded intra-height variance in four of the seven height categories (Appendix 1: Figure S7), supporting our decision to pool replicates by height. Height category was subsequently used as a factor in the analysis.

Effects of height and time of day on gust frequency, mean hourly speed, and relative speed

To assess wind dynamics across the forest height gradient, we used several indices: absolute (i.e., raw) **up-wind** and **up-gust speeds**, **up/down-gust frequency**, **mean up-/down-gust speeds** calculated separately, and **mean vertical gust speed** as an index of net vertical airflow. These indices were calculated either by hour of the day, for some visualisations, or by diel period, for

most statistical tests. A day began at 06:00 and ended at 18:00; the remaining time was treated as night. This roughly corresponded to the sunrise and sunset times at the study site during the sampling period (±30 minutes). Differences in means among heights, diel period, and position (in/out) were tested using KW-tests followed by Dunn's post hoc tests with Bonferroni correction.

We calculated the frequency of all up- and down-gusts ≥0.33 m s^{-1} (the measurement threshold) for each height, date, and hour-of-day subset. For this calculation, we excluded the first three vertical profiles because their measurement intervals exceeded 3 seconds and were therefore not directly comparable with the remaining data. Relative up-gust and down-gust proportions were calculated relative to the total number of measured gusts per height category. Mean hourly up-gust and down-gust speeds were calculated for the same subsets, with measurements of 0 m s^{-1} divided evenly between up-gusts and down-gusts because they are essentially directionless but still contribute to the mean. To determine whether net vertical airflow was predominantly upward or downward, we calculated mean vertical gust speed per diel period for each height category. For this signed mean, down-gusts were assigned negative values before averaging.

Effects of combined environmental factors on within-canopy gust speed

To test the effect of the environment on within-canopy mean gust speed, we fitted a Bayesian hierarchical model using the brms library (Bürkner, 2017). We calculated the 5-minute mean vertical gust speed (μ), matching the temporal resolution of the above-canopy predictors, which had been interpolated to 5-min intervals as described previously. To reduce computational load and avoid over-representing certain height categories, the data were balanced by down-sampling each height group to the smallest group (~2,200 data rows). Residual spread (σ) was modelled

simultaneously to allow variability around the mean to also depend on environmental conditions. Early model testing showed that some relationships were not well described by straight lines, so we allowed moderate non-linearity in the effects of all predictors by using smooth terms. Predictors included above-canopy wind speed, temperature, and vegetation structure, which was represented by two variables: PAD_{local}—defined as *PAD* at anemometer height—and cumulative *PAD* above anemometers (PAD_{above}), calculated as the sum of *PAD* per vertical metre above. We also modelled the linear interaction between above-canopy wind speed and both *PAD* variables. Sensor height was strongly negatively associated with PAD_{above} (Pearson's *R*: –0.9) and therefore excluded. Vertical profile ID was included as a random intercept to account for repeated measurements. All predictors were z-standardised before modelling.

Mean vertical gust speed was modelled with a Student-*t* distribution to accommodate occasional extreme values:

$$y_i \sim Student\ t(\nu, \mu_i, \sigma_i),$$

(Equation 1)

where y_i is the observed mean gust speed for observation i, μ_i is the predicted mean gust speed for observation i, σ_i is the predicted residual scale (i.e. variability) for observation i, and ν is the degrees-of-freedom parameter controlling tail heaviness, allowing the model to accommodate extreme values better than a Gaussian distribution. The predicted mean μ_i was modelled as:

$$\mu_i = \beta_0 + s(above\ canopy\ wind_i, k = 5) + s(PAD_{above_i}, k = 5) + s(PAD_{local_i}, k = 5) + s(mean\ temperature_i, k = 5) + \beta_1(above\ canopy\ wind_i \times PAD_{above_i}) + \beta_2(above\ canopy\ wind_i \times PAD_{local_i}) + b_{vertical\ profile\ ID[i]},$$

(Equation 2)

where β_0 is the intercept, $s(\cdot)$ denotes a smooth term, and k is the basis dimension controlling the maximum flexibility of the smooth. The coefficients $\beta_1$and $\beta_2$describe interaction effects between above-canopy wind and PAD_{above}, and between above-canopy wind and PAD_{local}, respectively; $b_{\text{vertical profile ID}[i]}$ is a random intercept for vertical profile identity.

The residual scale parameter was modelled as:

$$\log(\sigma_i) = \alpha_0 + s(above\ canopy\ wind_i, k = 5) + s\left(PAD_{above_i}, k = 5\right) +$$

$$s\left(PAD_{local_i}, k = 5\right) + s(mean\ temperature_i, k = 5),$$

(Equation 3)

where α_0 is the intercept.

Weakly informative regularising priors were used throughout. Because predictors were z-standardised, population-level coefficients were assigned zero-centred normal(mean = 0, SD = 0.15) priors to favour modest effect sizes while remaining broad enough to accommodate stronger effects if supported by the data. The mean intercept was assigned a normal(mean = 0, SD = 0.2) prior, centred on zero because mean vertical gust speed was generally close to zero. Random-effect and smooth-term standard deviations were assigned exponential(10) and exponential(2) priors, respectively, to limit implausibly large between-group variation and excessive complexity in smooth terms while preserving flexibility. In the σ model, the intercept was assigned a normal(mean = log[0.03], SD = 0.5) prior, corresponding to a low but uncertain residual standard deviation under average predictor conditions. The Student-*t* degrees-of-

freedom parameter was assigned a gamma(α = 2, β = 0.1) prior, where α controls the shape of the distribution and β its rate, allowing for heavy-tailed residual variation.

Stable fitting and convergence were achieved after increasing the target acceptance rate to 0.995 and the maximum tree depth to 15. Convergence diagnostics, including trace plots, posterior predictive checks, and Bayesian R^2, indicated that this sampling effort was sufficient. We report beta coefficients (β) for estimated linear effects and interactions, standard deviations (sds) for the magnitude of non-linear smooth variation, the standard deviation (sd) for random-effect variation, the residual standard deviation for residual spread (σ), the degrees-of-freedom parameter (v) governing the heaviness of the Student-*t* residual tails, and 95% credible intervals (CrI).

Additional R libraries used in our analyses are: data.table (Barrett et al., 2025) for working with large data; circular (Agostinelli & Lund, 2025) for calculating circular means; png (Urbanek, 2025) to add background images to the plots; patchwork (Pedersen, 2025) to join plots; PMCMRplus (Pohlert, 2024) and biostat (Gegzna, 2020) to create clds to add to the plots; ggtext (Wilke & Wiernik, 2022) for generating plot annotations and figure titles; ggbreak (Xu et al., 2021) to create axis breaks; viridis (Garnier et al., 2024) for colourblind-friendly colour scales; ggpmisc (Aphalo, 2025) and modelR (Wickham, 2023) for fitting generalised linear models; scales (Wickham et al., 2025) for (pseudo-)log transformation of axes and legends; moments (Komsta & Novomestky, 2022) to test for skewness and kurtosis, and RColorBrewer (Neuwierth, 2022) for the colour grading in Figure 1. Most of the generated figures were further manipulated using the free software Inkscape (Inkscape's contributors, 2023).

Diaspore dispersal simulation

To estimate **primary dispersal** success within the forest height gradient, we developed a trajectory model (*EpiDisp 1.0*) that is based on the winds and gusts measured at the different heights. As in other trajectory models, our model calculates the cumulative vertical and horizontal dispersal distance of a diaspore based on its trajectory during shorter time intervals.

Input parameters

The model incorporates three independent variables: release height (assumed to be the heights at which the anemometers were installed), terminal velocity (V_{term}), and plant area density (*PAD*). Reported terminal velocities for epiphytes range from 0.06 m s^{-1} in (not truly epiphytic) ferns to 0.09 m s^{-1} in orchids and to 0.5 m s^{-1} in bromeliads (Bennett, 1988; Chilpa-Galván et al., 2018; Zotz et al., 2016; Hoensbroech, pers. data, unpublished); *EpiDisp 1.0* considers a terminal velocity range of 0.01 m s^{-1} to 1 m s^{-1}. Like other trajectory models, this model neglects the short (relative to its subsequent flight period) initial acceleration period of the diaspore (usually < 0.5 s) and assumes that V_{term} remains constant during the diaspore's flight (Nathan et al., 2002; Nathan, Katul et al., 2011; Tackenberg, 2003).

Plant area density (*PAD*) affects a diaspores flight: as a rule of thumb, the more obstacles in the form of, e.g., leaves, branches, or stems are present (the higher the *PAD*), the more likely it is that a diaspore is intercepted by (deposited on) them early during its trajectory. Because bark generally forms the outermost layer of the woody parts of trees, the wood component was used as a proxy for potential bark interception. As the available lidar data did not allow us to distinguish leaves from wood, we estimated this partition from values reported in the literature: in tropical forests, woody surfaces, i.e., bark, contribute approximately 20% to horizontal plant

area density (PAD_h; Kalacska et al., 2005; Olivas et al., 2013). We therefore assumed that 20% of PAD_h represented bark, while vertical plant area density (PAD_v), being derived from stem surfaces, was assumed to consist entirely of bark. Based on these assumptions, we calculated **bark area density (*BAD*)** as: $BAD = 0.2 \times PADh + PADv$, and leaf area density (*LAD*) as the difference between *PAD* and *BAD* (*LAD* = *PAD*–*BAD*).

Simulation experiments

EpiDisp 1.0 calculates primary dispersal distance as the sum of the wind/gust speeds (the effective wind) minus the diaspore's falling velocity for every measured time increment (Equations 4a and 4b). Per increment, the maximum absolute gust speed contributes one third, the 1-minute wind average two thirds to the effective wind (the sum of the two components). For the vertical distance, the terminal velocity is subtracted from wind/gust speeds, so that

$$D_w = \sum \begin{cases} \frac{w' + 2\overline{w}}{3} - V_{term}\,), if\ \frac{w' + 2\overline{w}}{3} > V_{term} \\ \frac{w' + 2\overline{w}}{3}, \quad if\ \frac{w' + 2\overline{w}}{3} < V_{term} \end{cases}$$

$$\text{and } D_u = \sum \left(\tfrac{1}{3}u' + \tfrac{2}{3}\overline{u}\right) t$$

(Equations 41a and 4b)

where D_w and D_u are the sum of the, respectively, vertical or horizontal dispersal distances, $w'$and u' the vertical and horizontal gust speeds, $\overline{w}$ and $\overline{u}$ the 1-minute vertical and horizontal wind averages, t is the time increment and V_{term} the (negative) terminal velocity of a diaspore. Dispersal distances are influenced by terminal velocity only when it exceeds the speed of the downward airflow. When the air moves downward faster than the diaspore's terminal velocity,

543 the airflow carries the diaspore entirely, effectively cancelling out the influence of terminal
544 velocity on its trajectory (Horn et al., 2012).

545 Simulations begin at a randomly selected time interval (T) at release height H within a vertical
546 profile. Each diaspore is assigned a terminal velocity (V_{term}) from a predefined set of 12 possible
547 values (0.01, 0.05, 0.10, 0.15, 0.20, 0.25, 0.30, 0.35, 0.40, 0.45, 0.50, and 1 m s^{-1}). At each time
548 step, the model evaluates whether the current wind speed or gust exceeds V_{term}. If yes, the
549 diaspore is abscised and enters flight. If no, the diaspore remains attached and advances to the
550 next time interval (T') without changing height. Once abscised, the diaspore moves horizontally
551 and vertically according to wind vectors and its V_{term}. On its way towards each new height (H'),
552 the diaspore potentially encounters obstacles represented by plant area density (PAD) and its
553 components (BAD and LAD).

554 $$I_{Pw} = 1 - exp(-PAD\ |D_w|) \text{ or } I_{Pu} = 1 - exp(-PAD\ |D_u|)$$

555 (Equations 5a and 5b)

556 The probability that a diaspore is intercepted by a substrate during its horizontal (P_u) or vertical
557 (P_v) trajectory is modelled as a function of the absolute horizontal or vertical distance it travels
558 ($|D_u|$ or $|D_v|$) and the plant area density (PAD) at its release height, following Equations 5a and 5b
559 based on Bohrer et al. (2008). To determine whether interception occurs, the model generates a
560 random number (R) between 0 and 1. The diaspore is intercepted by a substrate when $R < P_u$ or
561 $R < P_v$. Dispersal is successful when that substrate is bark ($R < BAD$) and unsuccessful when it is
562 a leaf ($R > BAD$) or when it is dispersed to the forest floor ($H' = 0$). When it is dispersed above
563 the canopy ($H' >$ crown height), possibly initiating LDD, the success remains undetermined. In
564 the latter three cases, the diaspore is removed from the simulation. If none of these conditions are

565 met, the trajectory continues until termination criteria are reached (see Figure 2, as well as
566 Appendix 3 for a detailed flowchart). The point of interception is calculated as D_u or D_v, i.e., the
567 distance it would have travelled without interception, multiplied by the random number *R*.

568 We ran the simulation per subset, defined by vertical profile ID, anemometer position (in/out),
569 and diel period. To capture finer temporal variation, we initially divided the day into four diel
570 periods (early day: 06:00–11:59; late day: 12:00–17:59; early night: 18:00–23:59; late night:
571 00:00–05:59). For each subset, trajectories were simulated across all V_{term} values using the same
572 randomly selected 1,000 time steps, corresponding to approximately 30 min of wind data, or
573 fewer if the subset was shorter.

574 ***Output analysis***

575 To answer our second question, how airflow, forest structure, release height, and diaspore traits
576 jointly determine dispersal success and escape from the canopy, we first quantified the relative
577 frequency of successful and canopy dispersal events. We calculated the relative proportion of the
578 different dispersal outcomes, i.e., the ratio of diaspores per outcome to the total diaspores
579 released per release height, V_{term}, and diel period. Because diel period contributed little
580 explanatory power (< 0.01%), we simplified it to a binary day/night factor for analysis,
581 combining early and late day into day and early and late night into night.

582 We then assessed whether the probability of successful and canopy dispersal increased with
583 decreasing V_{term} and increasing release height using binomial regression. However, we observed
584 that the binomial regression performed poorly for canopy dispersal, and instead used general
585 additive models (GAMs), which showed a relatively lower Akaike Information Criterion (AIC)
586 indicating better model fit. Both the binomial regression for successful and GAM for canopy

dispersal considered V_{term}, release height, and diel period as predictor variables. Diaspores that dispersed successfully or above the canopy received a value of 1, the remaining outcomes a value of 0. Diaspores still "in dispersal" at the end of the simulation were excluded from both regressions as the outcome remained uncertain. Vertical profiles with a crown height ≤15 m were excluded from the canopy dispersal regression as the respective tree crowns were too low to model dispersal above the forest canopy. We ran the model on all V_{term} values to visually identify those that exhibited the most pronounced differences in probabilities. Only those (V_{term}: 0.01, 0.1, 0.3, 0.5, and 1 m s^{-1}) were considered for the manuscript.

We interpreted statistical significance with caution, as inferential outcomes can be strongly influenced by the number of simulated replicates rather than by the biological relevance of an effect. Following Murray and Conner (2009), we therefore emphasized variable importance rather than significance testing by first screening predictors using zero-order associations with the binary response and then quantifying their independent contributions using hierarchical partitioning. For the binomial response models, hierarchical partitioning was implemented with the R library hier.part (Mac Nally & Walsh, 2004), using a binomial error structure and log-likelihood as the goodness-of-fit metric. We report the independent contribution of each predictor and its percentage of the total independent explanatory contribution to describe the dominant tendencies generated by the simulations, rather than treating small *p*-values as evidence of biological importance.

For bark interception probability, hierarchical partitioning indicated that V_{term} was the dominant predictor of simulated outcomes, followed by diel period and release height. In the full model, V_{term}, diel period, and release height accounted for 82%, 12%, and 6% of the total independent

609 contribution, respectively. Because removal of release height after zero-order screening produced
610 nearly the same ranking of the remaining predictors, we report the full model in the Results.

611 For LDD probability, hierarchical partitioning of the full model ranked V_{term} first, release height
612 second, and diel period third, each accounting for 63%, 37%, and < 0.1% of the total
613 independent contribution, respectively. After removal of diel period following zero-order
614 screening, the reduced model retained the same ranking of the remaining predictors. Again,
615 because removing diel period after zero-order screening produced nearly the same ranking, we
616 present the full model in the Results.

617 To assess our third question, to what extent these processes generate dispersal limitation and
618 contribute to the spatial and vertical structuring of epiphyte communities, we used linear
619 regression models to quantify the influence of $V_{term,}$ release height, and diel period on vertical
620 and horizontal dispersal distances of successfully dispersed diaspores. We compared the simpler
621 models (release height, V_{term} or diel period alone) with the more complex models (their
622 combination) using AIC to evaluate whether additional predictors improved model fit. In all
623 cases, the more complex model had a lower AIC, indicating they captured the signal better. We
624 repeated the linear regression models on only parts of the forest height gradient to determine
625 whether the degree of influence of predictor variables varied between different forest zones, but
626 the effect was not significant.

627 We fitted dispersal kernel models to the observed vertical and horizontal dispersal distances of
628 diaspores intercepted by bark using the R dispfit library (Proença-Ferreira et al., 2025). We
629 excluded distances of 0 m and converted negative distances to their absolute values. Dispersal
630 directions (downward, upward, and horizontal) as well as groups (V_{term} × release height) were

modelled separately. For visualisation, we selected the best-supported model (lowest AIC) and used this model for plotting. We then summarised kernels across groups by calculating the mean kernel estimate and its standard error (SE). We estimated the distances at which 50%, 75%, and 95% of diaspores were predicted to be bark-intercepted by deriving these quantiles from the cumulative bark-interception curve. We additionally used 2d relative densities (i.e., densities per V_{term} × release height group) to visualise their distribution in the forest post-bark interception.

Finally, we developed a continuous metric of dispersal limitation by combining the proportion of diaspores that successfully dispersed with the distances they moved within the 1 ha forest plot. Vertical and horizontal dispersal distances were expressed relative to their respective maximum possible distances (i.e., from release height to ground or canopy, and across the plot extent, ~140 m, roughly reflecting the maximum dispersed distance of ca. 146 m), describing how broadly diaspores spread away from the parent plant. Both vertical and horizontal displacement were scaled linearly between zero and one.

The relative importance of vertical positioning and horizontal spread was controlled using weighting parameters (α and β, respectively), which determine how strongly each component contributes to the realised dispersal contribution of individual diaspores (ranging from 0 = no influence to 1 = proportional influence, with values >1 increasing emphasis). For example, values around 0.5 indicate moderate importance, whereas values ≥0.8 reflect a dominant role of that component.

For each release height × terminal velocity × diel period combination, the realised dispersal contribution of an individual diaspore *i* was defined as:

$$C_i = S_i \cdot (V_i^{\alpha}) \cdot \left(H_i^{\beta}\right),$$

(Equation 6)

where C_i is the contribution of diaspore i, S_i is a binary indicator of dispersal success (1 = successful interception, 0 = unsuccessful), V_i is the scaled vertical displacement, and H_i is the scaled horizontal displacement. Both V_i and H_i range from 0 to 1 relative to their maximum achievable distances. The parameters α and β control the relative weighting of vertical and horizontal components.

Rather than averaging contributions arithmetically, we aggregated dispersal contributions using a power mean of order q:

$$\bar{C}_q = \left(\frac{1}{n} \sum_{i=1}^{n} C_i^q \right)^{1/q},$$

(Equation 7)

where $\bar{C}_q$ is the mean realised dispersal contribution and q controls the weighting of contributions across diaspores. When q = 1, this reduces to the arithmetic mean, such that all diaspores contribute equally. For q > 1, higher-contribution diaspores exert disproportionately greater influence on the aggregate metric, thereby reducing the dominance of abundant low-distance dispersal events and increasing the importance of rare greater dispersal distances.

To incorporate fecundity, we scaled the aggregated contribution by a fecundity term, such that dispersal limitation was defined as:

$$\text{Dispersal limitation} = (1 - \bar{C}_q)^{\log(1+F)},$$

(Equation 8)

where F is fecundity. The logarithmic scaling of fecundity reflects diminishing returns of increasing diaspore supply, such that additional diaspores increase the likelihood of successful dispersal but with progressively smaller marginal gains. This prevents unrealistically rapid collapse of dispersal limitation at high fecundity.

Values of dispersal limitation close to zero indicate weak limitation, whereas values close to one indicate strong limitation. Overall, this framework assumes that dispersal success depends jointly on arrival probability and spatial redistribution, while allowing rare greater dispersal distances to disproportionately influence outcomes through the power-mean formulation.

Results

Effects of height and diel period on gust speed, frequency, and net airflow

Highest raw gust speeds occurred within the trunk zone (~20 m) and lowest gust speeds below the low crown zone (5–10 m; Appendix 4: Figure S1A) The interaction of height and position (Appendix 4: Figure S1A,B) on raw gust speeds was significant ($p < 0.001$, KW-$H_{df=13,n=9,864,421}$ = 632,588; Dunn's $p < 0.001$ for all except one combination (at 30–35 m, the difference between the in and out position was $p < 0.005$). Height also significantly increased 1-minute maximum up-gust speeds ($p < 0.001$, KW-$H_{df=3,n=36,946}$ = 11,895; Dunn's $p < 0.001$ for all combinations; Appendix 4: Figure S2). Across heights, the majority of up-gusts remained below 1 m s^{-1}, though we also recorded up-gust speeds > 5 m s^{-1} at all heights except in the 5–10 m category, where up-gusts did not exceed 2 m s^{-1}, and up-gust speeds > 10 m s^{-1} at 0–5 m and 15–20 m (Appendix 4: Figure S2).

The frequency of up- and down-gusts increased with height (Figure 3A, Appendix 4: Figure S3A), peaked at around noon, and plummeted to nearly 0 occurrences at night. Consistent with this, height ($p < 0.001$, KW-$H_{df=5,n=558,442} = 140,206$), diel period ($p < 0.001$, KW-$H_{df=1,n=558,442} = 4931$), and their interaction ($p < 0.001$, KW-$H_{df=1,n=558,442} = 144,770$) significantly increased hourly up-gust frequency as well as down-gust frequency (height: $p < 0.001$, KW-$H_{df=5,n=605,061} = 70,003$, diel period: $p < 0.001$, KW-$H_{df=1,n=605,061} = 14,895$, height × diel period: $p < 0.001$, KW-$H_{df=11,n=605,061} = 98,232$). For instance, near the forest floor, the frequency of up-gusts peaked at 50 gusts per hour, while at 25–30 m it peaked at more than 200 gusts per hour (Figure 3A). Down-gusts were relatively more common than up-gusts from the forest floor up to ca. 15 m (Appendix 4: Figure S3A), where up-gusts became more dominant, increasing from 0.1 near the forest floor to 0.3–0.4 in the high crowns (25–30 m; difference between heights: $p < 0.001$, KW-$H_{df=13,n=4728} = 1542$). Yet, overall, horizontal gusts prevailed at all heights (Appendix 4: Figure S3A).

Mean hourly gust speeds showed similar diurnal variation as gust frequency (Figure 3B, Appendix 4: Figure S3B), with peaks at noon and lows throughout the night at all heights. Again, height ($p < 0.001$, KW-$H_{df=6,n=2,031,308} = 784,187$), diel period ($p < 0.001$, KW-$H_{df=1,n=2,031,308} = 75,220$), and their interaction ($p < 0.001$, KW-$H_{df=13,n=2,031,308} = 896,367$) significantly increased the hourly mean of up-gust speeds and of down-gust speeds (height: $p < 0.001$, KW-$H_{df=6,n=1,841,283} = 523,294$, diel period: $p < 0.001$, KW-$H_{df=1,n=1,841,283} = 8,146$, height × diel period $p < 0.001$, KW-$H_{df=13,n=1,841,283} = 567,638$). Both peaked at 25–30 and 30–35 m, though down-gusts were relatively stronger than up-gusts, and horizontal gusts were stronger yet (Appendix 4: Figure S3B).

Mean (signed) vertical gust speed, i.e., net airflow, mostly fell within a range of ± 0.25 m s^{-1}, though variation was substantial, particularly above 15 m (Figure 3C). Height ($p < 0.001$, KW-$H_{df=6,n=3,872,591} = 414{,}620$), diel period ($p < 0.001$, KW-$H_{1,\ 3,872,591} = 22{,}594$), and their interaction ($p < 0.001$, KW-$H_{df=13,n=3,872,591} = 456{,}575$) significantly increased net airflow. At night, net airflow was downward throughout the height gradient. During the day, net airflow was downward only below 15 m, increased relatively sharply toward 20 m, and became upward above that. This transition zone coincided with a pronounced decrease in plant area density (*PAD*) and its components (leaf are density [*LAD*] and bark area density [*BAD*]); Figure 3D), which was even more prominent when considering only the seventeen vertical profiles (Appendix 4: Figure S4).

Effects of combined environmental factors on within-canopy gust speed

The Bayesian model explained only a small proportion of the variation in mean signed gust speed (Bayesian $R^2 = 0.02$, 95% CrI = 0.02 to 0.03), indicating weak overall structure in the fitted mean. Smooth-term variation in the mean (μ) model was relatively small for above-canopy wind (sds = 0.03, 95% CrI < 0.01 to 0.11), PAD_{above} (sds = 0.16, 95% CrI = 0.06 to 0.45), PAD_{local} (sds = 0.2, 95% CrI = 0.08 to 0.55), and temperature (sds = 0.12, 95% CrI = 0.04 to 0.35). Predicted mean gust speed nevertheless varied with above-canopy wind speed, and there was evidence that this relationship depended on canopy structure (Figure 4A,B), with a weak positive interaction with PAD_{local} ($\beta < 0.01$, 95% CrI = 0 to < 0.01; Figure 4A) and PAD_{above} ($\beta = 0.01$, 95% CrI = 0 to < 0.01; Figure 4B). The fitted mean decreased towards negative values with higher above-canopy wind, especially when PAD_{local} was intermediate (Figure 4A). When plotted against above-canopy wind speed, μ was more positive at low PAD_{above} but declined more strongly as above-canopy wind speed increased (Figure 4B). At higher PAD_{above}, μ

remained closer to zero across above-canopy wind speeds. Additional interactions can be explored in our shinyApp (Appendix 2).

In contrast, the σ sub-model showed substantially stronger structure, with larger smooth-term variation for above-canopy wind (sds = 1.71, 95% CrI = 0.97 to 2.96), PAD_{above} (sds = 0.79, 95% CrI = 0.35 to 1.68), PAD_{local} (sds = 1.06, 95% CrI = 0.48 to 2.01), and especially temperature (sds = 2.04, 95% CrI = 1.22 to 3.38). Residual spread increased strongly with above-canopy wind speed, and it decreased strongly with increasing PAD_{above} and PAD_{local} across the observed range (Figure 4A,B). Temperature was also strongly associated with σ, indicating overall that predictor variables were more strongly associated with variability around the mean than with the fitted mean itself. Variation among vertical profiles was modest (sd = 0.02, 95% CrI = 0.02 to 0.04), and the low Student-*t* degrees-of-freedom parameter indicated heavy-tailed residuals (ν = 1.95, 95% CrI = 1.86 to 2.04).

Diaspore dispersal

Based on the wind dynamics at San Lorenzo during the sampling period, *EpiDisp 1.0* predicts that, overall, approximately 74% of diaspores are effectively lost during primary dispersal: 16% of diaspores remain unabscised, 59% are intercepted by a leaf, 7% are still in dispersal at the end of the simulation, 2% fall to the ground. Less than 0.1% are dispersed above the canopy, and only 16% are intercepted by bark and, as per our definition, successfully dispersed (Appendix 4: Figure S5). These proportions, however, vary strongly with V_{term}, release height, and diel period (Appendix 4: Figure S5, Table S1), and differences become most evident at the extremes of the predictors' ranges. For example, more than 7% of diaspores with a V_{term} of 0.01 m s^{-1} released (and abscised; refer to Table 1 for the difference between released and abscised) at 30–35 m

759 during the day dispersed above the canopy—but none below 5 m did. In fact, nearly all diaspores
760 (> 99%) with a V_{term} of 1 m s^{-1} released below 10 m and at night remain unabscised. Between
761 10% and 30% of diaspores released below 5 m end up on the ground, whereas this proportion
762 decreases to < 3% when released above 10 m.

763 Bark interception probability and long-distance dispersal probability were both affected by V_{term},
764 release height, and diel period. Higher V_{term} strongly reduced both bark interception probability
765 (Figure 5A, Table 2) and above-canopy emergence probability (Figure 5B, Table 2). Release
766 height and diel period showed contrasting effects: higher release heights and nighttime
767 conditions decreased bark interception probability (Figure 5A, Table 2) but increased long-
768 distance dispersal probability (Figure 5B, Table 2). Interaction terms indicated that these effects
769 depended on one another, particularly for the combinations of release height and V_{term}, V_{term} and
770 nighttime, and the three-way interaction among release height, V_{term}, and nighttime (Table 2).

771 Vertical and horizontal dispersal distances of bark-intercepted diaspores were also shaped by
772 V_{term}, release height (Figure 6A,B, Appendix 4: Figures S6−S8), and diel period (Table 2).
773 According to GAMs, higher V_{term} reduced vertical dispersal distance but increased horizontal
774 dispersal distance, whereas nighttime conditions reduced both vertical and horizontal distances
775 (Table 2).

776 Within-canopy spread after successful dispersal varied with both V_{term} and release height: lower
777 V_{term} and higher release heights were associated with broader distributions across horizontal
778 distance and interception height, whereas higher V_{term} produced more compact distributions
779 closer to the point of release and showed greater spread towards lower heights (Appendix 4:
780 Figure S6). Kernel densities of bark-intercepted diaspores were overall concentrated near the

781 release point and declined steeply with distance in both the vertical and horizontal dimensions
782 across nearly all release height × V_{term} groups (Appendix 4: Figure S7A,B). Diaspores released
783 from 30–35 m tended to show a less distinct peak and more often reached greater dispersal
784 distances. Across all groups, kernel density peaked strongly near 1 m from the release point and
785 declined rapidly in all directions (Figure 6A,B). Downward, 75% of intercepted diaspores
786 occurred within < 5 m of the release point, whereas upward, 95% occurred within < ~6 m of
787 release point (Figure 6A). Horizontally, 50% of intercepted diaspores occurred within 5 m, 75%
788 within 10 m, and 95% within 25 m of the release point (Figure 6B). It seemed that release height
789 added less variation to vertical (Appendix 4: Figure S7A) than to horizontal spread (Appendix 4:
790 Figure S7B), whereas terminal velocity strongly shaped both (Appendix 4: Figure S8A,B).

791 Dispersal limitation remained generally high across all release height × V_{term} × diel period
792 combinations (Figure 7, Appendix 4: Figure S9), typically ranging between ~80% and 100%
793 when horizontal spread was moderately weighted ($\beta > 0.5$). The degree of dispersal limitation
794 declined when neither vertical nor horizontal spread were weighted ($\alpha = 0$, $\beta = 0$) and with
795 increasing power-mean exponent (q), reflecting the growing influence of rare longer distance
796 dispersal events.

797 Increasing release height generally reduced dispersal limitation, with a slight peak in the trunk
798 zone. This decline was most pronounced under daytime conditions and for low terminal
799 velocities, particularly when vertical positioning was not considered ($\alpha = 0$). When vertical
800 positioning was included ($\alpha > 0$), higher terminal velocities exhibited comparatively lower
801 dispersal limitation, reflecting their greater downward dispersal.

Discussion

Understanding how dispersal operates within forest canopies is essential for explaining the spatial and vertical structure of epiphyte communities. Our results show that dispersal contributes to the patchy and vertically stratified distribution patterns commonly observed in epiphyte communities but is unlikely to explain these patterns alone. Instead, dispersal in forests emerges as a context-dependent, three-dimensional process in which success, horizontal and vertical dispersal distances, and fecundity jointly determine the degree to which diaspores reach suitable substrates. At the per-diaspore level, epiphytes appear strongly constrained: the probability of being intercepted by bark is low, and most successful diaspores remain close to their parent plant. However, this constraint varies with terminal velocity, release height, and canopy context, and may be substantially reduced at the individual or community level when high fecundity is considered. Thus, dispersal limitation should not be interpreted as a fixed property of epiphytes or other organisms, but as a scale- and context-dependent outcome of dispersal success, dispersal distances, and diaspore supply.

This perspective is important because wind dispersal in forests is often conceptualised from a terrestrial point of view, in which vegetation interception represents loss from the dispersal process and success is defined by arrival at ground-level habitat. Yet many wind-dispersed organisms and particles—canopy soil (and soil organisms), pollen, fungal spores, ballooning spiders—move through forests without necessarily requiring ground deposition. Epiphytes provide a particularly clear reversal of this framework: their diaspores must be intercepted by suitable aboveground substrates, such as bark, to disperse successfully. To capture this process, we developed *EpiDisp 1.0*, a mechanistic within-canopy dispersal model using epiphytes as a model system. In the following, we discuss how canopy context and diaspore traits shape

dispersal outcomes in epiphytes, while highlighting their broader relevance for wind dispersal in vertically structured environments.

Patterns of dispersal in a stratified forest canopy

Dispersal success in forests depends on the target surface of the dispersal unit. For epiphytes, dispersal success is defined by interception on suitable aboveground substrates, here modelled as bark. A central assumption in epiphyte ecology is that dispersal success is extremely low. Seed-trap studies, for example, report retention values of ~0.5% for epiphyte diaspores (Cascante-Marín et al., 2009; Mondragón & Calvo-Irabién, 2006; Paggi et al., 2010). Our results suggest that such methods may underestimate primary dispersal success in epiphytes. Using a mechanistic trajectory model, we estimate that ~16% of diaspores are initially intercepted by bark and thus disperse successfully during primary dispersal. This indicates that the initial dispersal bottleneck may be weaker than previously assumed, although most diaspores still fail to reach suitable substrates. The discrepancy likely reflects methodological differences. Seed-trap studies rely on the chance recovery of tiny diaspores at their final resting positions and may miss a large fraction of dispersal events. In contrast, *EpiDisp 1.0* tracks each diaspore to its first point of interception and therefore quantifies primary dispersal rather than the full dispersal pathway. Incorporating diaspore retention (Tay et al., work in progress) and secondary dispersal could refine these estimates by accounting for how many diaspores are later removed from—or added to—interception sites. Nevertheless, mechanistic estimates of primary interception are likely to remain higher than values inferred from seed-trap studies because they are not constrained by the incomplete recovery of dispersed diaspores. Even this higher estimate, however, indicates that dispersal represents a demographic bottleneck, consistent with earlier suggestions for epiphytes (e.g., Ackerman et al., 1996) and plants more broadly (van der Pijl, 1982).

For other wind-dispersed organisms, interception by vegetation may also constitute successful dispersal. This is evident, for instance, in ballooning arthropods such as spiders, which even show vertical stratification comparable to that in epiphytes (Costa et al., 2025). Unlike epiphyte diaspores, however, spiders may be able to move to a more suitable microhabitat after interception. In foliar pathogens, successful dispersal may occur when wind-borne fungal spores are intercepted directly by susceptible leaf tissue. In ash dieback, for example, wind-borne spores of *Hymenoscyphus fraxineus* enter ash (*Fraxinus* L. spp.) leaves before spreading into and infecting petioles and shoots (e.g., Mansfield et al., 2018). Our results suggest that, when leaves are the target substrate, interception rates can be very high (Appendix 4: Figure S5), which could help explain rapid local transmission in ash dieback. Thus, whether vegetation functions as a dispersal barrier or as a successful destination depends on the organism and, critically, on the surface required for establishment.

Dispersal success, however, captures only whether diaspores reach their destination, not how far they disperse. To understand dispersal in a three-dimensional environment, horizontal and vertical dispersal distances must also be considered. In wind-dispersed plants, dispersal kernels are typically characterised by a strong concentration near the source and a thin tail of rare long-distance events (e.g., Nathan & Muller-Landau, 2000; Qin et al., 2025). Our model reproduces this general pattern for both horizontal and vertical dispersal distances (Figure 6). As a consequence, most successful diaspores move only short distances. In a forest context, these short dispersal distances would often keep diaspores within the same or neighbouring trees and, vertically, within the same or adjacent strata, consistent with earlier observations on epiphyte distributions (Schimper, 1908; Torres et al., 2018; Zotz & Vollrath, 2003). Dispersal can

therefore contribute to the patchy and vertically stratified distribution patterns commonly observed in epiphyte communities.

In addition to bark interception and within-canopy dispersal distances, *EpiDisp 1.0* also quantified above-canopy dispersal, a separate outcome that may initiate long-distance dispersal (LDD). In our simulations, the probability of above-canopy dispersal remained low overall, especially for diaspores released from lower forest strata. Fewer than 0.1% of diaspores released below 10 m dispersed above the canopy, regardless of V_{term}, reinforcing the assumption that diaspores originating from lower forest strata rarely undergo LDD (Bohrer et al., 2008). In contrast, up to 8% of diaspores released between 30 and 35 m dispersed above the canopy (Figure 5B, Appendix 4: Table S1), likely because they experienced a shorter vertical distance to the canopy boundary and more favourable wind conditions in the high crowns, where upward airflow was more common at San Lorenzo (Figure 3C). Thus, although above-canopy dispersal was generally rare, its probability depended on the interaction between release height and V_{term} (discussed below).

Dispersal above the canopy, however, does not guarantee success. On the contrary, the farther a diaspore travels from its parent plant, the lower its chances for survival may become (Winkler et al., 2009), and even surviving diaspores might still fail to land in a suitable site. Consequently, our above-canopy dispersal estimates are only a coarse proxy for LDD, and effective LDD is likely to be lower due to post-dispersal demographic filters. In this sense, our results fully agree with the view that LDD events are rare in epiphytes (Givnish et al., 2016; Trapnell et al., 2013) and understorey plants in general (Bohrer et al., 2008).

Canopy context and diaspore traits shape dispersal

Terminal velocity emerged as the main driver of dispersal outcomes, but its effects depended on canopy context and on which dispersal outcome was considered. For bark interception, terminal velocity was more important than release height. Against our expectation, bark interception probability was broadly similar across release heights, while terminal velocity emerged as the stronger predictor of primary dispersal success (Table 2). This contrasts with studies identifying release height as a dominant driver of wind dispersal in forests (Heydel et al., 2014; Soons et al., 2004), although few studies have modelled release from the understorey, and none considered bark as the final destination. In *EpiDisp 1.0*, especially diaspores with $V_{term} < 0.5$ m s^{-1} were only weakly affected by release height. This may partly reflect our decision to keep vertical bark surface (PAD_v) constant in *EpiDisp 1.0*, which constrained interception probabilities similarly across heights. By contrast, diaspores with $V_{term} > 0.5$ m s^{-1} showed a near-linear increase in dispersal success with increasing release height, possibly because their predominantly downward trajectories (Appendix 4: Figure S6) exposed them to more cumulative bark surface before reaching the ground. However, this pattern may have limited relevance for epiphyte dispersal, because terminal velocities reported so far for wind-dispersed epiphyte diaspores do not appear to exceed 0.4 m s^{-1}—although they may approach higher values when wet or dispersed in clusters (Zotz et al., 2016). Thus, for most wind-dispersed epiphytes, primary dispersal success appears to be governed less by where diaspores are released than by how slowly they fall.

Although terminal velocity remained the main determinant of dispersal outcomes, release height became more important for dispersal distances and above-canopy dispersal than it was for bark interception. However, its effect appeared to be driven less by height per se than by the highly localised airflow associated with different forest zones. Diaspores released from the lower strata

914 were most dispersal-limited (Figure 7), showing lower dispersal success (Figure 5A), shorter
915 dispersal distances (Figure 6A,B), and rarely dispersing to other strata, neighbouring trees, or
916 above the canopy (Appendix 4: Figures S6–S8). Similar constraints on understorey dispersal
917 have been observed in other forest systems (Heydel et al., 2014; Svahnström et al., 2025), likely
918 reflecting dense vegetation and weak, possibly downward, airflow (Figure 3C). At San Lorenzo,
919 conditions beneath the low crowns (<15 m)—predominantly downward flow, high *PAD*, and a
920 weaker gust regime—would be expected to restrict the upward transport of ascending diaspores
921 while retaining those descending from above, effectively creating a partial one-way filter. Yet
922 this filter was not impermeable: although most diaspores released in the lower forest strata were
923 retained locally, intermittent up-gusts appear to lift some diaspores above the low crowns
924 (Appendix 4: Figure S6), or transport them from the low crowns beyond the canopy (Figure 5B).

925 In contrast, release from higher strata, and particularly the trunk zone, increased dispersal
926 distances (Appendix 4: Figure S6), consistent with previous studies reporting greater dispersal
927 distances from higher release points (Heydel et al., 2014; Lee & Yoon, 2025; Soons et al., 2004).
928 These longer dispersal distances reduced dispersal limitation (Figure 7), likely due to stronger
929 horizontal airflow in these layers (Appendix 4: Figure S3A,B). Yet stronger or more turbulent
930 airflow did not promote all forms of dispersal.

931 The trunk zone, despite lower *PAD* (Figure 3D) and stronger, more turbulent airflow (Figure
932 3A–C), showed neither higher bark interception (Figure 5A) nor greater above-canopy dispersal,
933 which instead declined (Figure 5B). This suggests that open, turbulent parts of the canopy may
934 promote horizontal transport without necessarily facilitating vertical transport out of the forest.

935 By contrast, densely vegetated crown zones, although characterised by higher *PAD* and reduced
936 airflow, do not necessarily impede dispersal. Instead, tree crowns may facilitate complex vertical

air movements, intermittently enabling uplift events while dampening horizontal winds (Pounden et al., 2008; Qin et al., 2022, 2025). This may explain the relatively high above-canopy dispersal probability from the low and high crown zones (Figure 5B), particularly the small peak in the low crown zone. The reduced prevalence and intensity of down-gusts at night (Figure 3A–C) may likewise help explain the greater nocturnal above-canopy dispersal observed for the diaspores with lowest V_{term} (Figure 5B, Table 2). Thus, intermediate gusts, rather than strong turbulence, may be particularly important for above-canopy dispersal in epiphytes, as also suggested for small diaspores more generally (Norros et al., 2014; Qin et al., 2025).

The effects of terminal velocity were comparatively consistent across these outcomes. Diaspores with low terminal velocities were transported farther horizontally and occasionally upward, whereas increasing terminal velocity progressively shifted dispersal downward, with terminal velocities >0.5 m s^{-1} producing the greatest downward dispersal distances (Appendix 4: Figures S6, S8A). Taken together, these results show that wind dispersal in forests is strongly structured by terminal velocity, but that canopy context determines how this trait translates into bark interception, horizontal and vertical dispersal distances, and above-canopy dispersal.

How dispersal-limited are epiphytes really?

In its strict sense, dispersal limitation quantifies the degree to which diaspores fail to arrive at all available suitable sites within their theoretical niche. Yet, in practice, it is often treated as a qualitative label, quantified only indirectly, or inferred from spatial patterns without testing whether environmental heterogeneity could also explain those patterns (Münzbergová & Herben, 2005). Existing quantitative approaches typically focus on expected seed shadows, recruitment limitation, or the proportion of sites reached relative to null expectations, and they explicitly recognise that arrival depends on both dispersal probabilities and diaspore supply (Clark et al.,

960 1999; Nathan & Muller-Landau, 2000; Terborgh et al., 2011). Building on these approaches, the
961 metric developed here aims to quantify dispersal limitation from mechanistic evidence by
962 integrating the probability of successful dispersal with horizontal and vertical dispersal distances
963 and fecundity. This makes it possible to compare how limitation changes across diaspore traits,
964 canopy positions, and biological scales, while retaining the distinction between low per-diaspore
965 arrival probabilities and potentially high absolute numbers of arriving diaspores.

966 Because our dispersal limitation metric integrates dispersal success, dispersal distances, and
967 fecundity, the context-dependent dispersal outcomes described above affected the degree of
968 dispersal limitation (Figure 7). Overall, they translated into strong limitation at the per-diaspore
969 level (fecundity = 1). Low bark interception probability and short horizontal and vertical
970 dispersal distances together mean that most diaspores fail to colonise sites far from their parent
971 plant.

972 However, this does not necessarily imply strong dispersal limitation at the level of individuals or
973 communities. Epiphytes can produce vast numbers of diaspores, from <300 diaspores per
974 individual in some Tillandsia spp. to several million diaspores per individual in many orchids
975 (e.g., Arditti & Ghani, 2000; Croat, 1978; Toledo-Aceves, 2012; Zotz, 1997, 1998). The 0.4 ha
976 subplot at San Lorenzo contains nearly 14,000 vascular epiphyte individuals (Mendieta-Leiva et
977 al., 2022; Zotz & Schultz, 2008). Tentatively assuming these are sexually reproductive and
978 produce an average of 100,000 diaspores each, this would imply 1.4 billion diaspores produced
979 every year (see also Gòmez Noguez & Flores Galván, 2019). Even if only 1% dispersed beyond
980 10 m vertically or horizontally, this would still yield 14 million diaspores escaping the
981 immediate vicinity of their parent plant, which is still an intentionally conservative estimate
982 (Figure 6A,B, Appendix 4: Table S1, Figures S7, S8). If only 0.1% dispersed above the canopy,

this would still translate to 1.4 million diaspores that can potentially colonise distant forests. Such numbers exceed even reports of relatively high colonisation rates at San Lorenzo (Mendieta-Leiva et al., 2022) and elsewhere (Einzmann & Zotz, 2017a,b), suggesting that strong per-diaspore dispersal limitation can coexist with relatively low community-level dispersal limitation.

High fecundity therefore changes the interpretation of dispersal limitation. It does not remove the per-diaspore bottleneck, but it means that low probabilities of successful dispersal, movement between strata, or dispersal to distant trees can still translate into large absolute numbers of arriving diaspores. If many diaspores move beyond their parent plant, neighbouring trees, or vertical zones, then dispersal alone should produce less distinct patches and weaker vertical stratification than are commonly observed. Therefore, dispersal cannot be solely responsible for epiphyte distribution patterns, and later demographic filters must strongly determine which arrivals are ultimately retained, germinate, and establish (Trapnell et al., 2013; Wagner et al., 2013; Winkler et al., 2009). Vertical zonation, as often demonstrated, is likely shaped more strongly by epiphyte physiology, microclimatic gradients, host-tree characteristics, bark properties, and other post-dispersal processes (Petter et al., 2016, 2021; Pittendrigh, 1948; Wagner et al., 2013). Nevertheless, because release height and terminal velocity determine where diaspores arrive in the first place, dispersal should not be excluded from explanations of vertical niche preferences.

Altogether, our study calls for a more nuanced and explicitly quantitative view of dispersal limitation. By integrating mechanistically derived dispersal success, horizontal and vertical dispersal distances, and fecundity into a single framework, our metric provides a way to quantify dispersal limitation beyond qualitative labels or indirect inference from spatial patterns. This

approach complements existing concepts based on seed shadows or site occupancy (Clark et al., 1999; Nathan & Muller-Landau, 2000; Terborgh et al., 2011) by explicitly linking dispersal processes to spatial dispersal outcomes. Applied to epiphytes, it shows that strong limitation at the per-diaspore level can coexist with much weaker limitation at the community level once fecundity is taken into account.

Importantly, this metric is inherently flexible, but its interpretation depends on the spatial scale and habitat definition considered. In its current form, it captures the dispersal component of limitation within the modelled plot, including whether diaspores reach a target surface and how far they disperse horizontally and vertically. However, it does not yet quantify the full spatial availability or suitability of recruitment sites. For example, it does not distinguish between occupied and available bark area, nor does it incorporate variation in bark suitability, microclimate, host-tree identity, or other factors that determine whether a site forms part of the theoretical niche of the species or dispersal unit of interest. Moreover, because our estimates are limited to the plot scale, expanding the spatial extent to larger forest areas, landscapes, or metacommunities would likely change the estimated degree of dispersal limitation. Processes that appear strongly limiting within a single plot may be less limiting when evaluated across larger populations with high diaspore production, while rare above-canopy dispersal events may become more important at broader spatial scales. These processes could be incorporated in future extensions, thereby moving closer to a strict definition of dispersal limitation as the failure to reach all suitable sites within the theoretical niche. Developing such an integrated metric represents a substantial step in itself, but it offers the potential to disentangle the relative contributions of dispersal, diaspore supply, habitat availability, spatial scale, and post-dispersal filtering to observed patterns. More broadly, by making these components explicit and

comparable, this framework provides a basis for more consistent, testable, and transferable interpretations of dispersal limitation across plant ecology (Münzbergová & Herben, 2005).

Wind dynamics across forest height and environmental conditions

Gust speed, frequency, and net airflow increased with height, indicating clear vertical structuring within the canopy. This is broadly consistent with previous studies showing that horizontal and vertical air movements generally increase from the forest floor towards the canopy (Dias-Júnior et al., 2017; Finnigan, 2000; Froelich et al., 2005; Heydel et al., 2014; Kruijt et al., 2000; Santana et al., 2018). On average, this increase has been described as exponential within and logarithmic above the canopy (Horn et al., 2001; Rodrigues et al., 2021), although profiles may vary within individual trees (Zhu et al., 2004). Our data diverged from such an average vertical profile and instead peaked in the trunk zone at ~20 m. This suggests that although height matters, its effect is modified, and in some layers even overridden, by local forest structure.

Wind dynamics at San Lorenzo were influenced by both atmospheric conditions, such as above-canopy wind and temperature, and forest structure (Figure 4A,B), although these effects were difficult to disentangle and relationships were generally weak. This is not unexpected given the complexity of the system (Froelich et al., 2005) and the many interacting controls involved, including radiation, temperature or humidity gradients, atmospheric stability (i.e., the resistance of the atmosphere against vertical motion), and topography (Bohrer et al., 2008; Brunet, 2020; Froelich et al., 2005; Tackenberg, 2003). With the diurnal cycle acting as an overarching control on several of these drivers, diel period emerged as a strong predictor of gust activity. Gusts became stronger and more frequent during the day and peaked around noon, consistent with diurnal patterns reported from other forests (Froelich et al., 2005; Maurer et al., 2013).

Mean vertical airflow within the forest was not predominantly upward during the day, as might be expected (Froelich et al., 2005; Maurer et al., 2013). Instead, at heights up to 15 m, mean vertical airflow remained downward both day and night. This discrepancy may partly reflect differences in measurement context, because earlier studies focused on airflow above the canopy and therefore did not capture within-canopy dynamics directly. Another possible explanation is that, at the very low wind speeds common in the lower half of the San Lorenzo forest, directional measurements become unreliable because of meandering (Anfossi et al., 2005). Even so, the daytime intensification of both up- and down-gusts may be important for driving diaspore movement through the forest interior.

Forest structure, expressed here through plant area density (*PAD*), appeared to be one of the key modifiers of wind dynamics in our study (Figures 3C,D, 4A,B). In general, turbulence increased where *PAD* decreased, with the clearest effect in the trunk zone (compare Figure 3C,D). Similar local peaks in airflow have been attributed to channelling or blow-through effects, whereby air is constricted and accelerated as it passes through gaps within or between crowns (e.g., Shaw, 1977; Zeng & Takahashi, 2000; Zhu et al., 2004). This same zone was also dominated by down-gusts (Figure 3B), consistent with studies describing strong sweeps or negative momentum fluxes in comparable forest layers (Kruijt et al., 2000; Rodrigues et al., 2021). At the same time, vertical airflow is often considered a “mean-zero process” (Maurer et al., 2013), in which horizontal turbulence generates both down- and up-gusts that largely cancel each other out over time. Indeed, mean net vertical airflow within the forest remained below |0.25| m s–1 overall (Figure 3C), as also described within and immediately above the canopy in other forests (Froelich et al., 2005; Heydel et al., 2014). Taken together, these patterns suggest that forest structure, especially gap dynamics, can redirect and intensify local airflow, creating aerodynamic

pathways that may enhance or inhibit dispersal within the canopy. This provides a mechanistic explanation for the contrasting dispersal outcomes among forest zones described above, including increased dispersal distances in the trunk zone but higher above-canopy dispersal from crown zones.

Limitations and perspectives

Several limitations of this study should be acknowledged, primarily with respect to wind-data quality. The temporal resolution of wind measurements, with one reading every 3 to 10 seconds (0.3 to 0.1 Hz), was relatively low. Heydel et al. (2014) recommend a minimum of 10 Hz to capture the effects of continuous turbulence on diaspore trajectories, and other studies have used even higher frequencies (Abdoli et al., 2023; Santana et al., 2018). Moreover, the anemometers used in this study had a detection threshold of 0.33 m s^{-1}, so weaker gusts went unrecorded. This threshold is substantial in the context of epiphyte dispersal, because many epiphyte diaspores have terminal velocities below this value and could potentially travel considerable distances in airflows weaker than those captured by our anemometers. However, because *EpiDisp 1.0* used mean wind speeds averaged over one-minute intervals, some effects of weak but persistent airflow may still have been captured in the model input. Further, horizontal winds were not filtered from the data, which may have obscured signals from vertical wind components (Abdoli et al., 2023). Especially strong horizontal winds passing through the anemometers could have induced turbulence within the sensor plates, falsely registering vertical motion (van der Molen et al., 2004). Additionally, ultrasonic anemometers are known to suffer from (co)sine response errors due to wind angle of attack (van der Molen et al., 2004). These errors should be assessed and corrected for the specific model used. Future studies could improve vertical wind

measurements by shielding anemometers from horizontal winds using shrouds (Abdoli et al., 2023), although excluding horizontal winds may also obscure important dispersal dynamics.

A particular challenge was the occurrence of extreme up-gusts of up to 32 m s^{-1}. These readings were an order of magnitude higher than the interpolated above-canopy gusts and may therefore foster doubt in the accuracy of the measurements. We failed to find comparable data, because vertical winds are commonly reported as time averages, normalised values, covariance, skewness, kurtosis, or turbulence intensity rather than as absolute maxima (Dias-Júnior et al., 2017; Finnigan, 2000; Kruijt et al., 2000; Santana et al., 2018). To the best of our knowledge, the highest absolute vertical winds reported from a forest under normal conditions, that is, without wildfires, were 7 m s^{-1} (Dias-Júnior et al., 2017). Some of our extreme gusts may therefore reflect measurement artefacts, for example if canopy elements such as leaves or twigs entered the measuring plate.

However, we also tentatively suggest that some extreme values may represent apparent rather than actual winds. Apparent wind is the wind experienced by an object in motion, whereas actual wind is relative to the motionless surface of the earth (Appendix 1: Figure S1). Trees and branches are flexible and can sway considerably (Einzmann et al., 2022; Gardiner, 1995; Mayer, 1987). When a flexible branch bends under external load, elastic potential energy accumulates and is released as kinetic energy when the load lifts, causing the branch or stem to spring back and forth until it reaches its resting position. Because the anemometers moved with the stems or branches to which they were attached, and sometimes independently of them (MH, pers. observation), they may have recorded apparent winds generated by this motion. When anemometer movement opposed the actual wind direction, apparent wind speeds could exceed actual wind speeds (Appendix 1: Figure S1; Video S1 and Video S1 Metadata).

This distinction is biologically relevant because epiphytes growing on moving substrates will experience some component of the same apparent wind. The magnitude of this movement varies with tree and attachment height, architecture, foliage (or lack thereof), epiphyte load, neighbouring trees, and, naturally, wind intensity (Einzmann et al., 2022; Jackson et al., 2021; Mayer, 1987; Rudnicki et al., 2001). Epiphytes near the stem base should experience weaker apparent winds than those growing in crowns, where sway is greater (Einzmann et al., 2022). Reported sway amplitudes range from centimetres to metres (Gardiner, 1995; Jackson et al., 2021), and branch velocities can reach approximately 6 m s^{-1} (Milne, 1991), although absolute speeds have rarely been quantified. Such apparent turbulence may trigger diaspore release even under relatively weak winds, perhaps more effectively than strong but laminar airflow (Niklas, 1992). Dynamic diaspore release under wind loading is a recurring theme in dispersal biology (Cousens et al., 2008; Murray, 1986; Salisbury, 1942) that, despite its importance for dispersal, remains poorly investigated. Thus, while apparent winds and possible contact artefacts may not fully explain all recorded extreme gusts, they highlight the need to consider substrate motion and apparent wind in dispersal models, because true wind alone may not adequately represent the aerodynamic conditions governing dispersal within forest canopies.

EpiDisp 1.0 incorporates apparent winds as epiphytes might experience them, but like other trajectory models, it relies on several simplifying assumptions. First, the model assumes that the abscission threshold equals the terminal velocity of diaspores, although gravity alone might sometimes suffice for abscission. The threshold may also decrease as diaspores mature or with changing environmental conditions, such as updrafts or a drop in relative humidity, whereas wet diaspores may not abscise at all (e.g., Cousens et al., 2008; Greene & Quesada, 2011). Incorporating a dynamic abscission threshold in future versions of *EpiDisp 1.0* or similar models

could improve model accuracy, but experimental work is needed to quantify and parameterize such thresholds.

Similarly, V_{term} is treated as constant, despite evidence that it can change under different environmental conditions. Diaspores may change shape when exposed to high humidity, thereby altering drag, lift forces, and ultimately V_{term} (e.g., Lee & Yoon, 2025; Seale et al., 2022). The model also assumes single-seed dispersal, although diaspores may disperse in clusters, as seen in orchids (Zotz et al., 2016) and bromeliads (MH, pers. observation). Such clustering may increase terminal velocity and, ultimately, dispersal success, although the range of terminal velocities modelled by *EpiDisp 1.0* may have covered at least some of these events.

Interception probability was also simplified. It was based on mean plant area density, which cannot fully capture the complex vertical stratification and heterogeneity of forests (Lee & Yoon, 2025). Although this structure was not represented explicitly in the interception term, it was included indirectly through wind speeds, which reflect local forest structure. We also ignored particle trapping: slow-falling diaspores, such as fern spores or orchid dust seeds, may remain trapped within an eddy for longer periods (Heydel et al., 2014; Horn et al., 2001; Nathan, Katul et al., 2011), potentially reducing interception likelihood. Finally, the model only accounts for primary dispersal, even though diaspores may later be uplifted by wind (and other agents) once more. In some cases, this would resemble release from a corresponding height already simulated by *EpiDisp 1.0*. Future work should therefore assess movement after first surface interception and may require dedicated secondary dispersal models that incorporate additional vectors such as water or animals.

Addressing these limitations would enhance the predictive power of future dispersal models. Priorities include higher-resolution wind measurements, improved quantification of apparent

winds and substrate motion, more detailed forest-structure data, dynamic abscission thresholds, environmental effects on V_{term}, multi-seed dispersal, eddy dynamics, and secondary dispersal. An especially informative empirical research direction would be to test whether epiphyte morphology or substrate movement enhances diaspore abscission through locally generated turbulence.

Given the spatial and temporal complexity of forests, *EpiDisp 1.0* represents an important step towards a realistic approximation of within-canopy (epiphyte) dispersal. Unlike models relying on derived rather than measured wind data, it incorporates empirical within-canopy airflow, an abscission threshold, interception on both horizontal and vertical surfaces, and explicit effects of release height and terminal velocity. This is particularly relevant given the scarcity of mechanistic within-canopy dispersal models. Future work should validate model predictions through empirical approaches, such as trap-based dispersal studies (Mondragón & Calvo-Irabién, 2006) or wind-tunnel experiments (Bennett, 1988), and test whether the framework can be extended to other wind-dispersed canopy guilds, such as trees, lianas, understorey plants, ***as well as*** pollen or fungal spores.

Conclusion

Epiphytes occupy the entire height gradient of many tropical forests, showing they have overcome the first major challenge of their life cycle: their diaspores landing on a suitable aboveground substrate. Yet this crucial aspect of their life history has remained poorly understood. Using a simulative trajectory model based on the wind conditions that epiphytes experience inside a tropical forest, this study provides evidence that dispersal limitation is high at a per-diaspore level: the probability of settling on suitable substrate is relatively low, and successful dispersal occurs mostly within a few meters of release. However, high fecundity

strongly reduces the degree of dispersal limitation at the community level. Our study therefore provides a mechanistic explanation for how dispersal contributes to patchy or vertically stratified epiphyte distributions, while also showing that they cannot be explained by dispersal alone. Overall, our study is a major advance in understanding epiphyte dispersal and within-canopy dispersal more broadly. By integrating tree-scale wind data into a mechanistic trajectory model, it provides a framework for studying dispersal in complex, vertically structured environments. Beyond epiphytes, similar approaches could be applied to other wind-dispersed organisms, including pollen, fungal spores (whether beneficial like mycorrhizae or harmful like those responsible for forest diseases such as ash dieback), understorey herbs, lianas, wind-dispersed trees, invasive plants, and ballooning arthropods. Such models could help inform conservation strategies aimed at improving habitat connectivity through corridors, isolated trees, or stepping-stone habitats that facilitate pollen-mediated gene flow and diaspore dispersal. Our study therefore opens new opportunities to understand how organisms overcome spatial barriers and how dispersal processes shape forest communities.

Acknowledgements

We are grateful to the Republic of Panama for making its fascinating nature available for research; the Deutsche Forschungsgemeinschaft (DFG), who funded it (grant number ZO 94/13–1); STRI for long-term financial support by the ESP program and for making the San Lorenzo field station (9.28°, –79.97°) available to us; STRI ForestGeo for funding and collecting the airborne Lidar data and Helene Muller-Landau, STRI, for forwarding it for the use in this study. Some of the data analyses as well as the diaspore dispersal model were performed using the HPC Cluster ROSA, located at the University of Oldenburg (Germany), which is funded by the DFG through its Major Research Instrumentation Programme (INST 184/225–1 FUGG) and the

Ministry of Science and Culture (MWK) of the Lower Saxony State—and in this context, we thank Christoph Nehrke, Oldenburg, for de-mystifying the HPC Cluster to us. Microsoft Copilot (Microsoft, 2024) was used to generate the silhouette graphic included in some of the figures. We are grateful to Vicky Tough for her teachings that went beyond mere rope-access to trees; Lourdes Vargas for consistently coordinating the use of the crane, and Edwin Andrade for safely manoeuvring us through and informing us on his trees; Anel Santamaria and Antonio Gonzalez, for the assistance and safeguarding on site; and, last but not least, Helena Einzmann, Mateo Fernández-Lucero, Erik Janner, and Jessica Tay for their indispensable help, company, and moral support during the fieldwork.

Author contributions

Marie Hoensbroech and Gerhard Zotz conceived and designed the study. Marie Hoensbroech collected the wind data, conducted the analyses, and wrote the dispersal model with input from Juliano Sarmento Cabral. Marie Hoensbroech wrote the first draft, and all authors subsequently revised the manuscript.

Conflict of Interest Statement

The authors declare no conflicts of interest.

References

Abdoli, M., K. Lapo, J. Schneider, J. Olesch, and C. K. Thomas. 2023. “Toward Quantifying Turbulent Vertical Airflow and Sensible Heat Flux in Tall Forest Canopies Using Fiber-Optic Distributed Temperature Sensing.” *Atmospheric Measurement Techniques* 16: 809–24. https://doi.org/10.5194/amt-16-809-2023.

Ackerman, J. D., A. Sabat, and J. K. Zimmerman. 1996. “Seedling Establishment in an Epiphytic Orchid: An Experimental Study of Seed Limitation.” *Oecologia* 106: 192–8.

Agostinelli, C., and U. Lund. 2025. “R Package circular: Circular Statistics.” R Package Version 0.5-2. https://CRAN.R-project.org/package=circular.

Almeida, D., S. C. Stark, C. A. Silva, C. Hamamura, and R. Valbuena. 2021. “leafR: Calculates the Leaf Area Index (LAD) and Other Related Functions.” R Package Version 0.3.5. https://CRAN.R-project.org/package=leafR.

Anfossi, D., D. Oettl, G. Degrazia, and A. Goulart. 2005. “An Analysis of Sonic Anemometer Observations in Low Wind Speed Conditions.” *Boundary-Layer Meteorology* 114: 179–203. https://doi.org/10.1007/S10546-004-1984-4.

Aphalo, P. J. 2025. “ggpmisc: Miscellaneous Extensions to ‘ggplot2’.” R Package Version 0.6.2. https://CRAN.R-project.org/package=ggpmisc.

Arditti, J., and A. K. A. Ghani. 2000. “Tansley Review No. 110. Numerical and Physical Properties of Orchid Seeds and Their Biological Implications.” *New Phytologist* 145(3): 367–421. https://doi.org/10.1046/j.1469-8137.2000.00587.x.

Augspurger, C. 2024. *Seed Dispersal by Wind.* Washington DC: Smithsonian Institution Scholarly Press. https://doi.org/10.5479/si.26880697.

Augspurger, C. K., and S. E. Franson. 1988. “Input of Wind-Dispersed Seeds into Light-Gaps and Forest Sites in a Neotropical Forest.” *Journal of Tropical Ecology* 4(3): 239–52. https://doi.org/10.1017/S0266467400002807.

Barrett, T., M. Dowle, A. Srinivasan, J. Gorecki, M. Chirico, T. Hocking, B. Schwendinger, and I. Krylov. 2025. “data.Table: Extension of ‘data.frame’.” R Package Version 1.17.8. https://CRAN.R-project.org/package=data.table.

Barrington, D. S. 1993. “Ecological and Historical Factors in Fern Biogeography.” *Journal of Biogeography*. 20(3): 275–79. https://doi.org/10.2307/2845635.

Bennett, B. C. 1988. “A Comparison of Life History Traits in Selected Epiphytic and Saxicolous Species of *Tillandsia* (Bromeliaceae) from Florida and Peru.” PhD diss., University of North Carolina.

Benzing, D. H. 1990. *Vascular Epiphytes: General Biology and Related Biota.* Cambridge: Cambridge University Press.

Bivand, R., E. Pebesma, and V. Gomez-Rubio. 2013. *Applied Spatial Data Analysis with R*, 2nd ed. New York: Springer.

Bohrer, G., G. G. Katul, R. Nathan, R. L. Walko, and R. Avissar. 2008. “Effects of Canopy Heterogeneity, Seed Abscission and Inertia on Wind-Driven Dispersal Kernels of Tree Seeds.” *Journal of Ecology* 96(4): 569–80. https://doi.org/10.1111/j.1365-2745.2008.01368.x.

1268 Brunet, Y. 2020. “Turbulent Flow in Plant Canopies: Historical Perspective and Overview.”
1269 *Boundary-Layer Meteorology* 177: 315–64. https://doi.org/10.1007/S10546-020-00560-7.

1270 Bürkner, P.-C. 2017. “Brms: An R Package for Bayesian Multilevel Models Using Stan.” *Journal*
1271 *of Statistical Software* 80:1–28. https://doi.org/10.18637/jss.v080.i01.

1272 Cascante-Marín, A., J. H. D. Wolf, J. G. B. Oostermeijer, and J. C. M. Den Nijs. 2008.
1273 “Establishment of Epiphytic Bromeliads in Successional Tropical Premontane Forests in Costa
1274 Rica.” *Biotropica* 40(4): 441–48. https://doi.org/10.1111/j.1744-7429.2008.00403.x.

1275 Cascante-Marín, A., N. von Meijenfeldt, H. M. H. de Leeuw, J. H. D. Wolf, J. G. B. Oostermeijer,
1276 and J. C. M. den Nijs. 2009. “Dispersal Limitation in Epiphytic Bromeliad Communities in a
1277 Costa Rican Fragmented Montane Landscape.” *Journal of Tropical Ecology* 25(1): 63–73.
1278 https://doi.org/10.1017/S0266467408005622.

1279 Chilpa-Galván, N., J. Márquez-Guzmán, G. Zotz, I. Echevarría-Machado, J. L. Andrade, C.
1280 Espadas-Manrique, and C. Reyes-García. 2018. “Seed Traits Favouring Dispersal and
1281 Establishment of Six Epiphytic *Tillandsia* (Bromeliaceae) Species.” *Seed Science Research*
1282 28(4): 349–59. https://doi.org/10.1017/S0960258518000247.

1283 Clark, J. S., M. Silman, R. Kern, E. Macklin, and J. HilleRisLambers. 1999. “Seed Dispersal near
1284 and far: Patterns across Temperate and Tropical Forests.” Ecology 80(5): 1475–94.
1285 https://doi.org/10.1890/0012-9658(1999)080[1475:sdnafp]2.0.co;2.

1286 CloudCompare. 2023. *CloudCompare Version 2.13*. http://www.cloudcompare.org/.

1287 Cousens, R., C. Dytham, and R. Law. 2008. *Dispersal in Plants: A Population Perspective.* Oxford:
1288 Oxford University Press.

1289 Costa, R., N. Macías-Hernández, F. Rigal, P. A. V. Borges, and P. Cardoso. 2025. “Do Island
1290 Spiders Descend From Trees? – A Tale of Island Colonisation and Niche Expansion.” *Journal*
1291 *of Biogeography* 52: e70093. https://doi.org/10.1111/jbi.70093.

1292 Croat, T. B. 1978. *Flora of Barro Colorado Island.* Sanford: Stanford University Press.

1293 Dias-Júnior, C. Q., L. D. A. Sá, E. P. Marques Filho, R. A. Santana, M. Mauder, and A. O. Manzi.
1294 2017. “Turbulence Regimes in the Stable Boundary Layer above and within the Amazon
1295 Forest.” *Agricultural and Forestry Meteorology* 233: 122–32.
1296 https://doi.org/10.1016/j.agrformet.2016.11.001.

1297 Dislich, R., and W. Mantovani. 2016. “Vascular Epiphyte Assemblages in a Brazilian Atlantic
1298 Forest Fragment: Investigating the Effect of Host Tree Features.” *Plant Ecology* 217: 1–12.
1299 https://doi.org/10.1007/S11258-015-0553-X.

1300 Einzmann, H. J. R., and G. Zotz. 2017a. “Dispersal and Establishment of Vascular Epiphytes in
1301 Human-Modified Landscapes.” *AoB Plants* 9(6): plx052.
1302 https://doi.org/10.1093/aobpla/plx052.

1303 Einzmann, H. J. R., and G. Zotz. 2017b. “No Signs of Saturation: Long-Term Dynamics of
1304 Vascular Epiphyte Communities in a Human-Modified Landscape.” *Biodiversity and*
1305 *Conservation* 26: 1393–410. https://doi.org/10.1007/s10531-017-1306-z.

Einzmann, H. J. R., G. Zotz, and J. Y. L. Tay. 2022. “What Happens to Epiphytic Bromeliads in a Windy Spot?” *Journal of Tropical Ecology* 38: 158–63. https://doi.org/10.1017/S0266467422000037.

Esri Inc. 2024. *ArcGIS Pro Version 3.4.3*. https://www.arcgis.com.

Finnigan, J. 2000. “Turbulence in Plant Canopies.” *Annual Review of Fluid Mechanics* 32: 519–71. https://doi.org/10.1146/annurev.fluid.32.1.519.

Francisco, T. M., D. R. Couto, M. L. Garbin, F. Misaki, and C. R. Ruiz-Miranda. 2021. “Role of Spatial and Environmental Factors in Structuring Vascular Epiphyte Communities in Two Neotropical Ecosystems.” *Perspectives in Plant Ecology, Evolution and Systematics* 51: 125621. https://doi.org/10.1016/J.PPEES.2021.125621.

Froelich, N. J., H. P. Schmid, C. S. B. Grimmond, H.-B. Su, and A. J. Oliphant. 2005. “Flow Divergence and Density Flows above and below a Deciduous Forest: Part I. Non-Zero Mean Vertical Wind above Canopy.” *Agricultural and Forestry Meteorology* 133(1–4): 140–52. https://doi.org/10.1016/j.agrformet.2005.09.005.

Gandawijaja, D., and J. Arditti. 1983. “The Orchids of Krakatau: Evidence for a Mode of Transport.” *Annals of Botany* 52(2): 127–30. https://doi.org/10.1093/oxfordjournals.aob.a086558.

García-Franco, J. G., and V. Rico-Gray. 1988. “Experiments on Seed Dispersal and Deposition Patterns of Epiphytes–The Case of *Tillandsia deppeana* Steudel (Bromeliaceae).” *Phytologia* 65: 73–8.

Gardiner, B. A. 1995. “The Interactions of Wind and Tree Movement in Forest Canopies.” In *Wind and Trees*, edited by M. P. Coutts and J. Grace, 41–59. Cambridge: Cambridge University Press.

Garnier, S., N. Ross, R. Rudis, A. P. Camargo, M. Sciaini, and C. Scherer. 2024. “viridis(Lite)–Colorblind-Friendly Color Maps for R.” R Package Version 0.6.5. https://github.com/sjmgarnier/viridis.

Gegzna, V. 2020. “biostat: Routines for Basic (Bio)Statistics.” R Package Version 0.0.20. https://github.com/gegznav/biostat/.

Givnish, T. J., M. H. J. Barfuss, B. Van Ee, R. Riina, K. Schulte, R. Horres, P. A. Gonsiska, et al. 2014. “Adaptive Radiation, Correlated and Contingent Evolution, and Net Species Diversification in Bromeliaceae.” *Molecular Phylogenetics and Evolution* 71: 55–78. https://doi.org/10.1016/j.ympev.2013.10.010.

Givnish, T. J., D. Spalink, M. Ames, S. P. Lyon, S. J. Hunter, A. Zuluaga, A. Doucette, et al. 2016. “Orchid Historical Biogeography, Diversification, Antarctica and the Paradox of Orchid Dispersal.” *Journal of Biogeography* 43(10): 1905–16. https://doi.org/10.1111/jbi.12854.

Gòmez Noguez, F., and C. Flores Galván. 2019. “Ferns in the Air.” *Bulletin of the American Fern Society* 46: 1–6.

Greene, D. F., and E. A. Johnson. 1996. “Wind Dispersal of Seeds from a Forest into a Clearing.“ *Ecology* 77(2): 595–609. https://doi.org/10.2307/2265633.

1345 Greene, D. F., and M. Quesada. 2011. “The Differential Effect of Updrafts, Downdrafts and
1346 Horizontal Winds on the Seed Abscission of *Tragopogon dubius*.” *Functional Ecology* 25(3):
1347 468–72. https://doi.org/10.1111/j.1365-2435.2010.01788.x.

1348 Harper, J. L., J. N. Clatworthy, I. H. McNaughton, and G. R. Sagar. 1961. “The Evolution and
1349 Ecology of Closely Related Species Living in the Same Area.” *Evolution* 15(2): 209–27.
1350 https://doi.org/10.1111/j.1558-5646.1961.tb03144.x.

1351 Heydel, F., S. Cunze, M. Bernhardt-Römermann, and O. Tackenberg. 2014. “Long-Distance Seed
1352 Dispersal by Wind: Disentangling the Effects of Species Traits, Vegetation Types, Vertical
1353 Turbulence and Wind Speed.” *Ecological Research* 29(4): 641–51.
1354 https://doi.org/10.1007/s11284-014-1142-5.

1355 Hijmans, R. J. 2025. “terra: Spatial Data Analysis.” R Package Version 1.8-80. https://CRAN.R-
1356 project.org/package=terra.

1357 Hijmans, R. J. 2025. ”raster: Geographic Data Analysis and Modeling.” R Package Version 3.6–32.
1358 https://doi.org/10.32614/CRAN.package.raster.

1359 Horn, H. S., R. A. N. Nathan, and S. R. Kaplan. 2001. “Long-Distance Dispersal of Tree Seeds by
1360 Wind.” *Ecological Research* 16(5): 877–85. https://doi.org/10.1046/J.1440-
1361 1703.2001.00456.X.

1362 Horn, S., A. Raabe, H. Will, and O. Tackenberg. 2012. “TurbSeed–A Model for Wind Dispersal of
1363 Seeds in Turbulent Currents Based on Publicly Available Climate Data.” *Ecological*
1364 *Modelling* 237–238: 1–10. https://doi.org/10.1016/J.ECOLMODEL.2012.04.009.

Inkscape's Contributors. 2023. *The Inkscape Project Version 1.3.2*. https://inkscape.org.

Jackson, T. D., S. Sethi, E. Dellwik, N. Angelou, A. Bunce, T. van Emmerik, M. Duperat, et al. 2021. "The Motion of Trees in the Wind: A Data Synthesis." *Biogeosciences* 18(13): 4059–72. https://doi.org/10.5194/BG-18-4059-2021.

Kalacska, M., J. C. Calvo-Alvarado, and G. A. Sanchez-Azofeifa. 2005. "Calibration and Assessment of Seasonal Changes in Leaf Area Index of a Tropical Dry Forest in Different Stages of Succession." *Tree Physiology* 25(6): 733–44. https://doi.org/10.1093/treephys/25.6.733.

Kassambara, A. 2025. "rstatix: Pipe-Friendly Framework for Basic Statistical Tests." R Package Version 0.7.3. https://cran.r-project.org/package=rstatix.

Kelly, D. L. 1985. "Epiphytes and Climbers of a Jamaican Rain Forest: Vertical Distribution, Life Forms and Life Histories." *Journal of Biogeography* 12(3): 223–41. https://doi.org/10.2307/2844997.

Kelly, D. L., G. O'Donovan, J. Feehan, S. Murphy, S. O. Drangeid, and L. Marcano-Berti. 2004. "The Epiphyte Communities of a Montane Rain Forest in the Andes of Venezuela: Patterns in the Distribution of the Flora." *Journal of Tropical Ecology* 20(6): 643–66. https://doi.org/10.1017/S0266467404001671.

Kessler, M. 2002. "Environmental Patterns and Ecological Correlates of Range Size among Bromeliad Communities of Andean Forests in Bolivia." *The Botanical Review* 68: 100–27. https://doi.org/10.1663/0006-8101(2002)068[0100:EPAECO]2.0.CO;2.

Komsta, L., and F. Novomestky. 2022. “moments: Moments, Cumulants, Skewness, Kurtosis and Related Tests.” R Package Version 0.14.1. https://CRAN.R-project.org/package=moments.

Krömer, T., M. Kessler, and S. R. Gradstein. 2007. “Vertical Stratification of Vascular Epiphytes in Submontane and Montane Forest of the Bolivian Andes: The Importance of the Understory.” *Plant Ecology* 189: 261–78. https://doi.org/10.1007/s11258-006-9182-8.

Kruijt, B., Y. Malhi, J. Lloyd, A. D. Norbre, A. C. Miranda, M. G. P. Pereira, A. Culf, and J. Grace. 2000. “Turbulence Statistics above and within Two Amazon Rain Forest Canopies.” *Boundary-Layer Meteorology* 94: 297–331. https://doi.org/10.1023/A:1002401829007.

Ladino, G., F. Ospina-Bautista, J. Estévez Varón, L. Jerabkova, and P. Kratina. 2019. “Ecosystem Services Provided by Bromeliad Plants: A Systematic Review.” *Ecology and Evolution* 9(12): 7360–72. https://doi.org/10.1002/ECE3.5296.

Lee, S., and T. K. Yoon. 2025. “Why Are Seed Dispersal Models Rarely Used? Limitations of Scalability and Improvement Measures.” *Forests* 16(5): 851. https://doi.org/10.3390/f16050851.

Madison, M. 1977. “Vascular Epiphytes: Their Systematic Occurrence and Salient Features.” *Selbyana* 2: 1–13.

Mac Nally, R., and C. J. Walsh. 2004. “Hierarchical Partitioning Public-Domain Software.” *Biodiversity and Conservation* 13: 659–60. https://doi.org/10.1023/B:BIOC.0000009515.11717.0b.

Mansfield, J. W., N. Galambos, and R. Saville. 2018. “The Use of Ascospores of the Dieback Fungus *Hymenoscyphus fraxineus* for Infection Assays Reveals a Significant Period of Biotrophic Interaction in Penetrated Ash Cells.” *Plant Pathology* 67: 1354–61. https://doi.org/10.1111/ppa.12844.

Maurer, K. D., G. Bohrer, D. Medvigy, and S. J. Wright. 2013. “The Timing of Abscission Affects Dispersal Distance in a Wind-Dispersed Tropical Tree.” *Functional Ecology* 27(1): 208–18. https://doi.org/10.1111/1365-2435.12028.

Mayer, H. 1987. “Wind-Induced Tree Sways.” *Trees* 1: 195–206. https://doi.org/10.1007/BF01816816.

Mendieta-Leiva, G., H. L. Buckley, and G. Zotz. 2022. “Directional Changes over Time in the Species Composition of Tropical Vascular Epiphyte Assemblages.” *Journal of Ecology* 110(3): 553–68. https://doi.org/10.1111/1365-2745.13817.

Mendieta-Leiva, G., K. Wagner, and G. Zotz. 2021. “Vascular Epiphyte Census Data at the San Lorenzo Crane Plot [dataset].” *Zenodo.* https://doi.org/10.5281/zenodo.5645775.

Microsoft. 2024. *Microsoft 365 tools*. https://microsoft.com/microsoft-365.

Milne, R. 1991. “Dynamics of Swaying of *Picea sitchensis*.” *Tree Physiology* 9(3): 383–99. https://doi.org/10.1093/TREEPHYS/9.3.383.

Mondragón, D., and L. M. Calvo-Irabién. 2006. “Seed Dispersal and Germination of the Epiphyte *Tillandsia brachycaulos* (Bromeliaceae) in a Tropical Dry Forest, Mexico.” *The Southwestern Naturalist.* 51(4): 462–70. https://www.jstor.org/stable/20424755.

1424 Mondragón, D., T. Valverde, and M. Hernández-Apolinar. 2015. “Population Ecology of Epiphytic
1425 Angiosperms: A Review.” *Tropical Ecology* 56(1): 1–39.
1426 https://doi.org/10.13140/2.1.4043.5849.

1427 Muller-Landau, H. C., S. J. Wright, O. Calderón, R. Condit, and S. P. Hubbell. 2008. “Interspecific
1428 Variation in Primary Seed Dispersal in a Tropical Forest.” *Journal of Ecology* 96(4): 653–67.
1429 https://doi.org/10.1111/J.1365-2745.2008.01399.X.

1430 Münzbergová, Z., and T. Herben. 2005. “Seed, Dispersal, Microsite, Habitat and Recruitment
1431 Limitation: Identification of Terms and Concepts in Studies of Limitations.” *Oecologia* 145:
1432 1–8. https://doi.org/10.1007/s00442-005-0052-1.

1433 Murray, D. R. 1986. *Seed Dispersal*. Sydney: Academic Press.

1434 Murray, K., and M. M. Conner. 2009. “Methods to Quantify Variable Importance: Implications for
1435 the Analysis of Noisy Ecological Data.” *Ecology* 90(2): 348-55. https://doi.org/10.1890/07-
1436 1929.1.

1437 Nathan, R., H. S. Horn, J. Chave, and S. A. Levin. 2002. “Mechanistic Models for Tree Seed
1438 Dispersal by Wind in Dense Forests and Open Landscapes.” In *Seed Dispersal and Frugivory:*
1439 *Ecology, Evolution and Conservation*, edited by D. J. Levey, W. R. Silva, and M. Galetti, 69–
1440 82. Wallingford: CAB International.

1441 Nathan, R., N. Horvitz, Y. He, A. Kuparinen, F. M. Schurr, and G. G. Katul. 2011. “Spread of
1442 North American Wind-Dispersed Trees in Future Environments.” *Ecology Letters* 14(3): 211–
1443 19. https://doi.org/10.1111/J.1461-0248.2010.01573.X.

Nathan, R., G. G. Katul, G. Bohrer, A. Kuparinen, M. B. Soons, S. E. Thomson, A. Trakhtenbrot, and H. S. Horn. 2011. “Mechanistic Models of Seed Dispersal by Wind.” *Theoretical Ecology* 4: 113–32. https://doi.org/10.1007/s12080-011-0115-3.

Nathan, R., and H. C. Muller-Landau. 2000. “Spatial Patterns of Seed Dispersal, their Determinants and Consequences for Recruitment.” *Trends in Ecology & Evolution* 15(7): 278–85. https://doi.org/10.1016/S0169-5347(00)01874-7.

Neuwierth, E. 2022. “RColorBrewer: ColorBrewer Palettes.” R Package Version 1.1–3. https://CRAN.R-project.org/package=RColorBrewer.

Nieder, J., and G. Zotz. 1998. “Methods of Analyzing the Structure and Dynamics of Vascular Epiphyte Communities.” *Ecotropica* 4: 33–9.

Niklas, K. J. 1992. *Plant Biomechanics: An Engineering Approach to Plant Form and Function.* Chicago: University of Chicago Press.

Norros, V., Ü. Rannik, T. Hussein, T. Petäjä, T. Vesala, and O. Ovaskainen. 2014. “Do Small Spores Disperse Further than Large Spores?” *Ecology* 95(6): 1612–21. https://doi.org/10.1890/13-0877.1.

Olivas, P. C., S. F. Oberbauer, D. B. Clark, D. A. Clark, M. G. Ryan, J. J. O’Brien, and H. Ordoñez. 2013. “Comparison of Direct and Indirect Methods for Assessing Leaf Area Index Across a Tropical Rain Forest Landscape.” *Agricultural and Forest Meteorology* 177: 110–6. https://doi.org/10.1016/j.agrformet.2013.04.010.

Onset Computer Corporation. 2022. *HOBOware Version 3.7.26.* https://www.onsetcomp.com/products/software/hoboware.

Paggi, G. M., J. A. T. Sampaio, M. Bruxel, C. Martini Zanella, M. Göetze, M. Valli Büttow, C. Palma-Silva, and F. Bered. 2010. “Seed Dispersal and Population Structure in *Vriesea gigantea*, a Bromeliad from the Brazilian Atlantic Rainforest.” *Botanical Journal of the Linnean Society* 164: 317–25. https://doi.org/10.1111/j.1095-8339.2010.01088.x.

Partomihardjo, T. 2003. “Colonisation of Orchids on the Krakatau Islands.” *Telopea* 10(1): 299–310. https://doi.org/10.7751/TELOPEA20035620.

Paton, S. 2019a. “Galeta–Wind Direction [dataset]." *Smithsonian Tropical Research Institute.* https://doi.org/10.25573/data.10042640.v25.

Paton, S. 2019b. “Galeta–Wind Speed [dataset].” *Smithsonian Tropical Research Institute.* https://doi.org/10.25573/data.10042658.v23.

Paton, S. 2019c. “San Lorenzo Crane–Wind Speed [dataset].” *Smithsonian Tropical Research Institute.* https://doi.org/10.25573/data.10042688.v23.

Paton, S. 2019d. “San Lorenzo Crane–Wind direction [dataset].” *Smithsonian Tropical Research Institute.* https://doi.org/10.25573/data.10042718.v23.

Paton, S. 2019e. “San Lorenzo Crane–Air Temperature [dataset].” *Smithsonian Tropical Research Institute*. https://doi.org/10.25573/data.10042694.v23.

Paton, S. 2019f. “San Lorenzo Crane–Precipitation [dataset].” *Smithsonian Tropical Research Institute*. https://doi.org/10.25573/data.10042679.v23.

Paton, S. 2020. “Yearly Reports–San Lorenzo Crane [dataset].” *Smithsonian Tropical Research Institute*. https://doi.org/10.25573/data.11799309.v6.

Pebesma, E. 2018. “Simple Features for R: Standardized Support for Spatial Vector Data.” *The R Journal* 10: 439–46. https://doi.org/10.32614/RJ-2018-009.

Pedersen, T. L. 2025. “patchwork: The Composer of Plots.” R Package Version 1.3.2. https://CRAN.R-project.org/package=patchwork.

Petter, G., K. Wagner, W. Wanek, E. J. Sánchez Delgado, G. Zotz, J. S. Cabral, and H. Kreft. 2016. “Functional Leaf Traits of Vascular Epiphytes: Vertical Trends within the Forest, Intra-and Interspecific Trait Variability, and Taxonomic Signals.” *Functional Ecology* 30(2): 188–98. https://doi.org/10.1111/1365-2435.12490.

Petter, G., G. Zotz, H. Kreft, and J. S. Cabral. 2021. “Agent-Based Modeling of the Effects of Forest Dynamics, Selective Logging, and Fragment Size on Epiphyte Communities.” *Ecology and Evolution* 11(6): 2937–51. https://doi.org/10.1002/ece3.7255.

Pittendrigh, C. S. 1948. “The Bromeliad-*Anopheles*-Malaria Complex in Trinidad. I–The Bromeliad Flora.” *Evolution* 2(1): 58–89. https://doi.org/10.1111/j.1558-5646.1948.tb02732.x.

Pohlert, T. 2024. “PMCMRplus: Calculate Pairwise Multiple Comparisons of Mean Rank Sums.” R Package Version 1.9.12. https://CRAN.R-project.org/package=PMCMRplus.

Pounden, E., D. F. Greene, M. Quesada, and J. M. Contreras Sánchez. 2008. “The effect of collisions with vegetation elements on the dispersal of winged and plumed seeds.” *Journal of Ecology* 96: 591-8. https://doi.org/10.1111/j.1365-2745.2008.01380.x.

Proença-Ferreira, A., L. Borda-de-Água, M. Porto, F. Moreira, A. Mira, and R. Pita. 2025. “dispfit: Fit Distributions to Species Dispersal Data.” R Package Version 0.1.0. https://github.com/apferreira/dispfit.

Qin, X., W. Liang, M. Liu, Z. Xin, Z. Wang, Q. Zhou, L. Tian, L. Zong, J. Zhu, and Z. Liu. 2025. “Effects of Plant Crown Characteristics on Dispersal Kernels of Wind-Dispersed Seeds under Low Wind Speeds.” *Journal of Plant Ecology* 18(1): rtae106. https://doi.org/10.1093/jpe/rtae106.

Qin, X., W. Liang, Z. Liu, C. C. Baskin, J. M. Baskin, Z. Xin, Z. Wang, and Q. Zhou. 2022. “Plant Canopy May Promote Seed Dispersal by Wind.” *Scientific Reports* 12: 63. https://doi.org/10.1038/s41598-021-03402-9.

R Core Team. 2023. *R: A Language and Environment for Statistical Computing*. Vienna: R Foundation for Statistical Computing. https://www.R-project.org/.

Ramos, P., P. Villareal, and H. Muller-Landau. 2024. “Tree Height Allometry Data for 5109 Trees in Twenty-Four Small ForestGEO Plots in Panama, 2011–2020 [dataset].” *Smithsonian Tropical Research Institute*. https://doi.org/10.25573/data.24954204.v1.

Rodrigues, A., R. A. Sardinha, and G. Pita. 2021. “Exchange of Energy and Mass over Forest Canopies.” In *Fundamental Principles of Environmental Physics*, 105–32. Cham: Springer. https://doi.org/10.1007/978-3-030-69025-0_4.

Roth, W. E. 1986. *Stratification of a Tropical Forest as Seen in Dispersal Types*. Dordrecht: Springer Netherlands.

1523 Roussel, J.-R., D. Auty, N. C. Coops, P. Tompalski, T. R. H. Goodbody, A. Sánchez Meador, J.-F.
1524 Bourdon, F. de Boissieu, and A. Achim. 2020. “LidR: An R Package for Analysis of Airborne
1525 Laser Scanning (ALS) data.” *Remote Sensing of Environment* 251: 112061.
1526 https://doi.org/10.1016/j.rse.2020.112061.

1527 Rudnicki, M., U. Silins, V. J. Lieffers, and G. Josi. 2001. “Measure of Simultaneous Tree Sways
1528 and Estimation of Crown Interactions among a Group of Trees.” *Trees* 15: 83–90.
1529 https://doi.org/10.1007/s004680000080.

1530 Ruiz-Cordova, J. P., V. H. Toledo-Hernández, and A. Flores-Palacios. 2014. “The Effect of
1531 Substrate Abundance in the Vertical Stratification of Bromeliad Epiphytes in a Tropical Dry
1532 Forest (Mexico).” *Flora* 209: 375–84. https://doi.org/10.1016/J.FLORA.2014.06.003.

1533 Salisbury, E. 1942. *The Reproductive Capacity of Plants*. London: Bells and Sons.

1534 Santana, R. A., C. Q. Dias-Júnior, J. Tóta, J. D. Fuentes, R. S. Vale, E. G. Alves, R. M. N. dos
1535 Santos, and A. O. Manzi. 2018. “Air Turbulence Characteristics at Multiple Sites in and above
1536 the Amazon Rainforest Canopy.” *Agricultural and Forestry Meteorology* 260–261: 41–54.
1537 https://doi.org/10.1016/j.agrformet.2018.05.027.

1538 Schimper, A. 1908. *Pflanzen-Geographie auf physiologischer Grundlage*, 2nd ed. Jena: Gustav
1539 Fischer.

1540 Schimper, A. 1888. *Die epiphytische Vegetation Amerikas*. Jena: Gustav Fischer.

1541 Seale, M., O. Zhdanov, M. B. Soons, C. Cummins, E. Kroll, M. R. Blatt, H. Zare-Behtash, et al.
1542 2022. “Environmental Morphing Enables Informed Dispersal of the Dandelion Diaspore.”
1543 *eLife* 11: e81962. https://doi.org/10.7554/eLife.81962.

1544 Shaw, R. H. 1977. “Secondary Wind Speed Maxima inside Plant Canopies.” *Journal of Applied*
1545 *Meteorology* 16: 514–521. https://doi.org/10.1175/1520-
1546 0450(1977)016%3C0514:SWSMIP%3E2.0.CO;2.

1547 Soons, M. B., G. W. Heil, R. Nathan, and G. G. Katul. 2004. “Determinants of Long-Distance
1548 Dispersal by Wind in Grasslands.” *Ecology* 85(11): 3056–68. https://doi.org/10.1890/03-0522.

1549 Soons, M. B., and W. A. Ozinga. 2005. “How Important is Long-Distance Seed Dispersal for the
1550 Regional Survival of Plant Species?” *Diversity and Distributions* 11(2): 165–72.
1551 https://doi.org/10.1111/J.1366-9516.2005.00148.X.

1552 Spicer, M. E., and J. Ortega. 2023. “Source Height and Contact with Terrestrial Soil Drive
1553 Transplanted Epiphyte Performance.” *Journal of Ecology* 111(11): 2388–400.
1554 https://doi.org/10.1111/1365-2745.14187.

1555 Spicer, M. E., and C. L. Woods. 2022. “A Case for Studying Biotic Interactions in Epiphyte
1556 Ecology and Evolution.” *Perspectives in Plant Ecology, Evolution and Systematics* 54:
1557 125658. https://doi.org/10.1016/J.PPEES.2021.125658.

1558 Svahnström, V. J., E. N. Lughadha, F. Forest, and T. C. C. Leão. 2025. ”Geographic Range Size
1559 and Rarity of Epiphytic Flowering Plants.” *Nature Plants 11:* 1380–89.
1560 https://doi.org/10.1038/s41477-025-02022-9.

Tackenberg, O. 2003. “Modeling Long-Distance Dispersal of Plant Diaspores by Wind.” *Ecological Monographs* 73(2): 173–89. https://doi.org/10.1890/0012-9615(2003)073[0173:MLDOPD]2.0.CO;2.

Tackenberg, O., P. Poschlod, and S. Kahmen. 2003. “Dandelion Seed Dispersal: The Horizontal Wind Speed Does Not Matter for Long-Distance Dispersal - It Is Updraft!” *Plant Biology* 5(5): 451–4. https://doi.org/10.1055/S-2003-44789.

Taylor, A., and K. Burns. 2015. “Plant Composition Patterns inside an Endemic Birds’ Nest Fern (*Asplenium goudeyi*) on Lord Howe Island: Effects of Fern Size, Fern Isolation and Plant Dispersal Abilities.” *Journal of Tropical Ecology* 31(5): 413–21. https://doi.org/10.1017/S0266467415000334.

Terborgh, J., P. Alvarez-Loayza, K. Dexter, F. Cornejo, and C. Carrasco. 2011. “Decomposing Dispersal Limitation: Limits on Fecundity or Seed Distribution?” *Journal of Ecology* 99: 935–44. https://dx.doi.org/10.1111/j.1365-2745.2011.01836.x.

Thomsen, M. S., A. H. Altieri, C. Angelini, M. J. Bishop, P. E. Gribben, G. Lear, Q. He, et al. 2018. “Secondary foundation species enhance biodiversity”. *Nature Ecology and Evolution* 2: 634–639. https://doi.org/10.1038/s41559-018-0487-5.

Toledo-Aceves, T., J. G. García-Franco, S. Landero Lozada, M. L. León Mateos, and K. MacMillan. 2012. “Germination and Seedling Survivorship of Three *Tillandsia* Species in the Cloud-Forest Canopy.” *Journal of Tropical Ecology* 28(4): 423–26. https://doi.org/10.1017/S0266467412000363.

Torres, E., M. L. Riofrío, and J. M. Iriondo. 2018. “Complex Fine-Scale Spatial Genetic Structure in *Epidendrum rhopalostele*: An Epiphytic Orchid”. *Heredity* 122: 458–67. https://doi.org/10.1038/s41437-018-0139-1.

Trapnell, D. W., J. L. Hamrick, C. D. Ishibashi, and T. R. Kartzinel. 2013. “Genetic Inference of Epiphytic Orchid Colonization; It May Only Take One.” *Molecular Ecology* 22(14): 3680–92. https://doi.org/10.1111/mec.12338.

Urbanek, S. 2025. “png: Read and Write PNG Images.” R Package Version 0.1-9. https://CRAN.R-project.org/package=png.

van der Molen, M. K., J. H. C. Gash, and J. A. Elbers. 2004. “Sonic Anemometer (co)sine Response and Flux Measurement: II. The Effect of Introducing an Angle of Attack Dependent Calibration.” *Agricultural and Forest Meteorology* 122(1–2): 95–109. https://doi.org/10.1016/J.AGRFORMET.2003.09.003.

van der Pijl, L. 1982. *Principles of Dispersal in Higher Plants*, 3rd ed. Berlin: Springer.

Vasquez V., M. Garcia, M. Hernandez, ForestGEO Smithsonian, and H. Muller-Landau. 2024. “Smithsonian ForestGEO San Lorenzo and Panama Small Plots Aerial Photogrammetry Orthomosaics, Digital Surface Models, Point Clouds and Raw Images for 2015–2024. [dataset]” *Smithsonian Research Data Repository*. https://doi.org/10.60635/C33W2K.

Vieira. E. M., and P. Izar. 1999. “Interactions Between Aroids and Arboreal Mammals in the Brazilian Atlantic Rainforest.” *Plant Ecology* 145: 75–82. https://doi.org/10.1023/A:1009859810148.

Wagner, K., W. Bogusch, and G. Zotz. 2013. “The Role of the Regeneration Niche for the Vertical Stratification of Vascular Epiphytes.” *Journal of Tropical Ecology* 29(4): 277–90. https://doi.org/10.1017/S0266467413000291.

Wickham, H. 2023. “modelr: Modelling Functions that Work with the Pipe.” R Package Version 0.1.11. https://doi.org/10.32614/CRAN.package.modelr.

Wickham, H., M. Averick, J. Bryan, W. Chang, L. D’Agostino McGowan, R. François, G. Grolemund, et al. 2019. “Welcome to the Tidyverse.” *Journal of Open Source Software* 4(43): 1686. https://doi.org/10.21105/joss.01686.

Wickham, H., T. Pedersen, and D. Seidel. 2025. “scales: Scale Functions for Visualisation.” R Package Version 1.4.0. https://CRAN.R-project.org/package=scales.

Wilke, C. O., and B. M. Wiernik. 2022. “ggtext: Improved Text Rendering Support for ‘ggplot2’.” R Package Version 0.1.2. https://CRAN.R-project.org/package=ggtext.

Winkler, M., K. Hülber, and P. Hietz. 2009. “Population Dynamics of Epiphytic Orchids in a Metapopulation Context.” *Annals of Botany* 104(5): 995–1004. https://doi.org/10.1093/AOB/MCP188.

POWO. 2026. Plants of the World Online. Facilitated by the Royal Botanic Gardens, Kew. Published on the Internet; https://powo.science.kew.org/. (accessed 29 June 2026)

Retrieved 01 July 2026."Wright, S. J., V. Horlyck. Y. Basset, H. Barrios, A. Bethancourt, S. A. Bohlman, G. S. Gilbert, et al. 2003. “Tropical Canopy Biology Program, Republic of Panama.” In *Studying Forest Canopies from above: The International Canopy Crane Network*

edited by Y. Basset, V. Horlyck, and S. J. Wright, 137–55. New York: United Nations Environmental Programme, Smithsonian Tropical Research Institute.

Wright, S. J., A. Trakhtenbrot, G. Bohrer, M. Detto, G. G. Katul, N. Horvitz, H. C. Muller-Landau, F. A. Jones, and R. Nathan. 2008. “Understanding Strategies for Seed Dispersal by Wind under Contrasting Atmospheric Conditions.” *Proceedings of the National Academy of Sciences USA* 105(49): 19084–9. https://doi.org/10.1073/pnas.0802697105.

Xu, S., M. Chen, T. Feng, L. Zhan, L. Zhou, and G. Yu. 2021. “Use Ggbreak to Effectively Utilize Plotting Space to Deal with Large Datasets and Outliers.” *Frontiers in Genetics* 12: 774846. https://doi.org/10.3389/fgene.2021.774846.

Zeng, P., and H. Takahashi. 2000. “A First-Order Closure Model for the Wind Flow within and above Vegetation Canopies.” *Agricultural and Forest Meteorology* 103(3): 301-13. https://doi.org/10.1016/S0168-1923(00)00133-7.

Zhu, J. J., X. F. Li, G. Yutaka, and M. Takeshi. 2004. “Wind Profiles in and over Trees.” *Journal of Forestry Research* 15: 305-12. https://doi.org/10.1007/BF02844959.

Zotz, G. 1997. “Substrate Use of Three Epiphytic Bromeliads.” *Ecography* 20(3): 264–70. https://doi.org/10.1111/J.1600-0587.1997.TB00370.X.

Zotz, G. 1998. “Demography of the Epiphytic Orchid, *Dimerandra emarginata*.” *Journal of Tropical Ecology* 14(6): 725–41. https://doi.org/10.1017/S0266467498000534.

Zotz, G. 2016. *Plants on Plants–The Biology of Vascular Epiphytes*. Cham: Springer.

1640 Zotz, G., and P. Hietz. 2001. “The Physiological Ecology of Vascular Epiphytes: Current
1641 Knowledge, Open Questions.” *Journal of Experimental Botany* 52(364): 2067–78.
1642 https://doi.org/10.1093/JEXBOT/52.364.2067.

1643 Zotz, G., P. Hietz, and H. J. R. Einzmann. 2021. “Functional Ecology of Vascular Epiphytes.”
1644 *Annual Plant Reviews Online* 4(4): 869–906. https://doi.org/10.1002/9781119312994.apr0777.

1645 Zotz, G., and S. Schultz. 2008. “The Vascular Epiphytes of a Lowland Forest in Panama—Species
1646 Composition and Spatial Structure.” *Plant Ecology* 195: 131–41.
1647 https://doi.org/10.1007/s11258-007-9310-0.

1648 Zotz, G., and B. Vollrath. 2003. “The Epiphyte Vegetation of the Palm *Socratea exorrhiza* -
1649 Correlations with Tree Size, Tree Age and Bryophyte Cover.” *Journal of Tropical Ecology*
1650 19(1): 81–90. https://doi.org/10.1017/S0266467403003092.

1651 Zotz, G., T. Weichgrebe, H. Happatz, and H. J. R. Einzmann. 2016. “Measuring the Terminal
1652 Velocity of Tiny Diaspores.” *Seed Science Research* 26(3): 222–30.
1653 https://doi.org/10.1017/S0960258516000155.

1654 Zotz, G., P. Weigelt, M. Kessler, H. Kreft, and A. Taylor. 2021. “EpiList 1.0: A Global Checklist of
1655 Vascular Epiphytes.” *Ecology* 102(6): e03326. https://doi.org/10.1002/ecy.3326.

Boxes

(none)

Tables

Table 1. Glossary of key terms used in this paper (in alphabetical order).

Term	Definition
Abscission	The point at which a diaspore detaches from the seed pod and dispersal begins.
Actual wind	The wind relative to the motionless surface of the earth.
Apparent wind	The wind an object in motion experiences.
Bark area density (*BAD*)	The bark area (unit^2) per forest volume (unit^3).
Diaspore	The plant reproductive unit that is dispersed, consisting of a seed or spore and any additional tissues or structures that facilitate dispersal.
Dispersal limitation	A continuous measure of how strongly dispersal constraints restrict a species from occupying its full theoretical niche, e.g., by limiting the distance or likelihood of reaching suitable sites.
Effective dispersal	Successful dispersal of a diaspore combined with subsequent success in germination and establishment.
Ejection	Gradual upward air motion.
Leaf area density (*LAD*)	The leaf area (unit^2) per forest volume (unit^3).
Long-distance dispersal (LDD)	The movement of a diaspore outside of the spatial limits of a stand and/or the genetic neighbourhood area of individuals.
Mean up/down-gust speed	The time average of either up-gusts or down-gusts occurring over a specified time interval.
Mean vertical gust speed	The time average of up- and down-gusts over a specified time interval, where up-gusts contribute positively and down-gusts negatively.
Plant area density (*PAD*)	Total plant area density constituting both leaf and wood components.
Primary dispersal	The first dispersal phase, in which a diaspore moves away from the parent plant immediately after release until its first deposition, as opposed to secondary dispersal, which refers to any subsequent movement after that initial deposition.
Release height	The height at which a diaspore is first exposed to the environment, either through fruit opening or at the start of the simulation.
Safe site	A site at which a dispersed diaspore settles and where conditions are suitable for it to germinate (also see vertical niche.)
Successful dispersal	The settling of an abscised epiphyte diaspore on suitable substrate (here: bark) of a suitable host after primary dispersal,

Term	Definition
	recognising that this state is not necessarily final and may be modified through secondary dispersal.
Sweep	Sudden downward air motion.
Terminal velocity (V_{term})	The constant speed at which a diaspore falls in still air after initial acceleration.
Up/down-gusts	The measured maxima of upward or downward flowing air during a specified time interval.
Up/down-gust frequency	The number of up-gusts or down-gusts during a specified time interval.
Up/down-winds	The time averages of upward or downward flowing air calculated over a 1-minute or 5-minute interval.
Vertical niche	The portion of the forest's vertical profile in which abiotic conditions are suitable for a given epiphyte species to establish and persist; differences among species' vertical niches can produce vertical stratification.
Vertical stratification	Non-random distribution of epiphyte species along host-tree or canopy height gradients, typically attributed to microclimatic variation.

Note: terms appear in when first mentioned in the text.

Table 2. Parameter estimates for predictors of bark interception, canopy dispersal, and dispersal distance in epiphyte diaspores.

Model	Term	Estimate	Std. error	Statistic	*p*-value
Bark interception probability (GAM)	Intercept (Release height = 0, V_{term} = 0, Day)	–1.2	< 0.1	–120.5	< 0.01
	Release height	< 0.1	< 0.1	–4.9	< 0.01
	V_{term}	–1.5	< 0.1	–67.4	< 0.01
	Night	–0.2	< 0.1	–12.6	< 0.01
	Release height × V_{term}	< 0.1	< 0.1	33.1	< 0.01
	Release height × Night	< 0.1	< 0.1	10.5	< 0.01
	V_{term} × Night	–0.9	< 0.1	–22.8	< 0.01
	Release height × V_{term} × Night	< 0.1	< 0.1	2.1	0.1
Vertical distance at bark interception (GLM)	Intercept (Release height = 0, V_{term} = 0, Day)	0.5	< 0.1	19.4	< 0.01
	Release height	–0.1	< 0.1	–21.3	< 0.01
	V_{term}	–2.3	< 0.1	–33.2	< 0.01
	Night	–0.4	< 0.1	–9.0	< 0.01
	Release height × V_{term}	–0.1	< 0.01	–28.0	< 0.01
	Release height × Night	< 0.1	< 0.01	4.3	< 0.01
	V_{term} × Night	0.5	0.1	3.8	< 0.01
	Release height × V_{term} × Night	< 0.1	< 0.1	–14.0	< 0.01
Horizontal distance at bark interception (GLM)	Intercept (Release height = 0, V_{term} = 0, Day)	3.6	< 0.1	49.6	< 0.01
	Release height	< 0.1	< 0.1	24.0	< 0.01
	V_{term}	0.9	0.2	4.7	< 0.01
	Night	< 0.1	0.1	0.1	0.9
	Release height × V_{term}	< 0.1	< 0.1	1.7	0.1
	Release height × Night	–0.1	< 0.1	–5.6	< 0.01
	V_{term} × Night	0.8	0.3	2.3	0.1
	Release height × V_{term} × Night	< 0.1	< 0.1	–0.1	0.9
Above–canopy emergence probability (GAM)	Intercept (Release height = 0, V_{term} = 0, Day)	–7.7	< 0.1	–97.0	< 0.01
	Release height	0.2	< 0.01	51.1	< 0.01
	V_{term}	–5.1	0.4	–12.1	< 0.01
	Night	1.6	0.1	15.1	< 0.01
	Release height × V_{term}	< 0.1	< 0.1	2.1	0.1
	Release height × Night	–0.1	< 0.1	–10.6	< 0.01
	V_{term} × Night	–7.3	1.0	–7.7	< 0.01
	Release height × V_{term} × Night	< 0.1	< 0.1	2.1	0.1

Note: Generalized additive models (GAMs) tested the effects of terminal velocity (V_{term}), release height, diel period, and their interaction on the probability of bark interception (relative to

landing on the ground, leaf interception, or non-abscission) and canopy dispersal. Generalized linear models (GLMs) tested the effects of the same predictors on vertical and horizontal dispersal distances. Shown are estimated regression coefficients, standard errors, test statistics (*z* for GAMs, *t* for GLMs), and *p*-values.

Figure captions

Figure 1. Map of the study site in the San Lorenzo National Park and its location within Panama (inset). Colours represent the height of the canopy, generated using lidar data; dots mark the locations of the seventeen vertical profiles. White lines and text show altitude contours.

Figure 2. Flow chart of the mechanistic dispersal (trajectory) model *EpiDisp 1.0*. Abbreviations used in the figure: Terminal velocity = V_{term}, time at release = *T*, time increment after release = *T'*, height at release = *H*, height after abscission = *H'*, plant area density = *PAD*, bark area density = *BAD*.

Figure 3. Day–night variation in wind dynamics **(A–B)** and across the height gradient **(C)** alongside different vegetation indices **(D)**. **(A)** Mean hourly frequency of up- and down-gusts ≥0.33 m s^{-1} (the lowest wind speed measurable by the anemometers) per 5 m height category. Because the first three vertical profiles were sampled at longer time intervals, up-gust frequency was computed only from the fourth vertical profile onward, resulting in no 30–35 m category in this panel. (**B)** Mean hourly speed of up- and down-gusts with measurements of 0 m s^{-1} included. (**C)** Mean hourly vertical wind speed, coloured by datetime, with all measurements of 0 m s^{-1} included, with down-gusts contributing negative and up-gusts positive values. The smoothed lines go through the means per 5 m height category. (**D)** Plant area density (*PAD*) and its components bark area density (*BAD*) and leaf area density (*LAD*) along the forest height gradient, averaged across the San Lorenzo 1 ha permanent plot. *PAD* was calculated from lidar data provided by Vasquez et al. (2024); the derivation *BAD* and *LAD* leaned heavily on previous censuses at San Lorenzo (Janner & Fernández-Lucero, work in progress; Ramos et al., 2024). The silhouette in the background illustrates the forest structure and was adapted from a graphic

generated with Microsoft Copilot (Microsoft, 2024). Points and whiskers show means and standard errors (SE) in panels A-C. In most cases, SE is much smaller than symbol size.

Figure 4. Model-predicted mean gust value (*mu*, solid lines) and residual variation (*sigma*, dashed lines) as functions of above-canopy wind speed and plant area density. **(A)** Predictions across PAD_{local} (0.1–0.4 m^2 m^{-3}), with colour indicating above-canopy wind speed. **(B)** Predictions across above-canopy wind speed, with colour indicating PAD_{above} (1–4 m^2 m^{-3}). All other covariates were held at their median reference values. Shaded ribbons indicate uncertainty around predictions. *PAD* indices were calculated from lidar data from the San Lorenzo plot provided by Vasquez et al. (2024), and above-canopy wind speed was derived from Paton (2019a–d).

Figure 5. Effects of release height, terminal velocity, and diel period on dispersal outcomes. **(A)** Predicted bark interception probability as a function of release height, shown for each terminal velocity and separated by day and night. **(B)** Predicted above-canopy emergence probability, used here as a proxy for long-distance dispersal probability, as a function of release height, shown for each terminal velocity and separated by day and night. Curves are fitted GAM smooths using cubic regression splines (k = 5), and grey ribbons indicate 95% confidence intervals. Note the different y-axis scales.

Figure 6. Distance density distribution of bark-intercepted diaspores. **(A)** Vertical and **(B)** horizontal dispersal kernels (black line) with standard errors (grey shading) calculated from the dispersal kernels in Supplement 2: Figure S7. Dashed vertical lines mark the distances at which the cumulative dispersed population reaches 50%, 75%, and 95%, respectively. Note the pseudo-log transformed x-axis and the different axis scales.

Figure 7. Dispersal limitation as a function of release height and terminal velocity under varying fecundity levels. Points represent release height × V_{term} group simulation outcomes during daytime and are sized by bark interception probability (%), lines show smoothed trends across release height, and colours indicate terminal velocity (m s^{-1}). Dispersal limitation was calculated assuming strong weighting of both vertical and horizontal displacement ($\alpha = 1$, $\beta = 1$), such that both vertical and horizontal spread contribute proportionally to dispersal success. Contributions were aggregated using a power mean of order $q = 2$, which increases the influence of longer distance dispersal events relative to the arithmetic mean while still retaining contributions from the broader distribution. Note the truncated y-axis.

Figures

Uploaded as separate files.

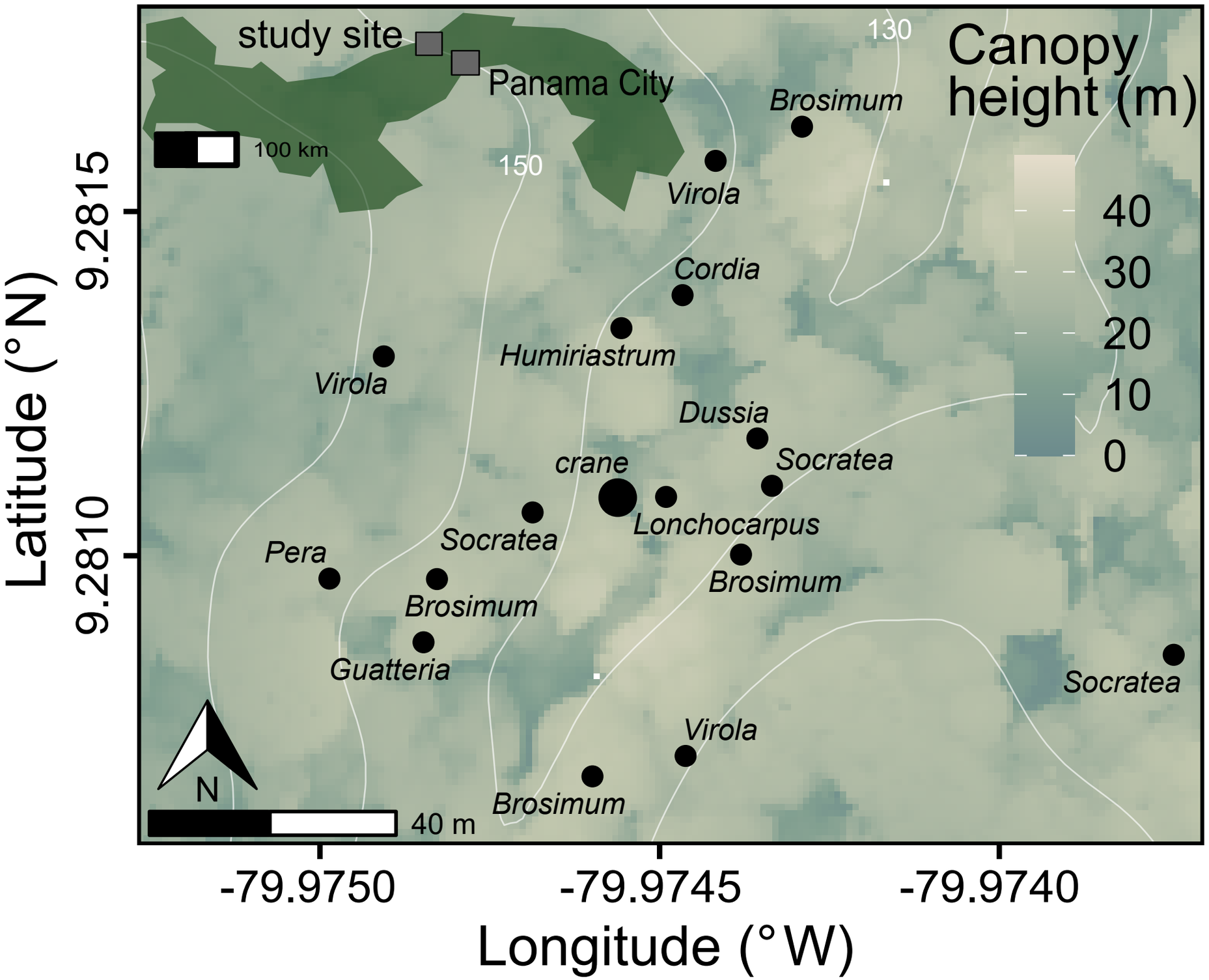
study site
Panama City
100 km
130
150
Canopy height (m)
40
30
20
10
0
Brosimum
Virola
Cordia
Humiriastrum
Virola
Dussia
Socratea
crane
Lonchocarpus
Socratea
Pera
Brosimum
Brosimum
Guatteria
Socratea
Virola
Brosimum
N
40 m
9.2815
9.2810
Latitude (°N)
-79.9750
-79.9745
-79.9740
Longitude (°W)

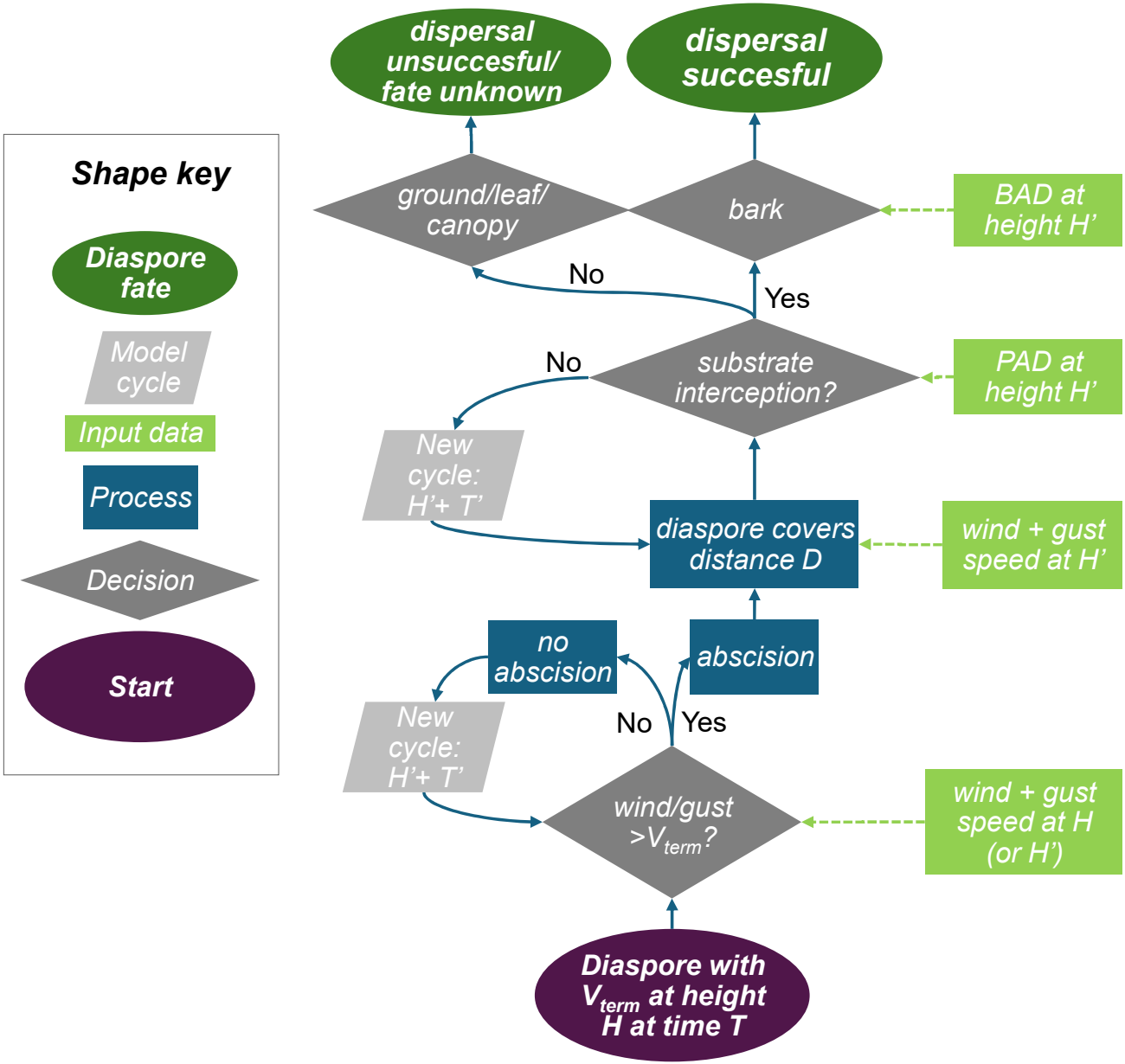
Shape key
Diaspore fate
Model cycle
Input data
Process
Decision
Start
dispersal unsuccesful/ fate unknown
dispersal succesful
ground/leaf/ canopy
bark
BAD at height H'
No
Yes
No
substrate interception?
PAD at height H'
New cycle: H'+ T'
diaspore covers distance D
wind + gust speed at H'
no abscision
abscision
New cycle: H'+ T'
No
Yes
wind/gust >V term ?
wind + gust speed at H (or H')
Diaspore with V term at height H at time T

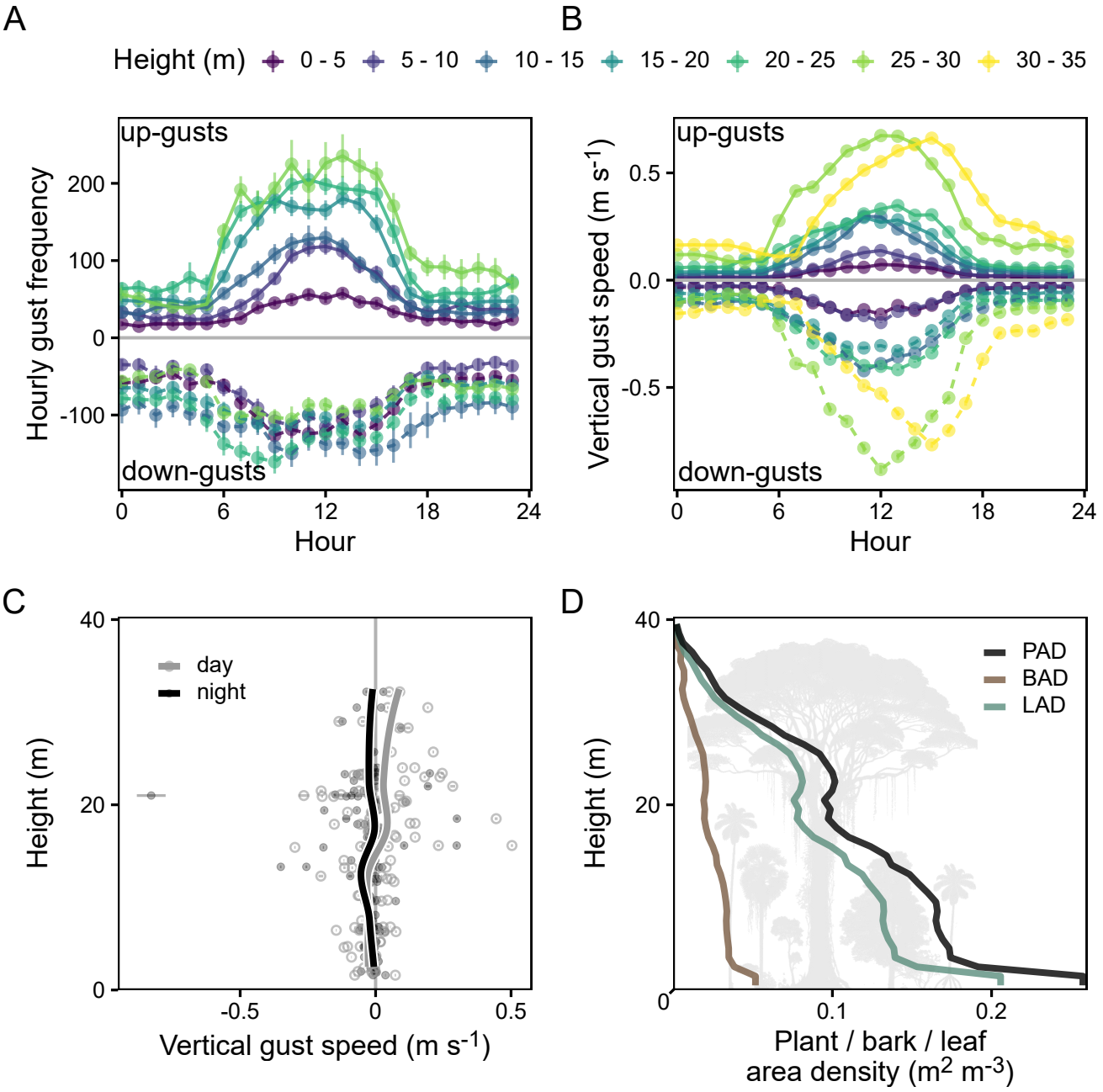
A
B
Height (m)
0 - 5
5 - 10
10 - 15
15 - 20
20 - 25
25 - 30
30 - 35
up-gusts
down-gusts
Hourly gust frequency
200
100
0
-100
0
6
12
18
24
Hour
Vertical gust speed (m s-1)
0.5
0.0
-0.5
C
D
day
night
Height (m)
40
20
0
-0.5
0
0.5
Vertical gust speed (m s-1)
PAD
BAD
LAD
0.1
0.2
Plant / bark / leaf
area density (m2 m-3)

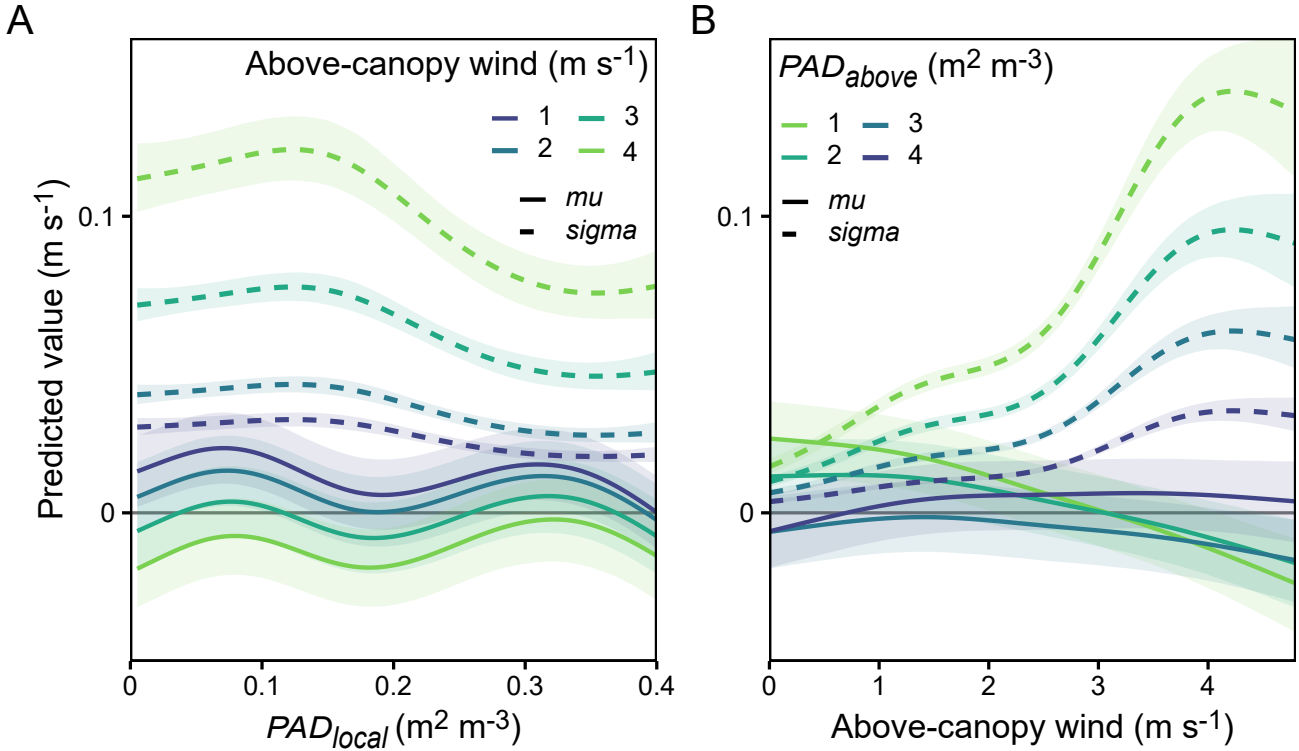
A
Above-canopy wind (m s-1)
1
2
3
4
mu
sigma
Predicted value (m s-1)
0.1
0
0
0.1
0.2
0.3
0.4
PADlocal (m2 m-3)
B
PADabove (m2 m-3)
1
2
3
4
mu
sigma
0.1
0
0
1
2
3
4
Above-canopy wind (m s-1)

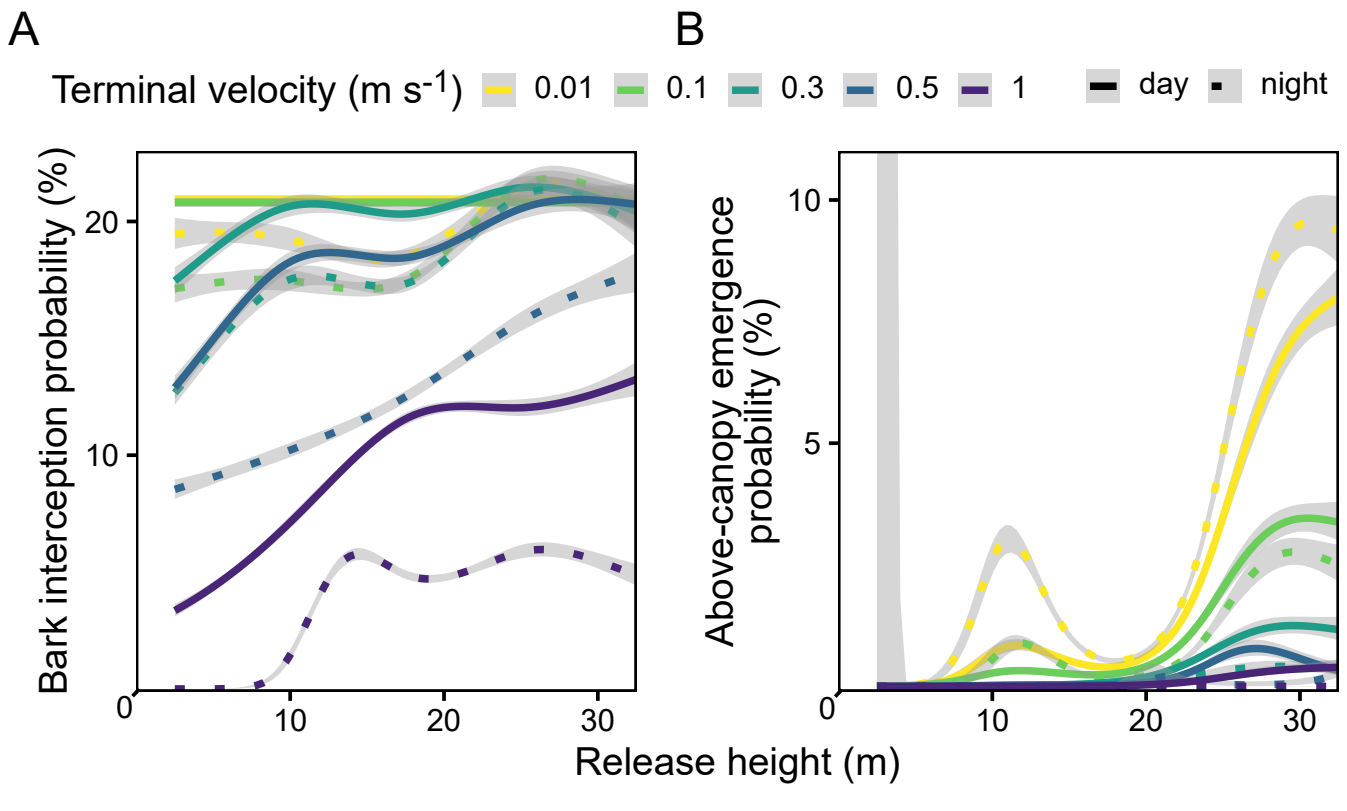
A
B
Terminal velocity (m s-1)
0.01
0.1
0.3
0.5
1
day
night
Bark interception probability (%)
Above-canopy emergence probability (%)
0
10
20
5
10
20
30
Release height (m)

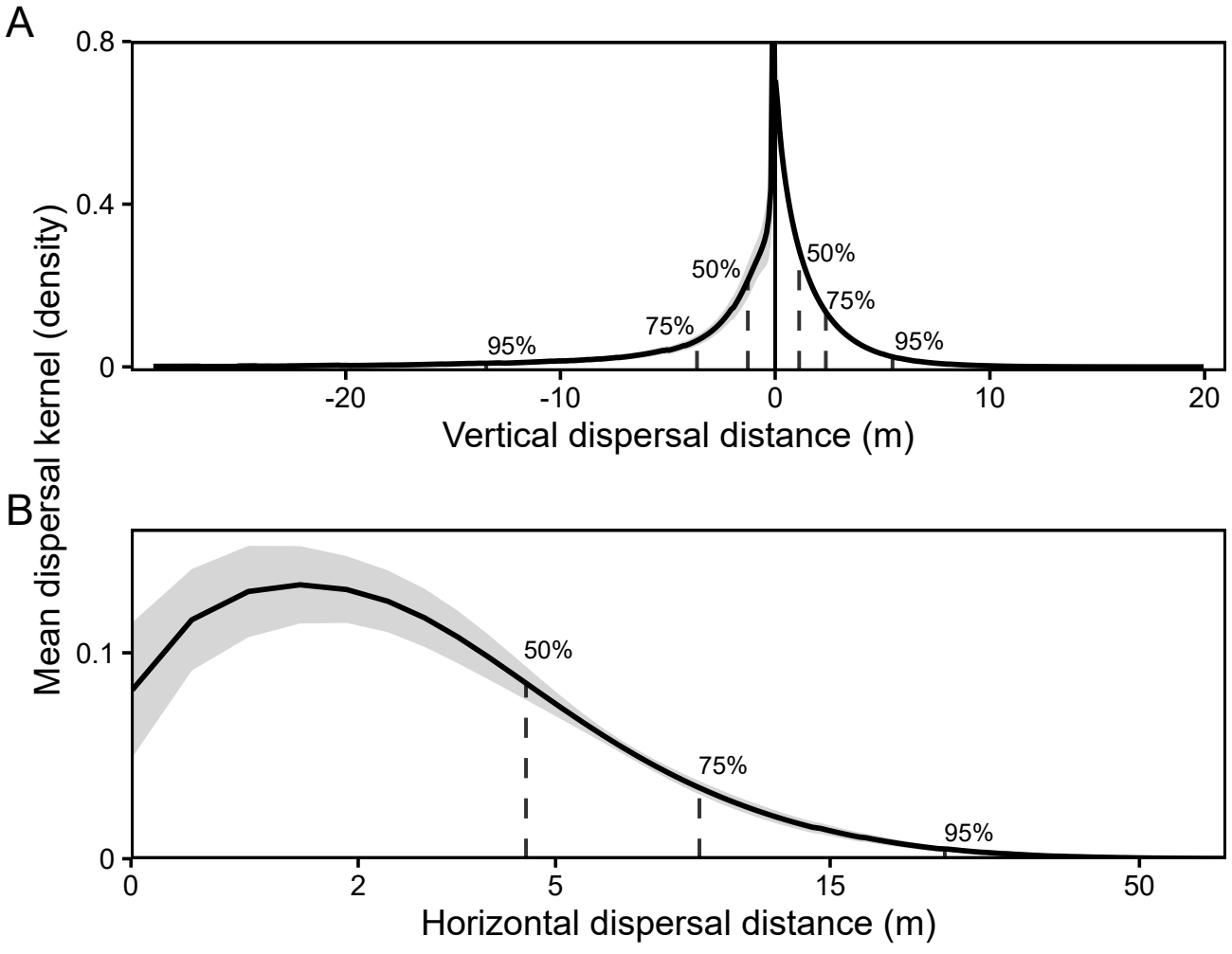
A
0.8
0.4
0
Mean dispersal kernel (density)
95%
75%
50%
50%
75%
95%
-20
-10
0
10
20
Vertical dispersal distance (m)
B
0.1
0
50%
75%
95%
0
2
5
15
50
Horizontal dispersal distance (m)

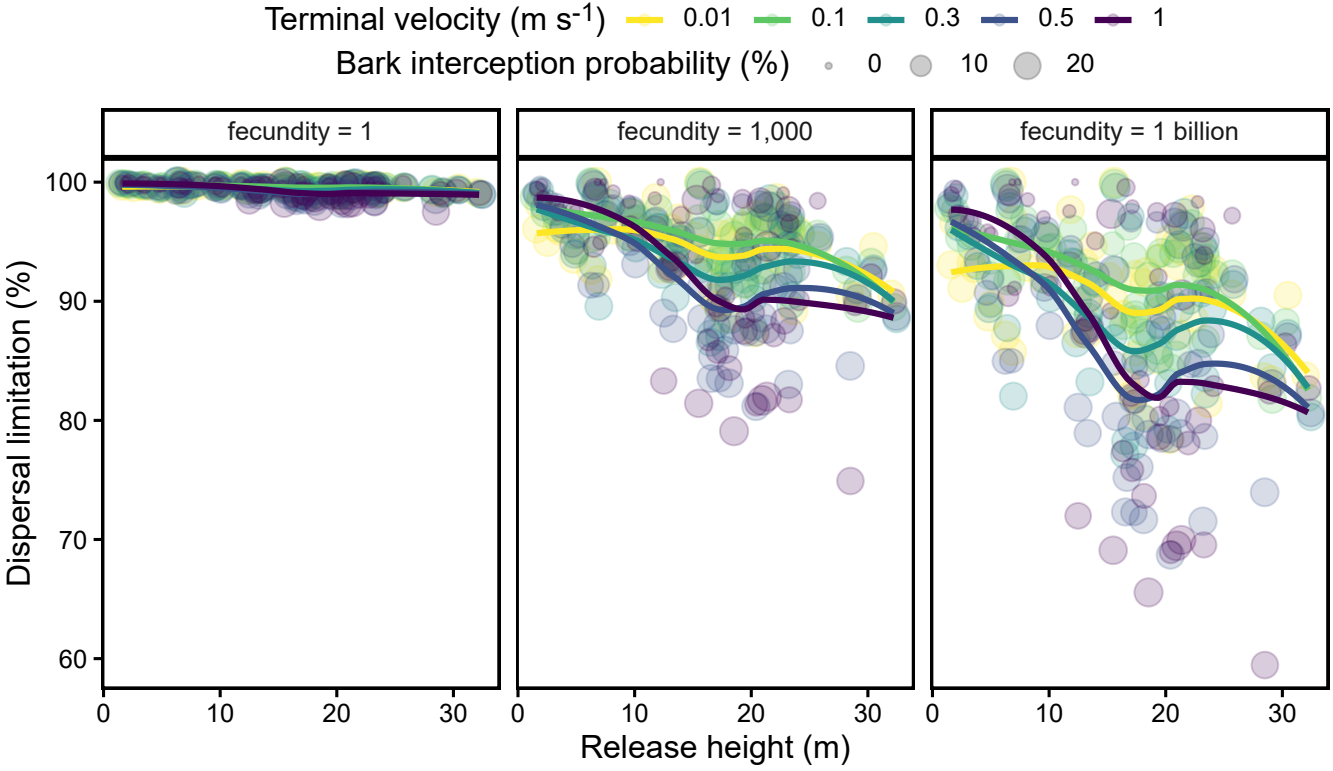
Terminal velocity (m s-1)
0.01
0.1
0.3
0.5
1
Bark interception probability (%)
0
10
20
fecundity = 1
fecundity = 1,000
fecundity = 1 billion
Dispersal limitation (%)
100
90
80
70
60
0
10
20
30
Release height (m)

Ecological Monographs

Appendix 1: Materials, Methods, Concepts

Patterns of wind dispersal within a forest canopy: An epiphyte perspective

Marie Hoensbroech[1], Juliano Sarmento Cabral[2], Gerhard Zotz[1,3]

1: Institute of Biology and Environmental Sciences, Carl von Ossietzky Universität Oldenburg, Ammerländer Heerstr. 114-118, 26129 Oldenburg, Germany

2: Ecological Modelling, Bonner Institute for Organismal Biology — Department of Plant Biodiversity, Universität Bonn, Venusbergweg 22, 53115 Bonn, Germany

3: Smithsonian Tropical Research Institute, Box 0843-03092, Panama, Republic of Panama

Correspondence: Marie Hoensbroech; email: marie.hoensbroech@uni-oldenburg.de

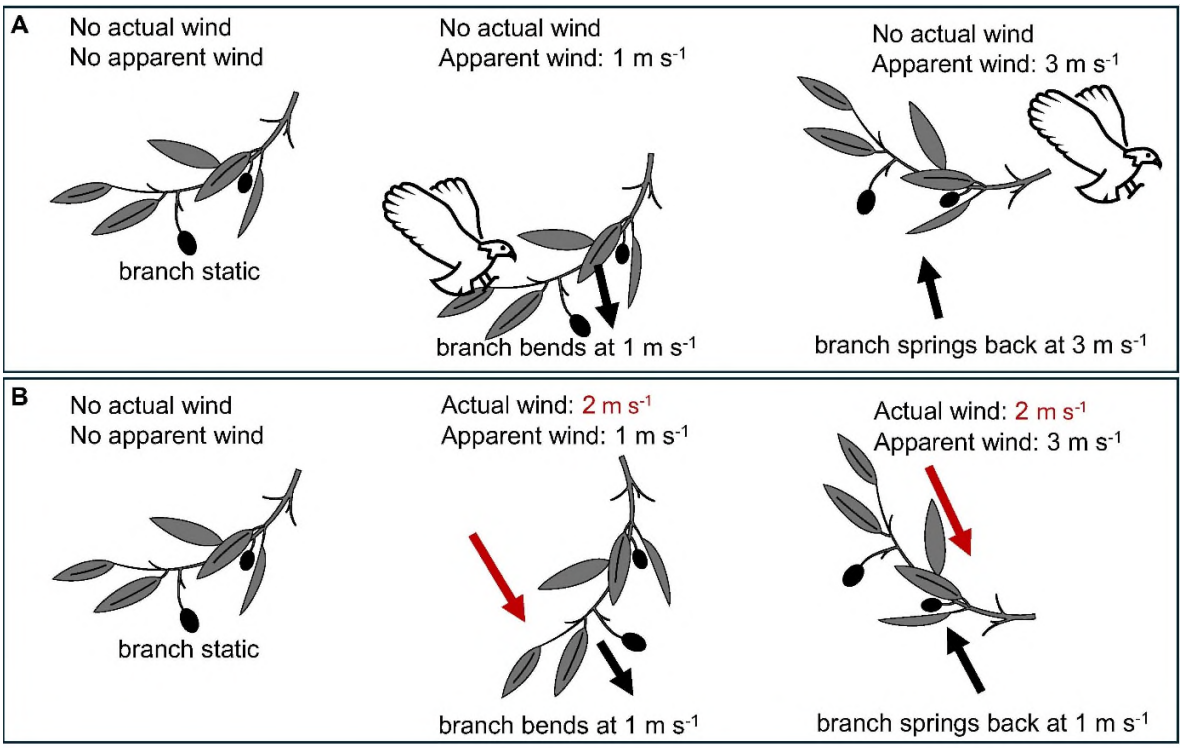

Figure S1. Conceptual diagram of branch movements and their apparent winds that diverge from the actual winds due to **(A)** mechanical disturbance and **(B)** branch sway due to wind loading. Note that other factors such as the direction of movement relative to the direction of the actual wind, inertia, resistance, or drag also play a role in the magnitude and the direction of the apparent wind. The icons used in this figure were sourced from the built-in icon library in Microsoft PowerPoint (Microsoft, 2024) and adapted by MH.

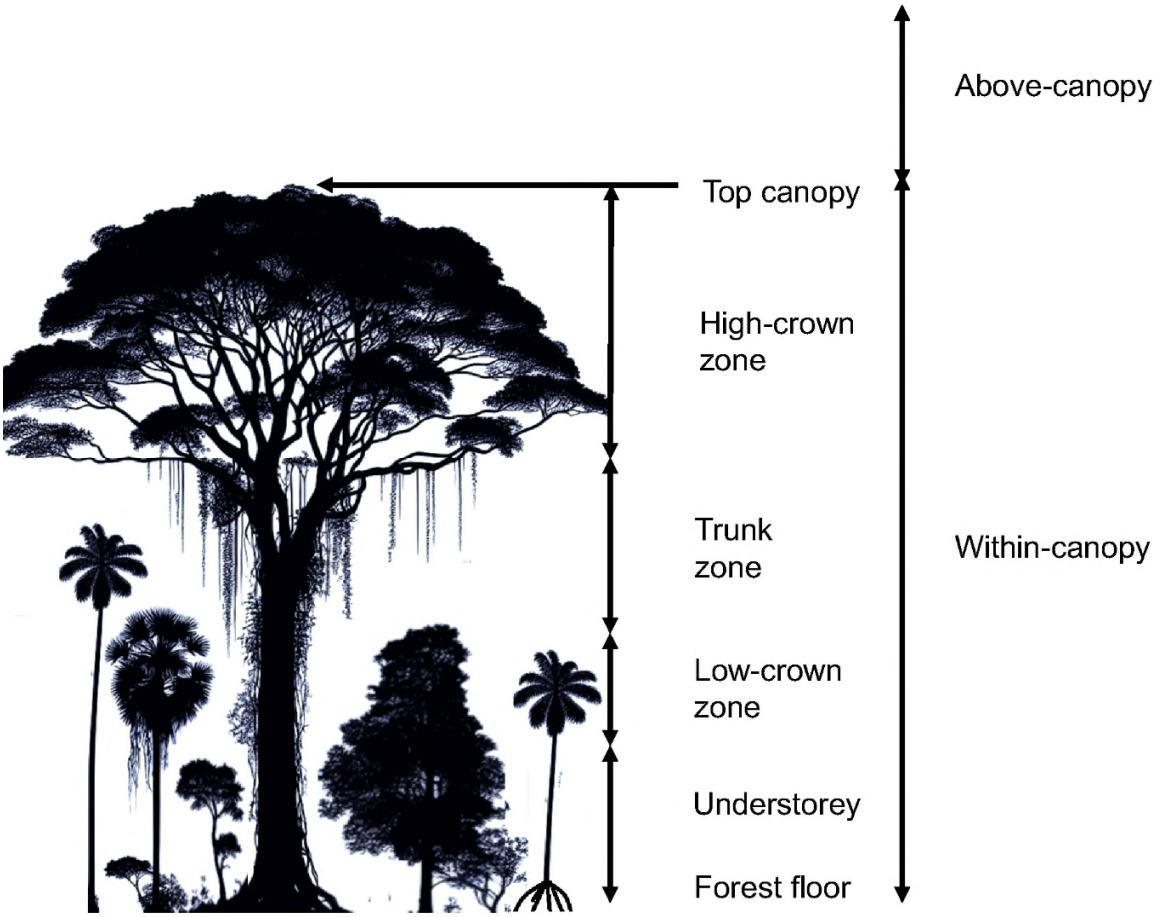

Figure S2. The different forest zones this study refers to and the terminology used. Note that the heights and vegetation densities of the zones may vary within and between forests, and that they are not necessarily representative of the San Lorenzo Forest studied here. The silhouette was adapted by MH from a graphic generated with Microsoft Copilot (Microsoft, 2024).

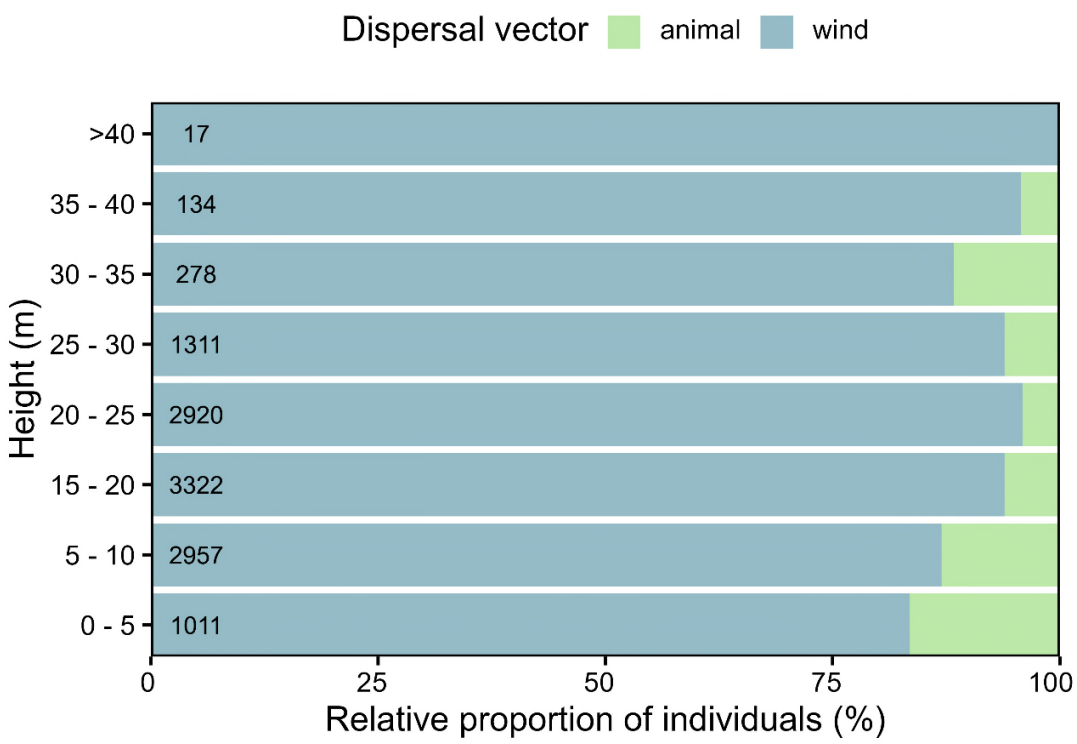

Figure S3. Percent of wind-dispersed vs. animal-dispersed epiphyte individuals at the San Lorenzo 0.4 ha forest plot with absolute numbers of wind-dispersed individuals given inside the columns. The data are based on the census by Zotz & Schultz (2008), encompassing 11,950 epiphyte individuals of 126 species.

Figure S4. Assessing wind dynamics along the forest height gradient. Sonic anemometers **(A)**, screwed to an aluminium frame at two positions (in = near the stem, out = 1.35 m away from the stem), were strapped to stems or branches of trees at four heights to measure winds, gusts, and wind direction for 3- to 10-second intervals (0.3 to 0.1 Hz) for one to five consecutive days. Loggers **(B)** logged the measurements. Every anemometer was additionally coupled with a temperature sensor **(C)**. The images were taken by MH.

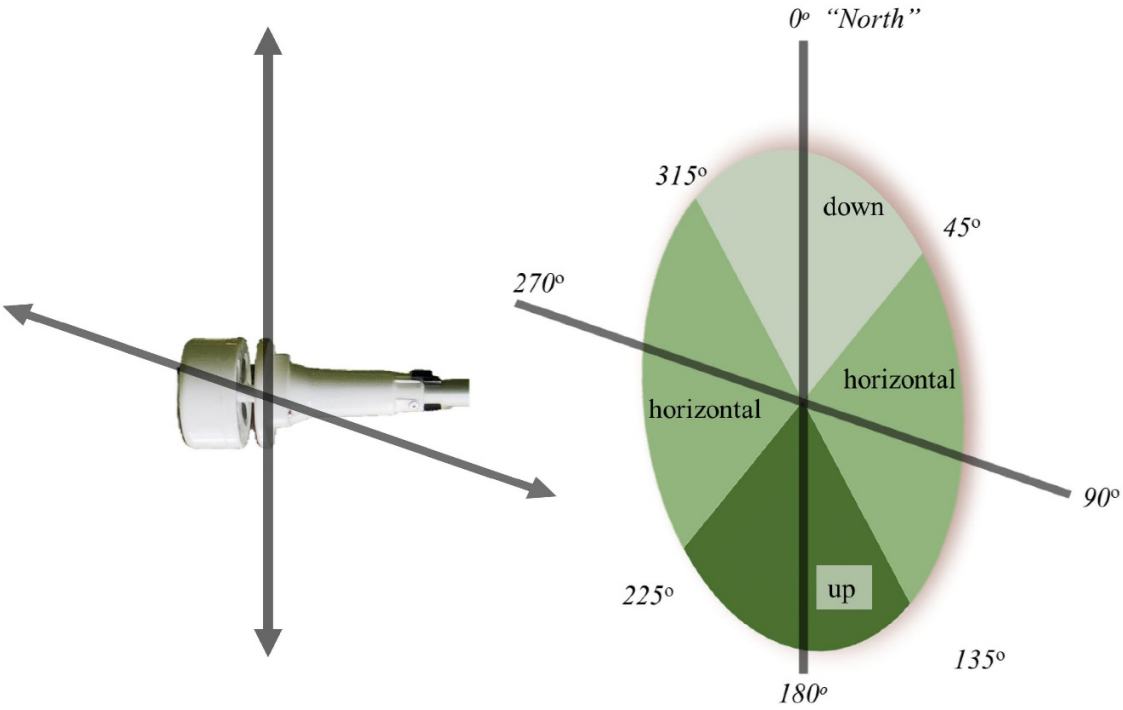

Figure S5. The plane of wind measurements during the study of the wind dynamics at San Lorenzo, Panama, showing measurement directions in cursive and geographic directions in bold. The measurement plane was divided into four equally sized portions, which denote the respective measurement direction categories (up, down, or horizontal [two times]). The geographic direction was derived with the help of the facing direction (see equations in Figure). However, because this horizontal alignment of the anemometers gave only two readings of horizontal direction, i.e., left (90°) and right (270°), horizontal winds/gusts were largely ignored during the analyses. The image of the anemometer was taken and modified by MH.

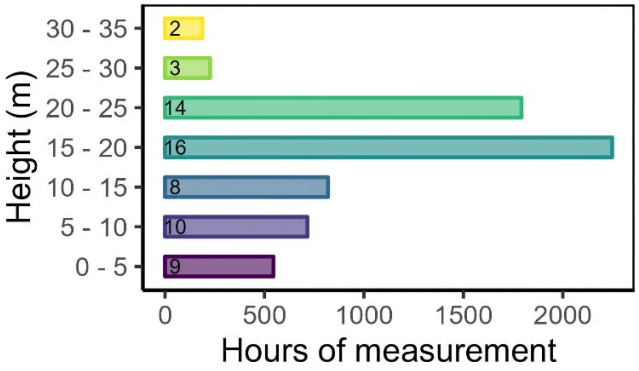

Figure S6. Hours of measurement per height category with numbers of replicates inside the bars. Note that this is for a single anemometer (i.e., the “in” treatment: 0.3 m from the stem); the hours of measurements duplicate when the second position ("out": 1.3 m from the stem) is added.

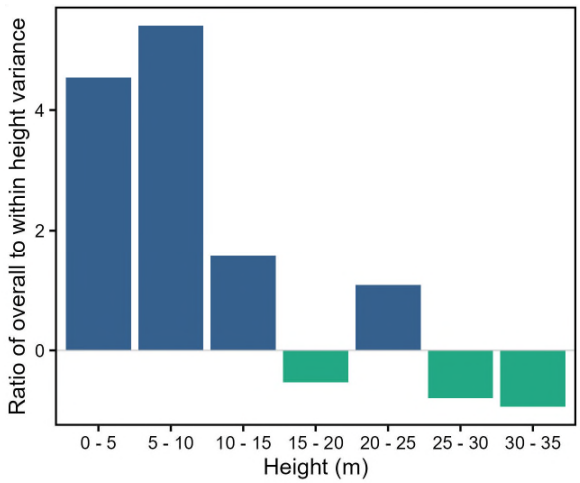

Figure S7. Ratio of inter-height to intra-height variance of gust speeds. A positive value indicates that the variance is greater between height categories than within a height category. Note that the axis is shifted down 1 unit to highlight the differences, i.e., a shown value of 0 corresponds to a ratio of 1, i.e., equal variances.

References

Microsoft. 2024. "Microsoft 365 tools [software]". https://microsoft.com/microsoft-365.

Zotz, G., and S. Schultz. 2008. “The Vascular Epiphytes of a Lowland Forest in Panama—Species Composition and Spatial Structure.” *Plant Ecology* 195: 131–41. https://doi.org/10.1007/s11258-007-9310-0.

Ecological Monographs

Appendix 2: ShinyApp

Patterns of wind dispersal within a forest canopy: An epiphyte perspective

Marie Hoensbroech[1], Juliano Sarmento Cabral[2], Gerhard Zotz[1,3]

1: Institute of Biology and Environmental Sciences, Carl von Ossietzky Universität Oldenburg, Ammerländer Heerstr. 114–118, 26129 Oldenburg, Germany

2: Ecological Modelling, Bonner Institute for Organismal Biology — Department of Plant Biodiversity, Universität Bonn, Venusbergweg 22, 53115 Bonn, Germany

3: Smithsonian Tropical Research Institute, Box 0843-03092, Panama, Republic of Panama

Correspondence: Marie Hoensbroech; email: marie.hoensbroech@uni-oldenburg.de

Figure S1. Screenshot of the interactive shinyApp, available at: https://mariehoensbroech.shinyapps.io/epi-wind-dispersal/. Users can explore the study site as a 3D lidar scene, inspect vertical profiles and anemometer wind sensor positions, and animate above-canopy wind and gust conditions measured at 50 m from the top of the canopy access crane, and discover how below-canopy gust speeds change with above-canopy wind, temperature, or vegetation density. The data and R scripts associated with the ShinyApp will be made available in the study's data repository such that the app can be run locally as well.

Reference List of R Libraries used in the ShinyApp

Barrett, T., M. Dowle, A. Srinivasan, J. Gorecki, M. Chirico, T. Hocking, B. Schwendinger, and I. Krylov. 2025. “data.Table: Extension of ‘data.Frame’.” R Package Version 1.17.8. https://CRAN.R-project.org/package=data.table.

Bürkner, P.-C. 2017. “brms: An R Package for Bayesian Multilevel Models Using Stan.” *Journal of Statistical Software* 80:1–28. https://doi.org/10.18637/jss.v080.i01.

Chang, W., J. Cheng, J. Allaire, C. Sievert, B. Schloerke, Y. Xie, J. Allen, J. McPherson, A. Dipert, and B. Borges. 2026. “shiny: Web Application Framework for R.” R Package Version 1.11.1. https://CRAN.R-project.org/package=shiny.

Cheng, J., B. Schloerke, B. Karambelkar, Y. Xie, and G. Aden-Buie. 2025. “leaflet: Create Interactive Web Maps with the JavaScript ‘leaflet’ Library.” R Package Version 2.2.3. https://CRAN.R-project.org/package=leaflet.

Hester, J., and J. Bryan. 2026. “glue: Interpreted String Literals.” R Package Version 1.8.0. https://CRAN.R-project.org/package=glue.

Hijmans, R. J. 2025. “terra: Spatial Data Analysis.” R Package Version 1.8-80. https://CRAN.R-project.org/package=terra.

North, A. 2026. “rdeck: Deck.gl Widget.” R Package Version 0.5.2. https://github.com/qfes/rdeck.

Ooms, J. 2014. “The jsonlite Package: A Practical and Consistent Mapping Between JSON Data and R Objects.” arXiv:1403.2805. https://arxiv.org/abs/1403.2805.

Pebesma, E. 2018. “Simple Features for R: Standardized Support for Spatial Vector Data.” The R Journal 10: 439–46. https://doi.org/10.32614/RJ-2018-009.

R Core Team. 2023. *R: A Language and Environment for Statistical Computing.* Vienna: R Foundation for Statistical Computing. https://www.R-project.org/.

Roussel, J.-R., D. Auty, N. C. Coops, P. Tompalski, T. R. H. Goodbody, A. Sánchez Meador, J.-F. Bourdon, F. de Boissieu, and A. Achim. 2020. “lidR: An R Package for Analysis of Airborne Laser Scanning (ALS) data.” *Remote Sensing of Environment* 251: 112061. https://doi.org/10.1016/j.rse.2020.112061.

Vaidyanathan, R., Y. Xie, J. J. Allaire, J. Cheng, C. Sievert, and K. Russell. 2023. “htmlwidgets: HTML Widgets for R.” R Package Version 1.6.4. https://CRAN.R-project.org/package=htmlwidgets.

Wickham, H., M. Averick, J. Bryan, W. Chang, L. D’Agostino McGowan, R. François, G. Grolemund, et al. 2019. “Welcome to the tidyverse.” *Journal of Open Source Software* 4(43): 1686. https://doi.org/10.21105/joss.01686.

References List of External Data Sources

Janner, L. E., and M. Fernández-Lucero, unpublished dataset.

Mendieta-Leiva, G., K. Wagner, and G. Zotz. 2021. “Vascular Epiphyte Census Data at the San Lorenzo Crane Plot [dataset].” *Zenodo.* https://doi.org/10.5281/zenodo.5645775.

Paton, S. 2019a. “Galeta–Wind Direction [dataset]." *Smithsonian Tropical Research Institute.* https://doi.org/10.25573/data.10042640.v25.

Paton, S. 2019b. “Galeta–Wind Speed [dataset].” *Smithsonian Tropical Research Institute.* https://doi.org/10.25573/data.10042658.v23.

Paton, S. 2019c. “San Lorenzo Crane–Wind Speed [dataset].” *Smithsonian Tropical Research Institute.* https://doi.org/10.25573/data.10042688.v23.

Paton, S. 2019d. “San Lorenzo Crane–Wind direction [dataset].” *Smithsonian Tropical Research Institute.* https://doi.org/10.25573/data.10042718.v23.

Paton, S. 2019e. “San Lorenzo Crane–Air Temperature [dataset].” Smithsonian Tropical Research Institute. https://doi.org/10.25573/data.10042694.v23.

Paton, S. 2019f. “San Lorenzo Crane–Precipitation [dataset].” Smithsonian Tropical Research Institute. https://doi.org/10.25573/data.10042679.v23.

Ramos, P., P. Villareal, and H. Muller-Landau. 2024. “Tree Height Allometry Data for 5109 Trees in Twenty-Four Small ForestGEO Plots in Panama, 2011–2020 [dataset].” Smithsonian Tropical Research Institute. https://doi.org/10.25573/data.24954204.v1.

Vasquez V., M. Garcia, M. Hernandez, ForestGEO Smithsonian, and H. Muller-Landau. 2024. “Smithsonian ForestGEO San Lorenzo and Panama Small Plots Aerial Photogrammetry Orthomosaics, Digital Surface Models, Point Clouds and Raw Images for 2015–2024.” Smithsonian Research Data Repository. https://doi.org/10.60635/C33W2K.

Zotz, G., and S. Schultz. 2008. “The Vascular Epiphytes of a Lowland Forest in Panama—Species Composition and Spatial Structure.” *Plant Ecology* 195: 131–41. https://doi.org/10.1007/s11258-007-9310-0.

Ecological Monographs

Appendix 3: Flowchart of the data wrangling and dispersal model for:

- **Patterns of wind dispersal within a forest canopy: An epiphyte perspective**
  Marie Hoensbroech[1], Juliano Sarmento Cabral[2], Gerhard Zotz[1,3]
- 1: Institute of Biology and Environmental Sciences, Carl von Ossietzky Universität Oldenburg, Ammerländer Heerstr. 114–118, 26129 Oldenburg, Germany
  2: Ecological Modelling, Bonner Institute for Organismal Biology — Department of Plant Biodiversity, Universität Bonn, Venusbergweg 22, 53115 Bonn, Germany
  3: Smithsonian Tropical Research Institute, Box 0843-03092, Panama, Republic of Panama

Correspondence: Marie Hoensbroech; email: marie.hoensbroech@uni-oldenburg.de

Joining below-canopy wind data with the tree data

speeds are in m/s,

temperature in ^{o}C,

heights in m

Below-canopy wind data

Replicate #

Position

Sensor ID

Datetime	Wind speed 11.3 in 1234567	Gust speed 11.3 in 1234567	Wind direction 11.3 in 1234567
2023-04-10 15:43:32	0	0.33	340
2023-04-10 15:43:35	0	0	10

Datetime	Replicate #	Position	Sensor ID	Wind speed	Gust speed	Wind direction
2023-04-10 15:43:32	11.3	in	1234567	0	0.33	340
2023-04-10 15:43:35	11.3	in	1234567	0	0	10

Replicate #	Measurement	Sensor ID	Position	Tree species	Sensor height	Sensor direction	Tree height	Canopy density (four readings)
11.3	Wind	1234567	in	*Brosimum*	17.4	60	36.1	24, 40, 5, 37
11.3	Temp	23456789	out	*Brosimum*	17.4	60	36.1	24, 40, 5, 37

Datetime	Replicate #	Position	Sensor ID	Wind speed	Gust speed	Wind direction
2023-04-10 15:43:32	11.3	in	1234567	0	0.33	340
2023-04-10 15:43:35	11.3	in	1234567	0	0	10

Datetime	Replicate #	Position	Sensor ID	Wind speed	Gust speed	Wind direction	Tree species	Sensor height	Sensor direction	Tree height	Canopy density
2023-04-10 15:43:32	11.3	in	1234567	0	0.33	340	*Brosiimum*	17.4	60	36.1	24, 40, 5, 37
2023-04-10 15:43:35	11.3	in	1234567	0	0	10	*Brosimum*	17.4	60	26.1	24, 40, 5, 37

Interpreting direction

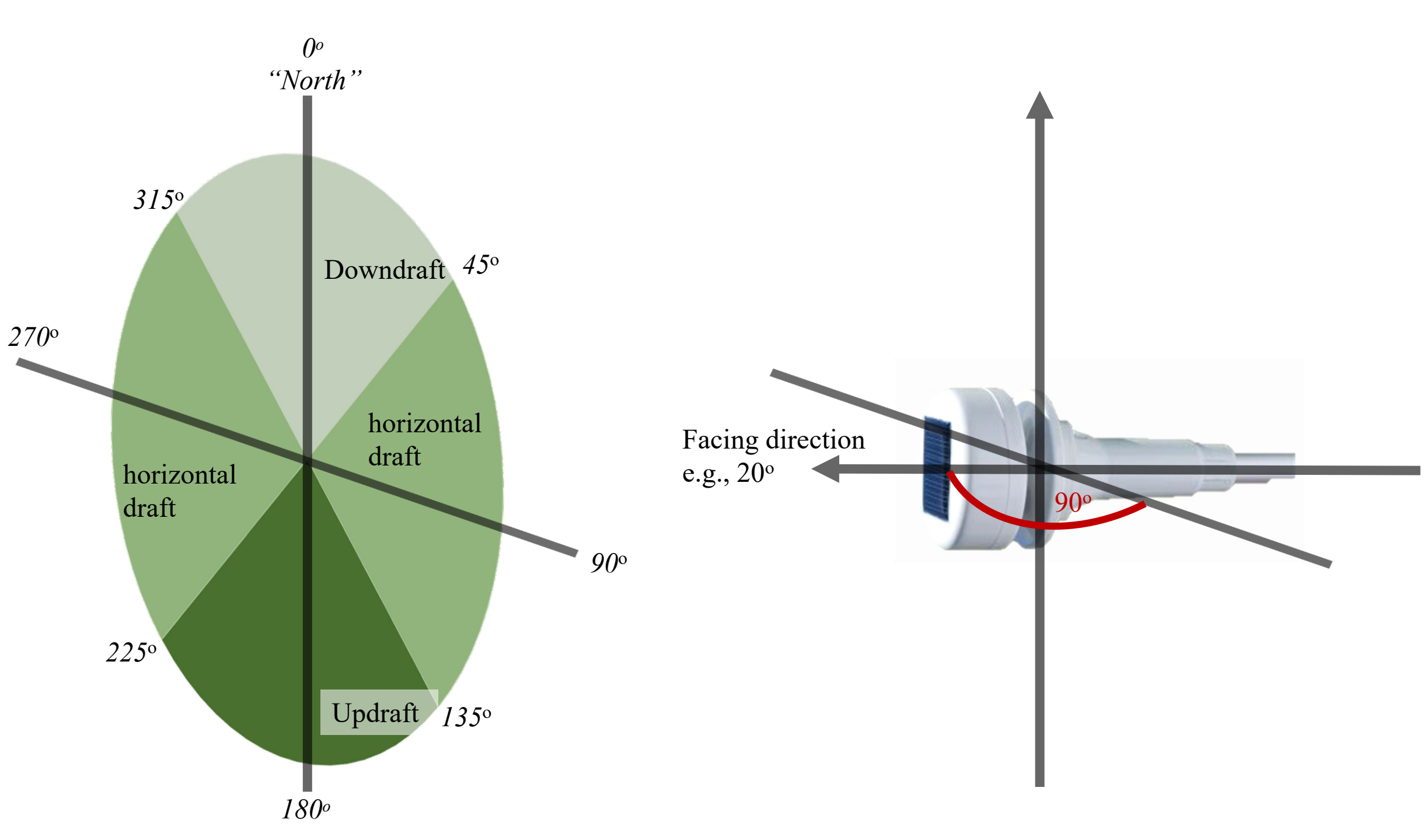
0°
"North"
315°
45°
Downdraft
270°
horizontal draft
horizontal draft
90°
225°
Updraft
135°
180°
Facing direction
e.g., 20°
90°

Datetime	Replicate #	Position	Sensor ID	Wind speed	Gust speed	Wind direction	**Direction**	Sensor height	**Height category**
2023-04-10 15:43:32	11.3	in	1234567	0	0.33	340	Down	17.4	15 – 20
2023-04-10 15:43:35	11.3	in	1234567	0	0	10	Down	17.4	15 – 20

Datetime	Replicate #	Position	Sensor ID	Wind speed	Gust speed	Wind direction	Direction	Sensor height	....
2023-04-10 15:43:32	11.3	in	1234567	0	0.33	340	Down	17.4	
2023-04-10 15:43:35	11.3	in	1234567	0	0	10	Down	17.4	

3 second data

lubridate::ceiling_date() -> 1 minute

mean

max

circular mean

per group: replicate # and position

Datetime	Replicate #	Position	Sensor ID	Wind speed	Gust speed	Wind direction	Direction	Sensor height
2023-04-10 15:44:00	11.3	in	1234567	0	0.33	350	Down	17.4
2023-04-10 15:45:00	11.3	in	1234567	0.12	0.66	345	Down	17.4
2023-04-10 15:46:00	11.3	in	1234567	0.22	1	270	Horizontal	Sensor height
2023-04-10 15.47:00	11.3	In	1234567	0.1	0.33	170	Up	17.4

1 minute data

Datetime	Replicate #	Position	Sensor ID	Wind speed	Gust speed	Wind direction	Direction	Sensor height
2023-04-10 15:44:00	11.3	in	1234567	0	0.33	350	Down	17.4
2023-04-10 15:45:00	11.3	in	1234567	0.12	0.66	345	Down	17.4
2023-04-10 15:46:00	11.3	in	1234567	0.22	1	270	Horizontal	17.4
2023-04-10 15.47:00	11.3	In	1234567	0.1	0.33	170	Up	17.4

lubridate::ceiling_date() -> 5 minutes

mean

max

circular mean

per group: replicate # and position **and direction**

Datetime	Replicate #	Position	Sensor ID	Wind speed	Gust speed	Wind direction	Direction	Sensor height
2023-04-10 15:45:00	11.3	in	1234567	0 .06	0.66	347.5	Down	17.4
2023-04-10 15:50:00	11.3	in	1234567	0.22	1	270	Horizontal	17.4
2023-04-10 15.50:00	11.3	In	1234567	0.1	0.33	170	Up	17.4

1 minute data

5 minute data

Joining below-canopy data with above-canopy data

Datetime	Mean wind	Max wind (gust)	Wind direction	Mean temperature	Rain
2023-04-10 15:45:00	5.4	7.7	0	29.5	10
2023-04-10 16:00:00	5.7	7.5	10	29.4	0

dplyr::na_spline()

Datetime	Mean wind	Gust	Wind direction	Mean temperature	Rain
2023-04-10 15:45:00	5.4	7.7	0	29.5	10
2023-04-10 15:50:00	5.5	7.64		29.46	
2023-04-10 15:55:00	5.6	7.57		29.42	
2023-04-10 16:00:00	5.7	7.5	10	29.4	0

Copy down

Divide by 3

Datetime	Mean wind	Gust	Wind direction	Mean temperature	Rain
2023-04-10 15:45:00	5.4	7.7	0	29.5	3.33
2023-04-10 15:50:00	5.5	7.64	0	29.46	3.33
2023-04-10 15:55:00	5.6	7.57	0	29.42	3.33
2023-04-10 16:00:00	5.7	7.5	10	29.4	0

Datetime	Replicate #	Position	Sensor ID	Wind speed	Gust speed	Wind direction	Direction	Sensor height	Mean wind	Gust	Wind direction	Mean temperature	Rain
2023-04-10 15:45:00	11.3	in	1234567	0 .06	0.66	347.5	Down	17.4	5.4	7.7	0	29.5	3.33
2023-04-10 15:50:00	11.3	in	1234567	0.22	1	270	Horizontal	17.4	5.5	7.64	0	29.46	3.33
2023-04-10 15.50:00	11.3	In	1234567	0.1	0.33	170	Up	17.4	5.5	7.64	0	29.46	3.33

Calculating up-gust proportion

Datetime	Replicate #	Position	Sensor ID	Wind speed	Gust speed	Wind direction	Direction	Sensor height	....
2023-04-10 15:43:32	11.3	in	1234567	0	0.33	340	Down	17.4	
2023-04-10 15:43:35	11.3	in	1234567	0	0	10	Down	17.4	

3 second data

Filter gusts above 0.33 m/s (the anemometers' threshold)

Datetime	Replicate #	Position	Sensor ID	Wind speed	Gust speed	Wind direction	Direction	Sensor height
2023-04-10 15:43:32	11.3	in	1234567	0	0.33	340	Down	17.4
2023-04-10 15:43:43	11.3	in	1234567	0	0	10	Up	17.4

Calculate total number of gusts per hour, the number of gusts in each direction category, and the relative proportion

Datehour	Datetime	Replicate #	Position	Sensor ID	Wind speed	Gust speed	Wind direction	Direction	Sensor height	Total number of gusts	Number of gusts per group	Proportion
2023-04-10 16:00:00	2023-04-10 15:43:32	11.3	in	1234567	0	0.33	340	Down	17.4	2500	100	0.04
2023-04-10 16:00:00	2023-04-10 15:43:43	11.3	in	1234567	0	0	10	Up	17.4	2500	323	0.13

EpiDisp 1.0 – the trajectory model

Mean wind speed for every minute per height.

Vertical winds and gusts received a negative sign when downward flow, positive when upward flow.

Negative when cardinal wind direction between 90.1° and 270°

Datetime	Daytime	Replicate #	Position	Vertical wind speed	Vertical gust speed	Horizontal wind speed	Horizontal gust speed	Sensor height	Tree height
2023-04-10 15:43:32	Late day	11.3	In	0.1	0.33	1.6	-2.3	10.2	36.1
2023-04-10 15:43:32	Late day	11.3	In	0	0	0	0	13.2	36.1
2023-04-10 15:43:32	Late day	11.3	In	0.1	-0.67	1.6	0	17.4	36.1
2023-04-10 15:43:32	Late day	11.3	In	0.1	0	1.6	1.2	21.1	36.1
2023-04-10 15:43:33	Late day	11.3	In	0.1	0	1.6	1.5	13.2	36.1

When at a certain time, at a given height, no measurements were taken, they received 0 as value

Dataframes were split by replicate #, position, and daytime

A ca. 30-min period (~1000 rows) were randomly chosen

Datetime	Daytime	Replicate #	Position	Vertical wind speed	Vertical gust speed	Horizontal wind speed	Horizontal gust speed	Sensor height	Tree height
2023-04-10 21:43:32	Early night	11.3	Out	0.1	0.33	1.6	-2.3	10.2	36.1
2023-04-10 21:43:32	Early night	11.3	Out	0	0	0	0	13.2	36.1
2023-04-10 21:43:32	Early night	11.3	Out	0.1	-0.67	1.6	0	17.4	36.1
2023-04-10 21:43:32	Early night	11.3	Out	0.1	0	1.6	1.2	21.1	36.1
2023-04-10 21:43:33	Early night	11.3	Out	0.1	0	1.6	1.5	13.2	36.1

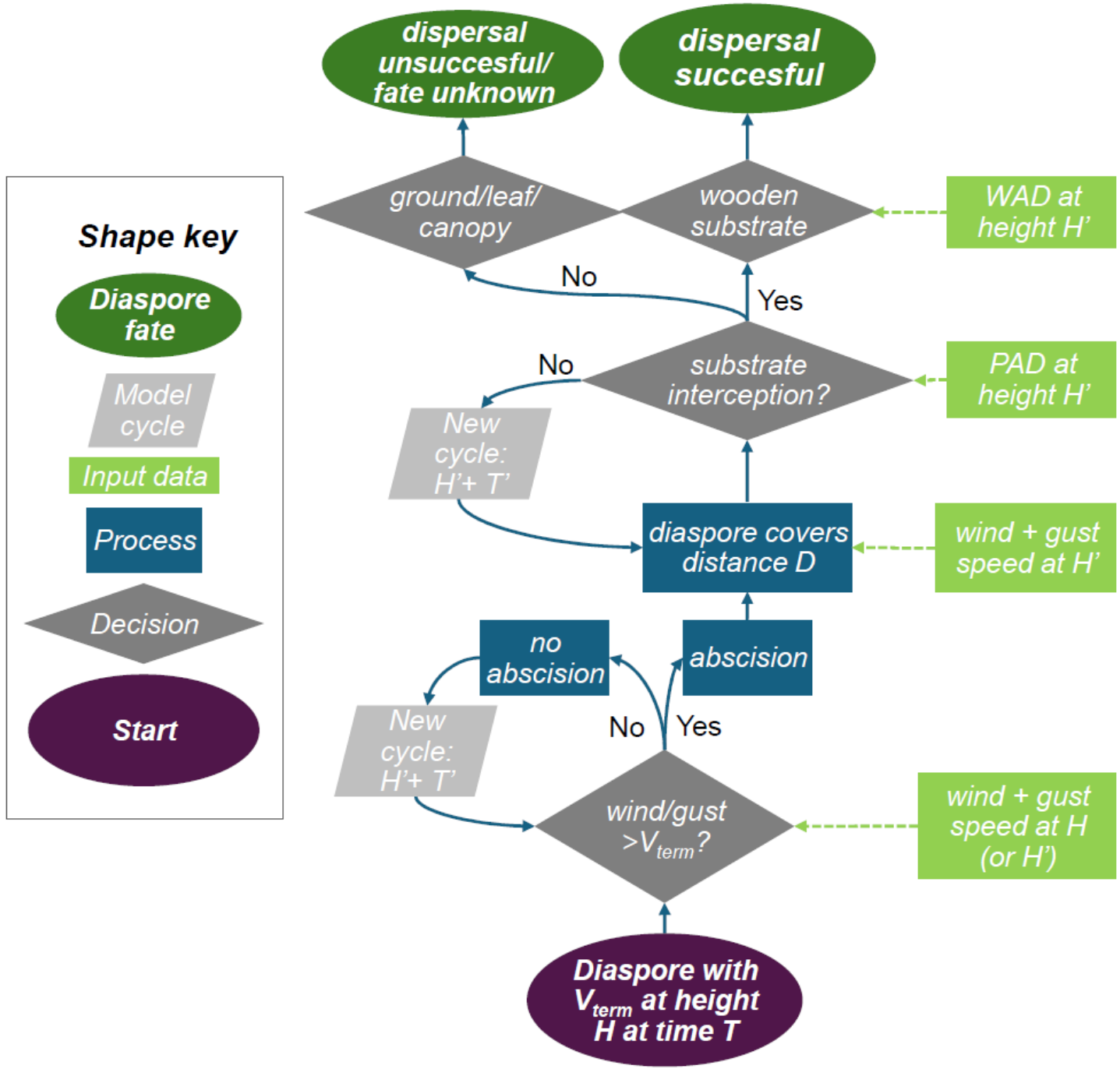
Shape key
Diaspore fate
Model cycle
Input data
Process
Decision
Start
dispersal unsuccesful/ fate unknown
dispersal succesful
ground/leaf/ canopy
wooden substrate
WAD at height H'
No
Yes
No
substrate interception?
PAD at height H'
New cycle: H'+ T'
diaspore covers distance D
wind + gust speed at H'
no abscision
abscision
New cycle: H'+ T'
No
Yes
wind/gust >V term ?
wind + gust speed at H (or H')
Diaspore with V term at height H at time T

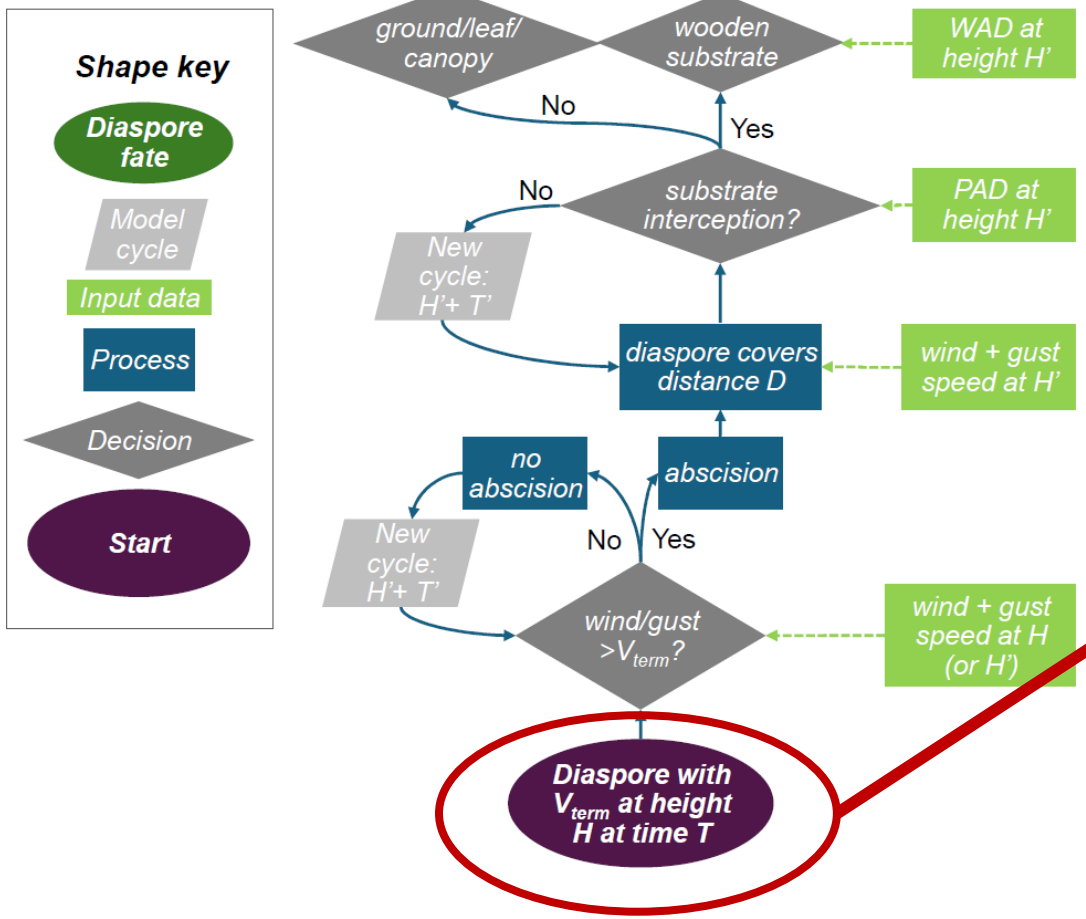
Shape key
Diaspore fate
Model cycle
Input data
Process
Decision
Start
dispersal unsuccesful/ fate unknown
dispersal succesful
ground/leaf/ canopy
wooden substrate
WAD at height H'
No
Yes
No
substrate interception?
PAD at height H'
New cycle: H'+ T'
diaspore covers distance D
wind + gust speed at H'
no abscision
abscision
New cycle: H'+ T'
No
Yes
wind/gust >V_term?
wind + gust speed at H (or H')
Diaspore with V_term at height H at time T

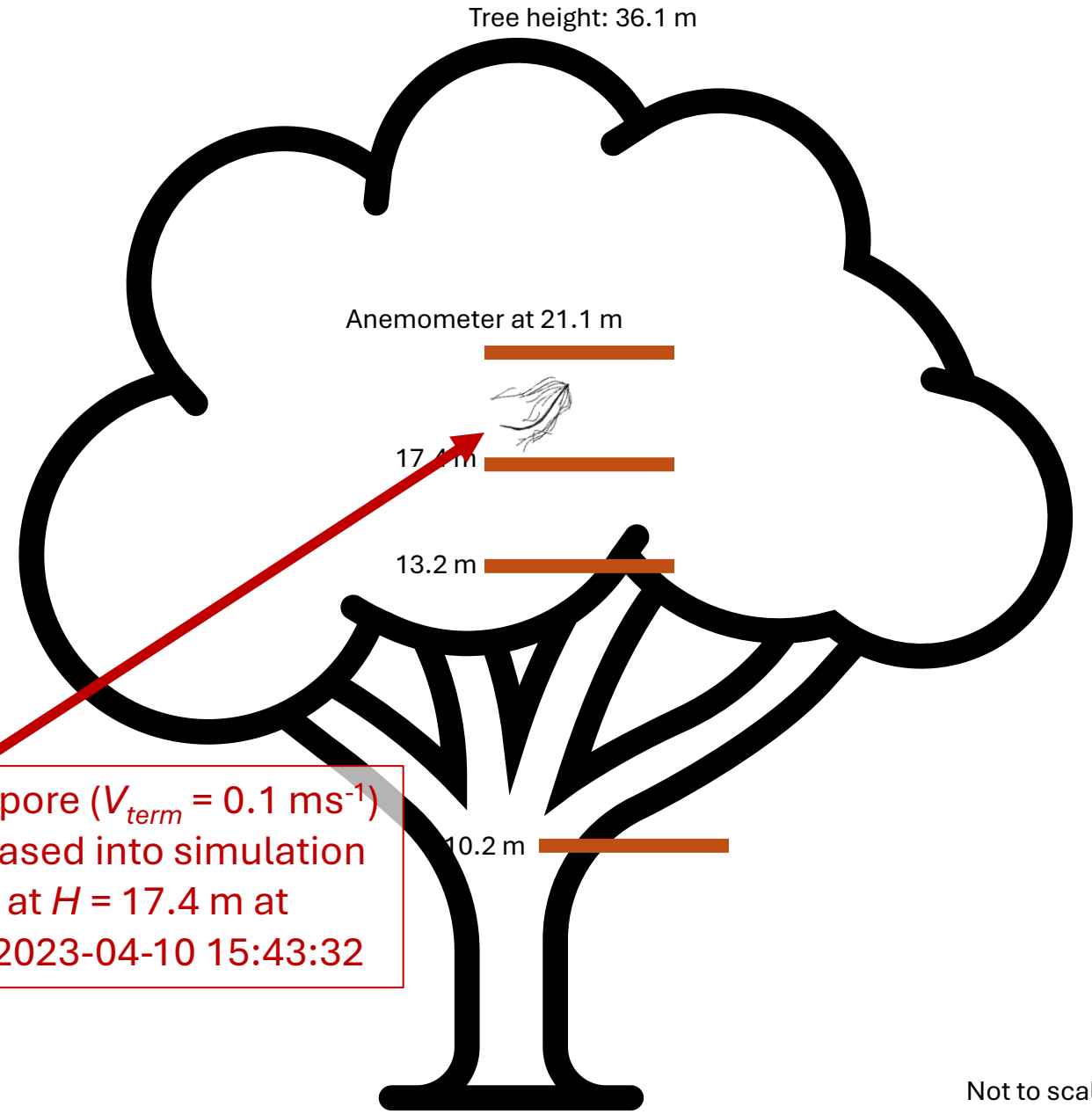
Tree height: 36.1 m
Anemometer at 21.1 m
17.4 m
13.2 m
10.2 m
Diaspore (V_{term} = 0.1 ms^{-1}) released into simulation at H = 17.4 m at T = 2023-04-10 15:43:32
Not to scale

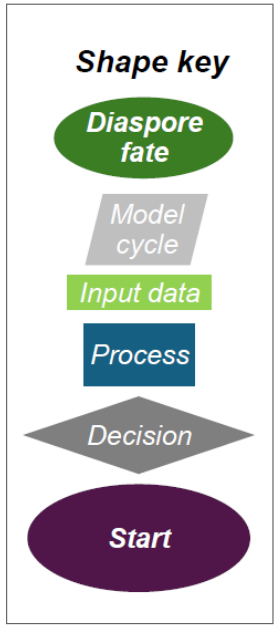

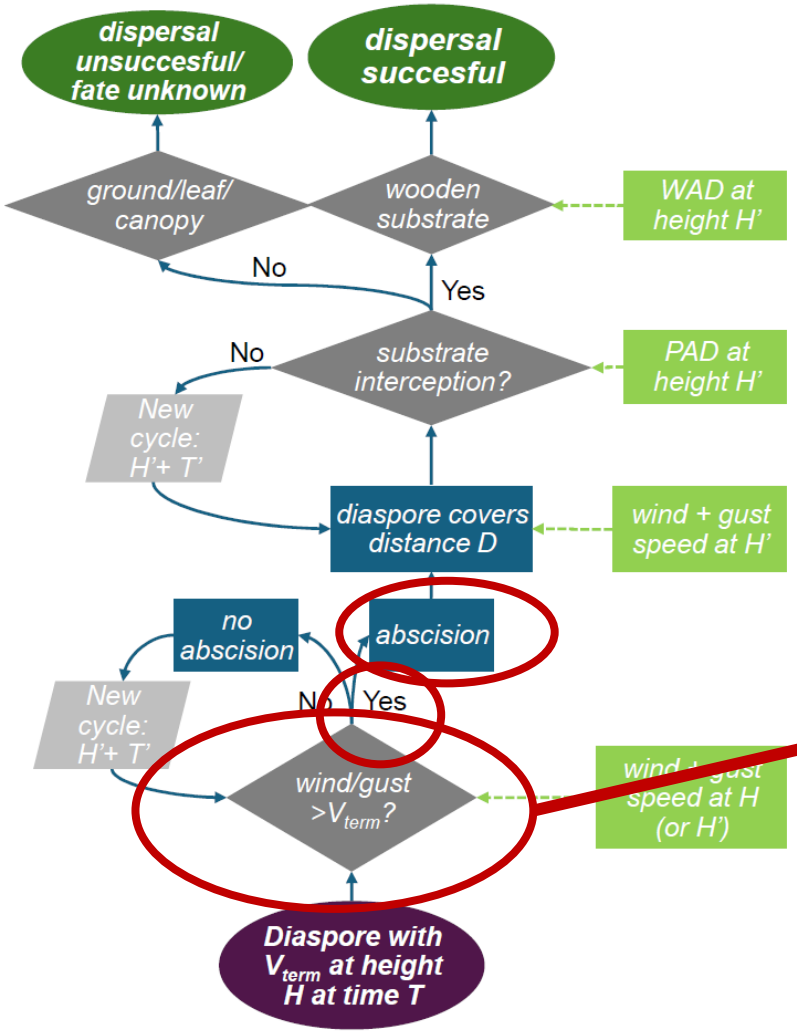

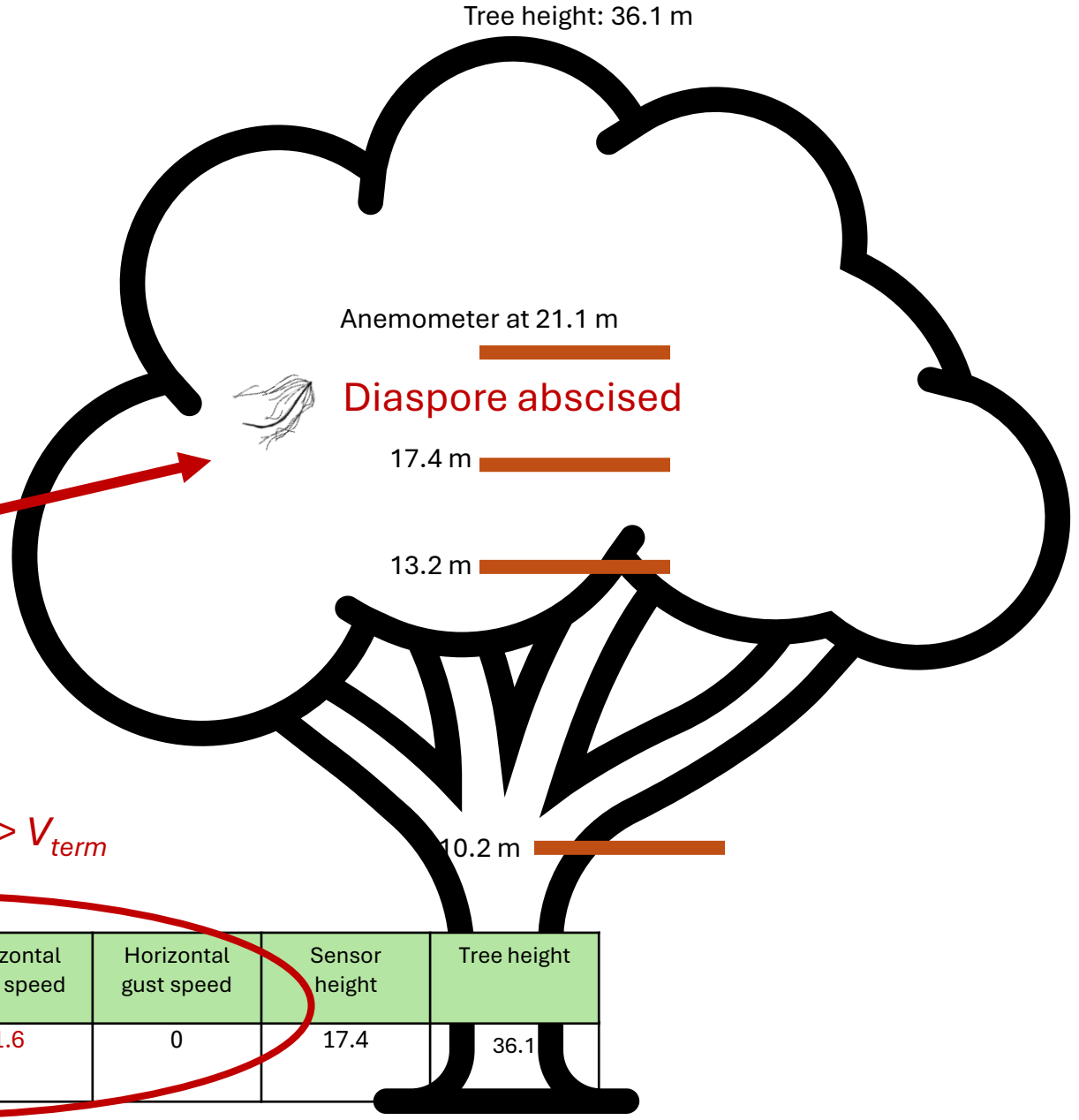

|gust| and |wind| > V_{term}

Datetime	Daytime	Replicate #	Position	Vertical wind speed	Vertical gust speed	Horizontal wind speed	Horizontal gust speed	Sensor height	Tree height
2023-04-10 15:43:32	Late day	11.3	In	0.1	-0.67	1.6	0	17.4	36.1

Additional columns are added now

When a seed was released, at what height, and at what position

True, if a vertical or horizontal gust speed was greater than Vterm terminal velocity (m/s)

Only filled when abscision = T and Time of abscision = NA

Datetime	Seed ID	Time interval (seconds)	Vertical wind speed	Vert. gust speed	Horizontal wind speed	Hor. gust speed	Sensor height = Original release height	Tree height	Vterm	Abscision	Time of abs.
2023-04-10 21:43:32	2023-04-10 21:43:32 __ 10.2 m __ Out	3	0.1	0.33	1.6	-2.3	10.2	36.1	0.1	T	2023-04-10 21:43:32
2023-04-10 21:43:32	2023-04-10 21:43:32__ 10.2 m __ Out	3	0	0	0	0	13.2	36.1	0.1	F	NA
2023-04-10 21:43:32	2023-04-10 21:43:32__ 10.2 m __ Out	3	0.1	-0.67	1.6	0	17.4	36.1	0.1	T	2023-04-10 21:43:32
2023-04-10 21:43:32	2023-04-10 21:43:32__ 10.2 m __ Out	3	0.1	0	1.6	1.2	21.1	36.1	0.1	T	2023-04-10 21:43:32

Calculating vertical and horizontal distances:

$$D_w = \sum \begin{cases} \frac{w' + 2\overline{w}}{3} - V_{term}), & if \ \frac{w' + 2\overline{w}}{3} > V_{term} \\ \frac{w' + 2\overline{w}}{3}, & if \ \frac{w' + 2\overline{w}}{3} < V_{term} \end{cases}$$

and $D_u = \sum \left(\frac{1}{3}u' + \frac{2}{3}\bar{u}\right) t$

(Equations 1a and 1b),

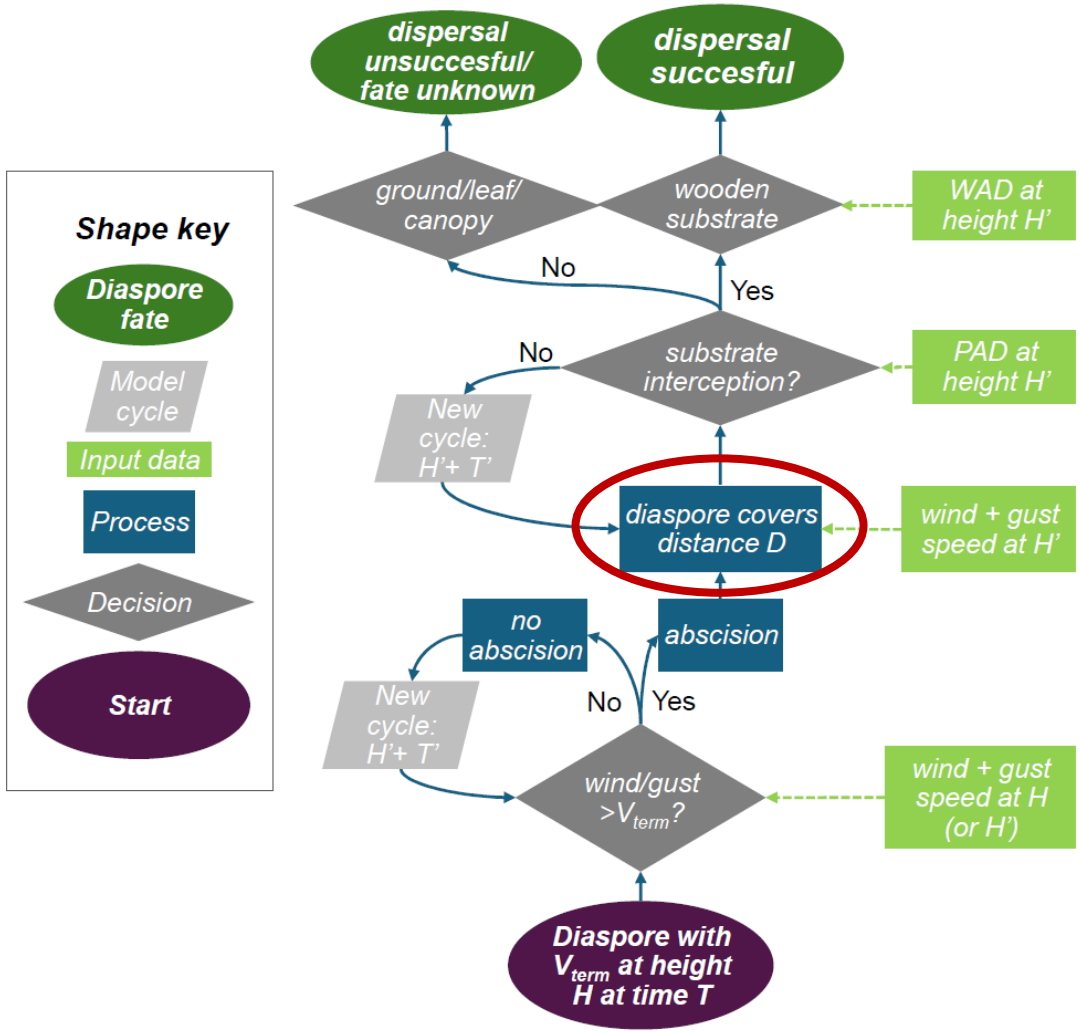

where D_w and D_u are the sum of the vertical and horizontal dispersal distances, $w'$and u' the vertical and horizontal gust speeds, $\overline{w}$ and $\overline{u}$ the 1-minute vertical and horizontal wind averages, t is the time interval and V_{term} the terminal velocity of a seed. The vertical distance was corrected for the apparent speed, meaning that the falling velocity did not affect the downward motion if winds were equal to or more negative than the falling velocity. For example, a seed with a terminal velocity of 0.1 m/s in a down-gust of 0.2 m/s does not fall at 0.3 m/s but at 0.2 m/s; conversely, a seed with a falling velocity of 0.5 m/s falls at 0.5 m/s. Wind vectors of the same direction cancel out; hence, the more negative value determines the downward distance.

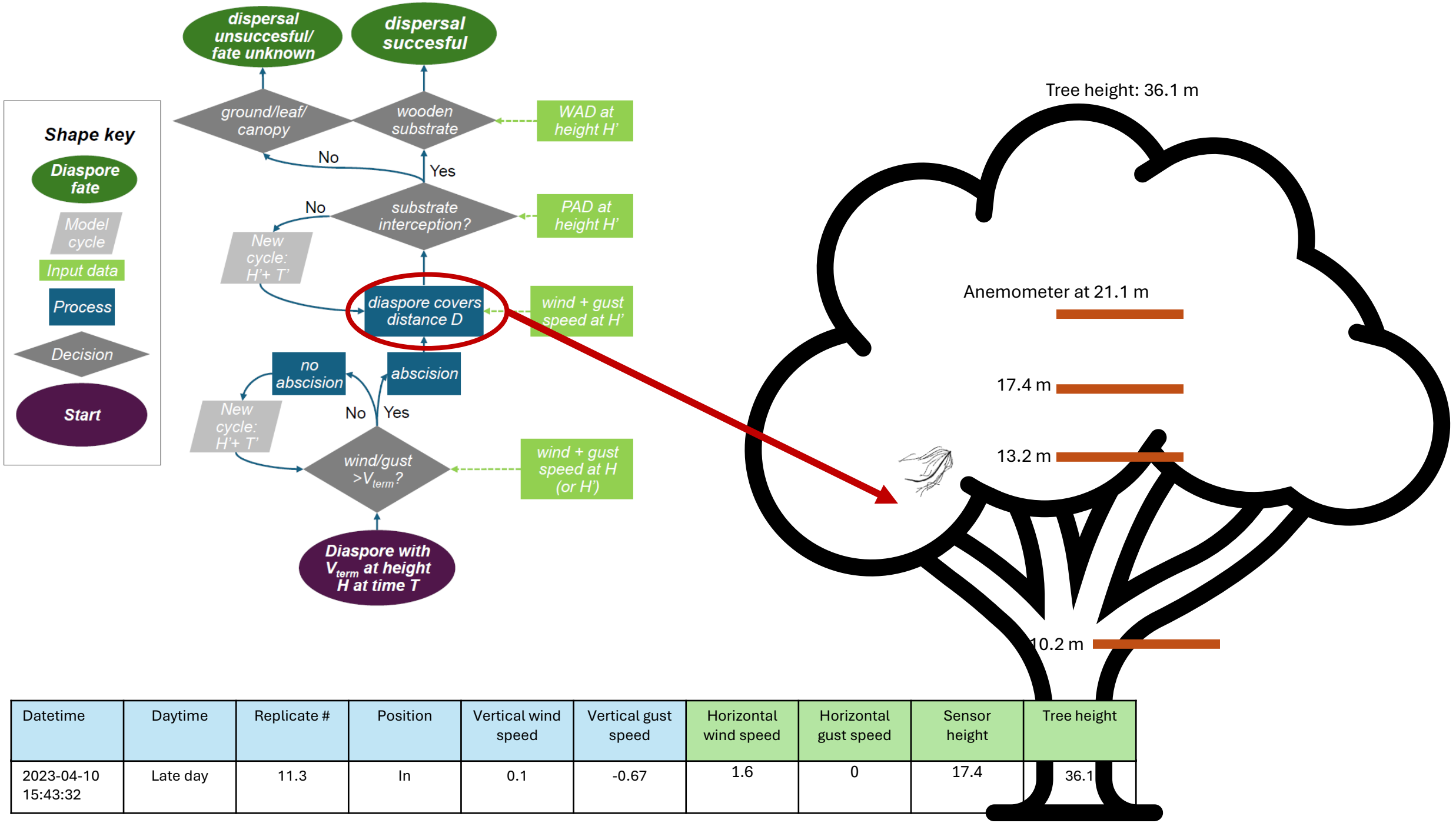

Datetime	Daytime	Replicate #	Position	Vertical wind speed	Vertical gust speed	Horizontal wind speed	Horizontal gust speed	Sensor height	Tree height
2023-04-10 15:43:32	Late day	11.3	In	0.1	-0.67	1.6	0	17.4	36.1

Calculating substrate interception proability

$$I_{Pw} = 1 - exp(-PAD\ |D_w|) \quad \text{or}$$

$$I_{Pu} = 1 - exp(-PAD\ |D_u|)$$

(Equations 2a and 2b)

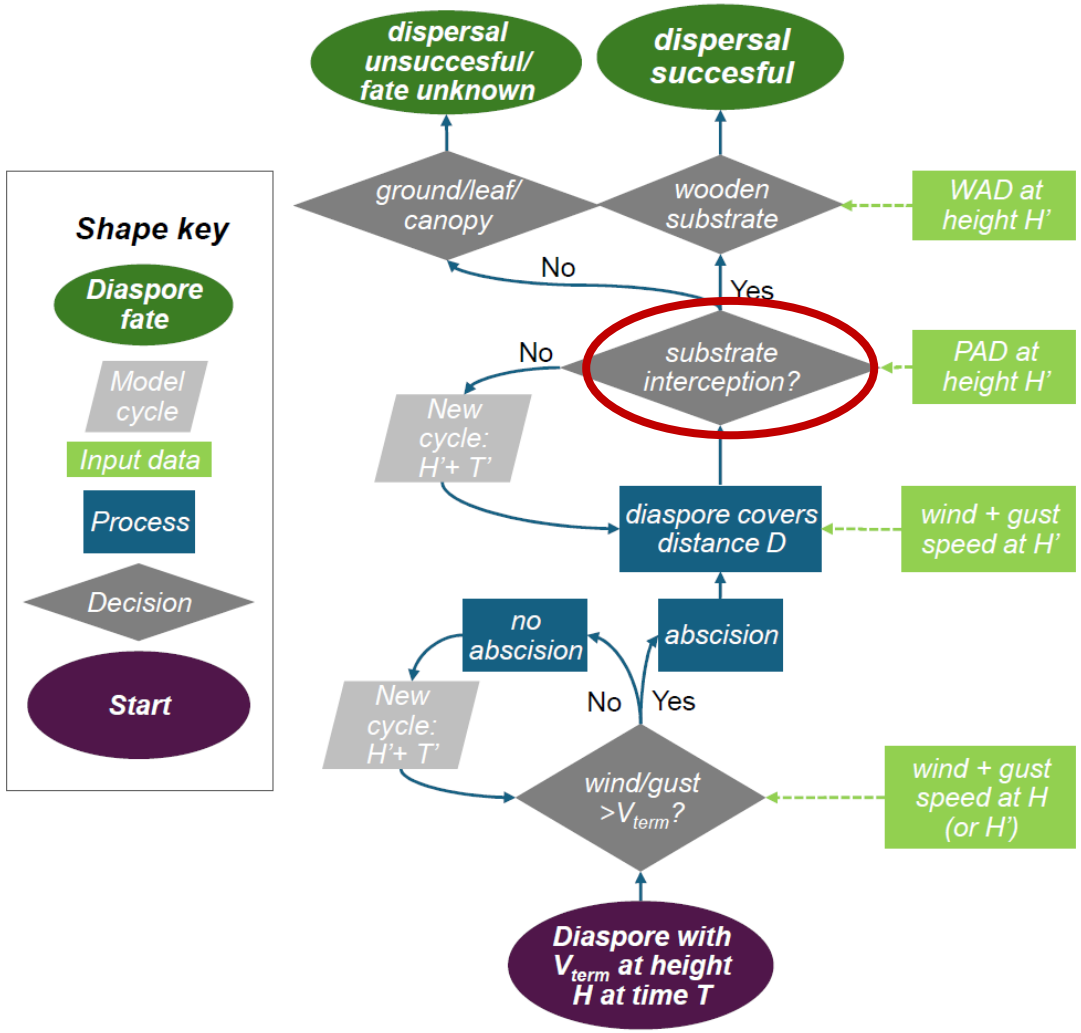

Where I_{Pw} and I_{Pv} are the probabilities that a diaspore is intercepted during the horizontal (P_u) or vertical (P_v) trajectory, ($|D_u|$ or $|D_v|$) the absolute horizontal or vertical distance it travels, and *PAD* is the plant area density (*PAD*) at height H.

The model generates a random number (*R*) between 0 and 1. When $R < P_u$ or $R < P_v$, interception occurs. Specifically, when *R* < wood area density (*WAD),* it was intercepted by wood and considered **successful.**

Calculating substrate interception proability

$$I_{Pw} = 1 - exp(-PAD\ |D_w|) \quad \text{or}$$

$$I_{Pu} = 1 - exp(-PAD\ |D_u|)$$

(Equations 2a and 2b)

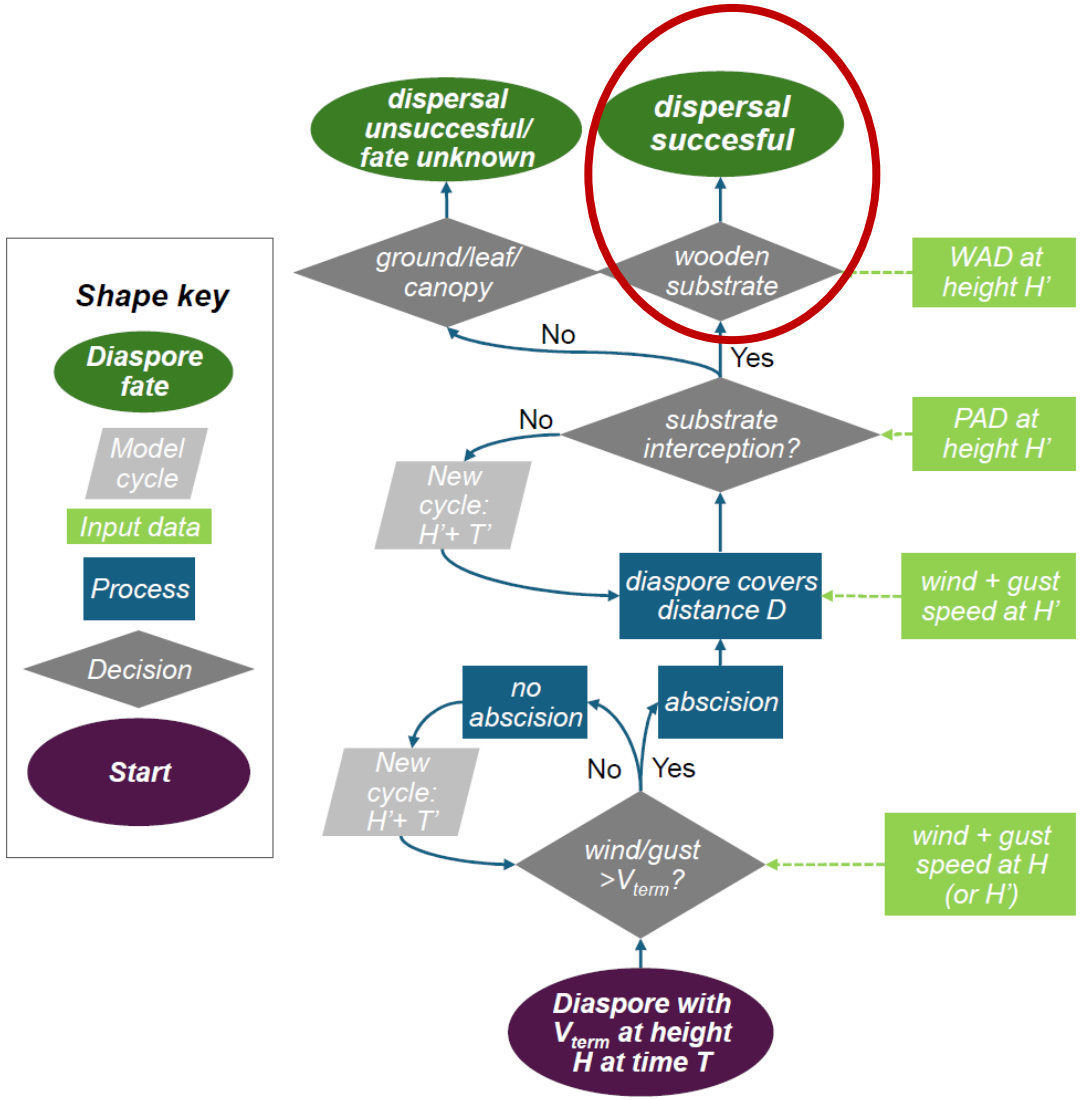

When random number *R* < wood area density (*WAD)*, it was intercepted by wood and considered **successfully dispersed**

Calculating substrate interception proability

$$I_{Pw} = 1 - exp(-PAD\ |D_w|) \quad \text{or}$$

$$I_{Pu} = 1 - exp(-PAD\ |D_u|)$$

(Equations 2a and 2b)

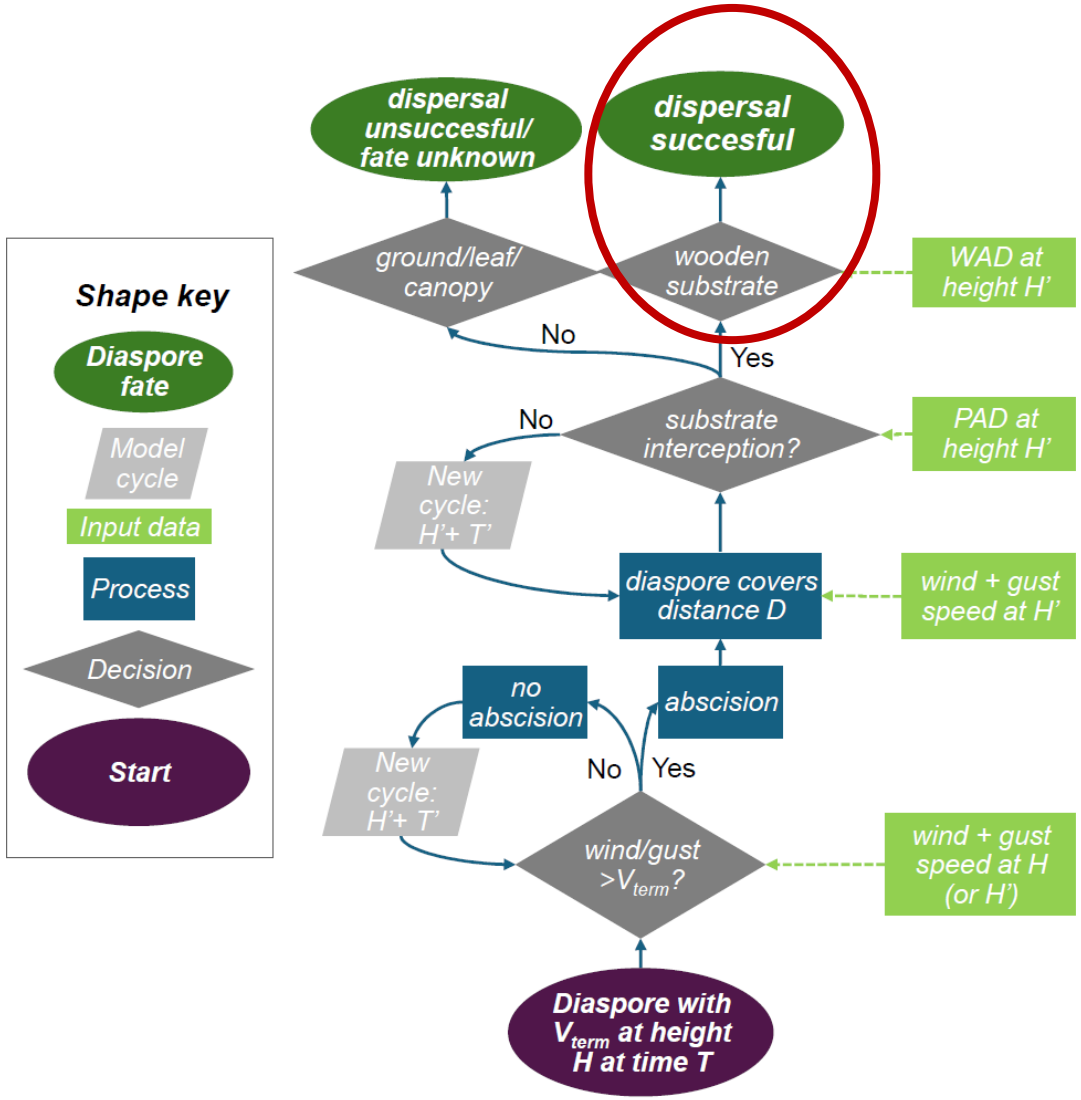

When random number *R* > wood area density (*WAD) but* < *PAD* it was intercepted by a leaf and considered **unsuccessfully dispersed.**

Calculating substrate interception proability

$$I_{Pw} = 1 - exp(-PAD\ |D_w|) \quad \text{or}$$

$$I_{Pu} = 1 - exp(-PAD\ |D_u|)$$

(Equations 2a and 2b)

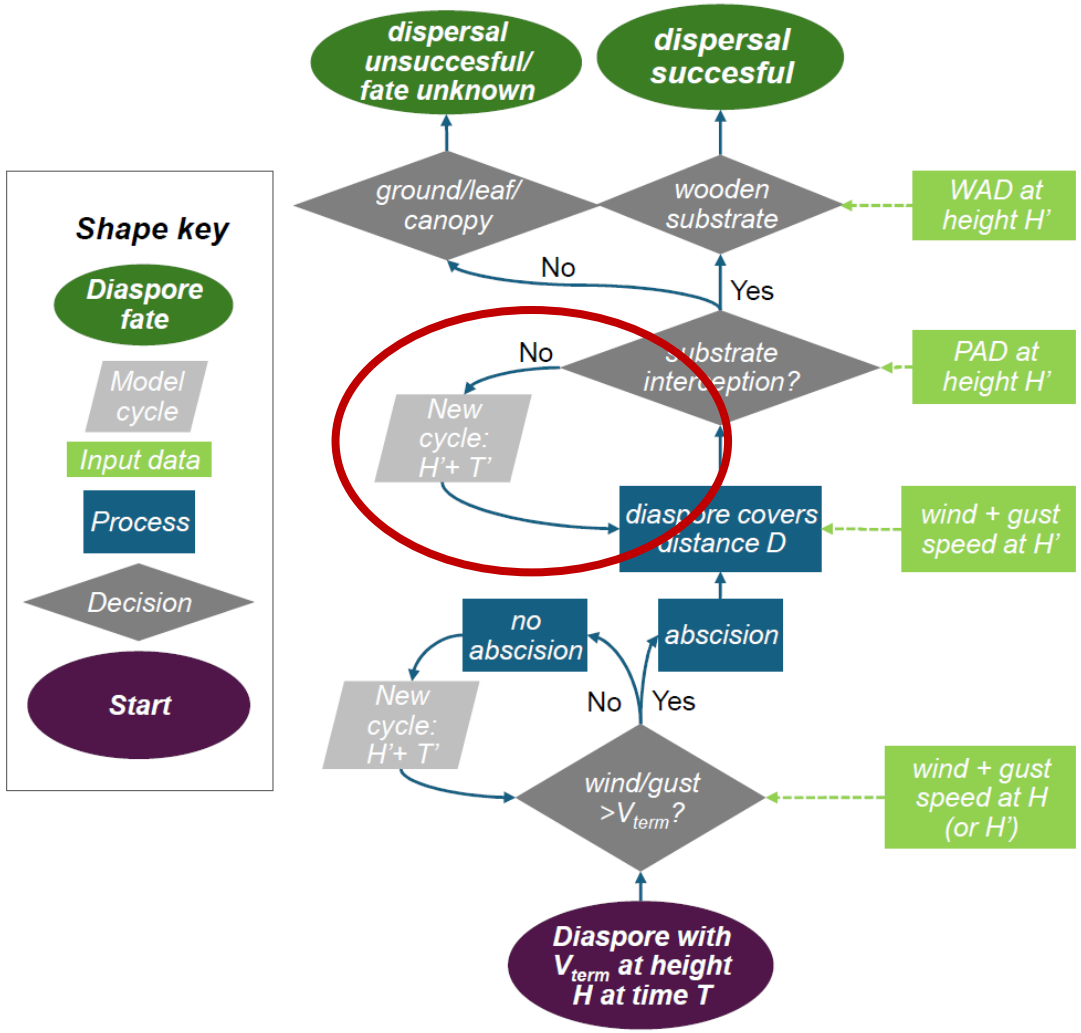

When random number R > PAD, it was not intercepted and the simulation continued

Additional columns are added now

Calculated using equations 1 and 2

The new distances were added to the value present here. First iteration = 0

Explained in the next slide

Date time	Seed ID	Time interval (s)	Vert. wind speed	Vert. gust speed	Hor.wind speed	Hor. gust speed	Sensor height = Original release height	Tree height	Vterm	Ab-scision	Time of abs.	New vert. dis-tance	New hor. dis-tance	Sum vert. distance	Sum hor. distance	New release height
2023-04-10 21:43:32	2023-04-10 21:43:32 __ 10.2 m __ Out	3	0.1	0.33	1.6	-2.3	10.2	36.1	0.1	T	2023-04-10 21:43:32	0.23	2.43	0 + 0.21 = 0.21	0 + 2.43 = 2.43	10.2
2023-04-10 21:43:32	2023-04-10 21:43:32_ _ 10.2 m __ Out	3	0	0	0	0	13.2	36.1	0.1	F	NA	0	0	0	0	13.2
2023-04-10 21:43:32	2023-04-10 21:43:32_ _ 10.2 m __ Out	3	0.1	-0.67	1.6	0	17.4	36.1	0.1	T	2023-04-10 21:43:32	-0.67	3.2	0 + 0.32 = 0.32	0 + 3.2 = 3.2	17.4
2023-04-10 21:43:32	2023-04-10 21:43:32_ _ 10.2 m __ Out	3	0.1	0	1.6	1.2	21.1	36.1	0.1	T	2023-04-10 21:43:32	0	3.6	0	0 + 3.6 = 3.6	21.1

If the total vertical distance travelled by a seed exceeded a higher or lower sensor, that sensor was used for the next wind calculations. For example:

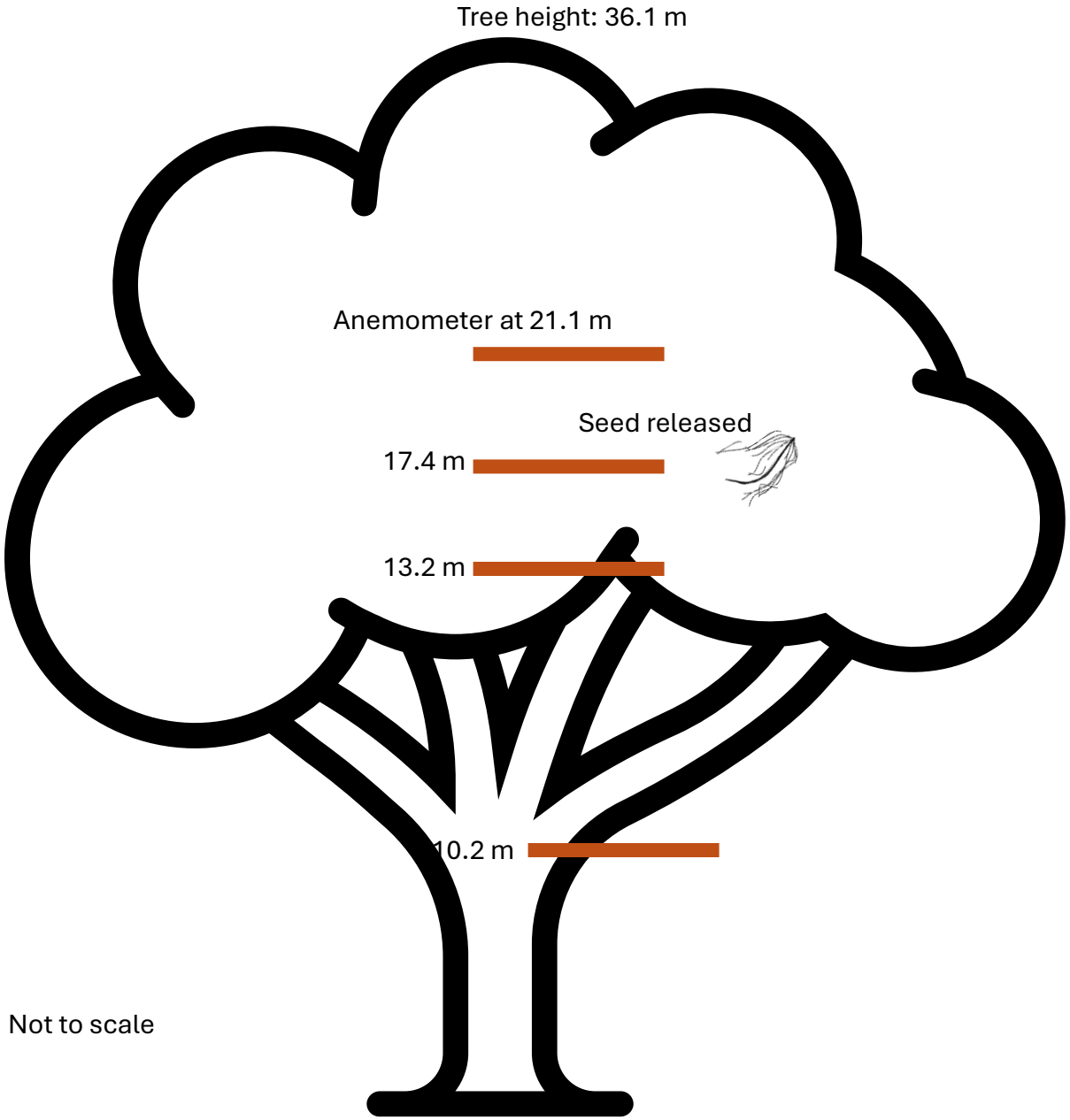

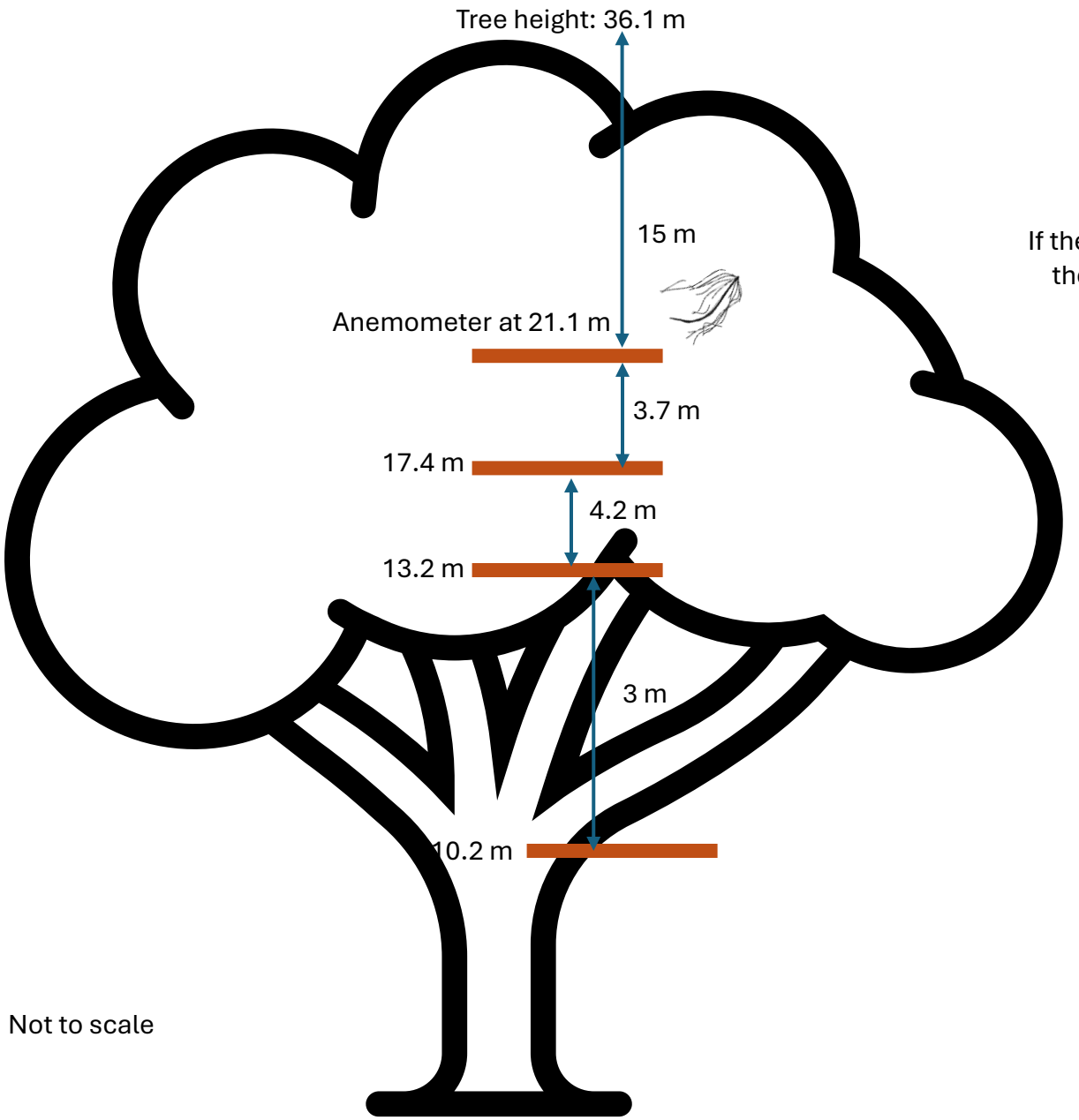

Not to scale

If the vertical distance travelled is equal to or greater than 3.7, the winds/igusts measured at 21.1 m height will affect the seeds trajectoy n the next loop

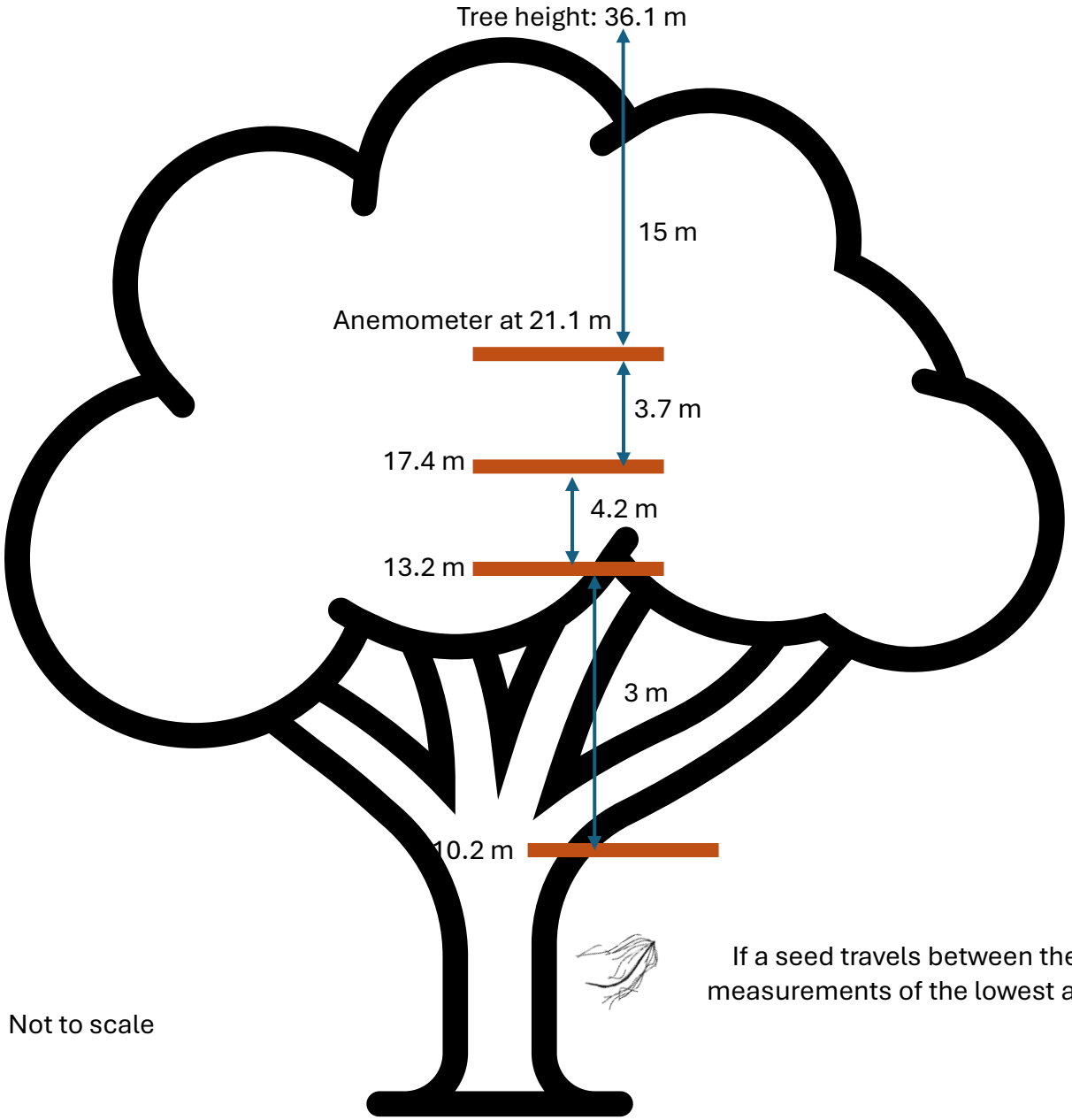

Not to scale

If a seed travels between the ground and the lowest anemometer, the measurements of the lowest anemometer will affect the seed's trajectory

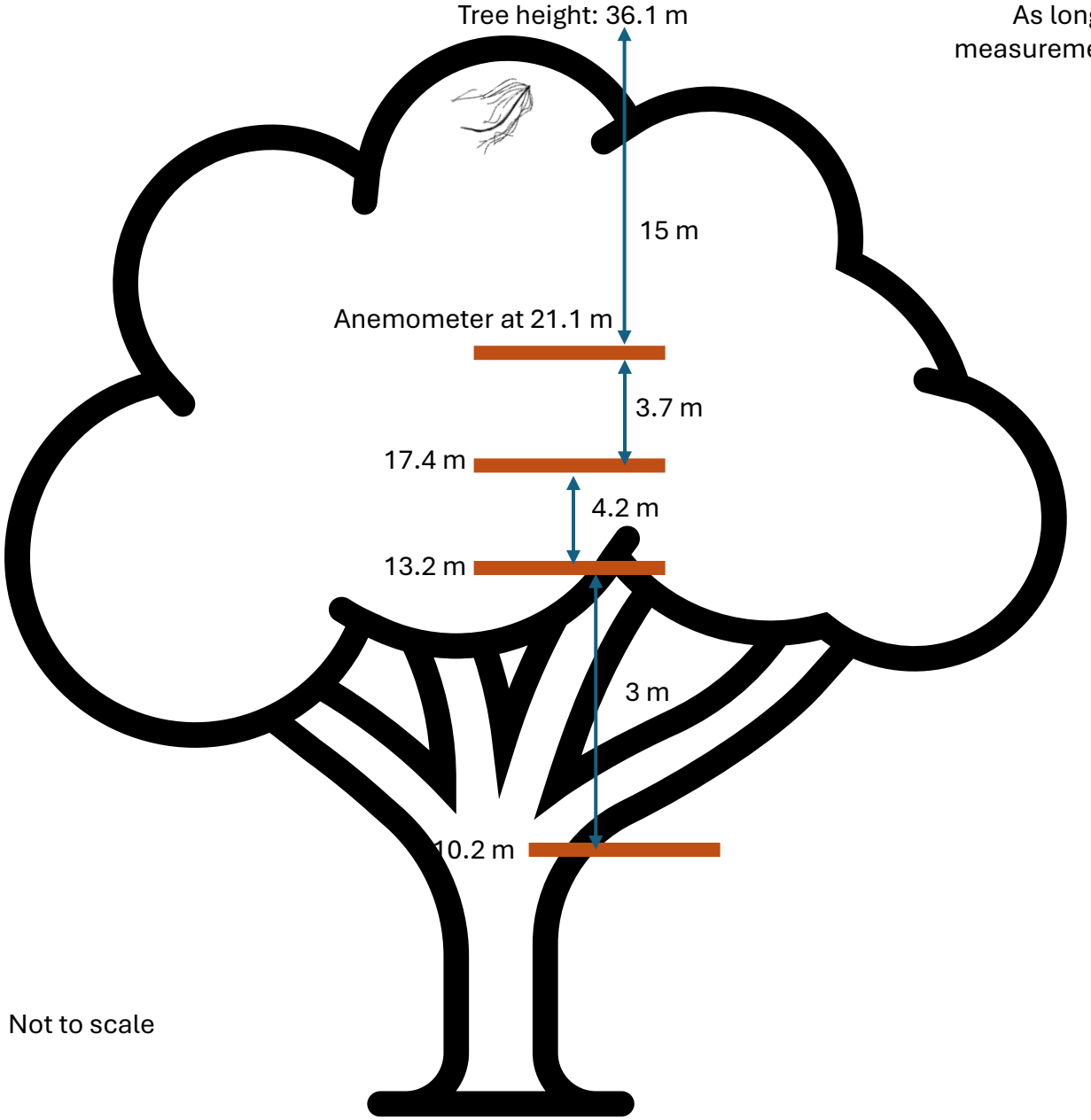

Not to scale

As long as the seed is below or at tree height, the measurements of highest anemometer affect its trajectory

Once the diaspore is intercepted, new columns are generated:

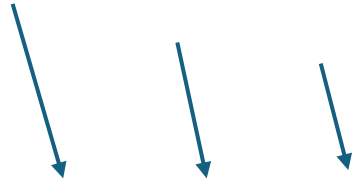

Date time	Seed ID	Time interval (s)	Vert. wind speed	Vert. gust speed	Hor.wind speed	Hor. gust speed	Sensor height = Original release height	Tree height	Vterm	Ab-scision	Time of abs.	New vert. dis-tance	New hor. dis-tance	Sum vert. distance	New release height	Inter-cepti-on	Inter-ception by wood	Height at inter-ception
2023-04-10 21:43:32	2023-04-10 21:43:32 __ 10.2 m __ Out	3	0.1	0.33	1.6	-2.3	10.2	36.1	0.1	T	2023-04-10 21:43:32	0.23	2.43	0 + 0.21 = 0.21	10.2	T	T	10.2 + 0.23 = 10.53
2023-04-10 21:43:32	2023-04-10 21:43:32_ _ 10.2 m __ Out	3	0	0	0	0	13.2	36.1	0.1	F	NA	0	0	0	13.2	NA	NA	NA
2023-04-10 21:43:32	2023-04-10 21:43:32_ _ 10.2 m __ Out	3	0.1	-0.67	1.6	0	17.4	36.1	0.1	T	2023-04-10 21:43:32	-0.67	3.2	0 + 0.32 = 0.32	17.4	F	NA	NA
2023-04-10 21:43:32	2023-04-10 21:43:32_ _ 10.2 m __ Out	3	0.1	0	1.6	1.2	21.1	36.1	0.1	T	2023-04-10 21:43:32	0	3.6	0	21.1	T	F	21.1 + 0 = 21.1

If seeds remain in the loop, results from previous iteration are added to the new iteration

New seeds

Datetime	Seed ID	Time interval (seconds)	Vertical wind speed	Vert. gust speed	Horizontal wind speed	Hor. gust speed	Sensor height = Original release height	Tree height	Vterm	Abscision	Time of abs.	New vert. distance	New hor. Distance	Sum vert. distance	Sum hor. distance	New release height
2023-04-10 21:43:33	2023-04-10 21:43:33 __ 10.2 m __ Out	3	0	0	0	0	10.2	36.1	0.1	F	NA	0	0	0	0	10.2
2023-04-10 21:43:33	2023-04-10 21:43:33__ 10.2 m __ Out	3	0.1	0.3	-1	-0.7	13.2	36.1	0.1	T	**2023-04-10 21:43:33**	0.2	-2.23	0 + 0.2 = 0.2	0 – 2.23 = -2.23	13.2
2023-04-10 21:43:33	2023-04-10 21:43:33__ 10.2 m __ Out	3	0	0	0	0	17.4	36.1	0.1	F	NA	0	0	0	0	17.4
2023-04-10 21:43:33	2023-04-10 21:43:33__ 10.2 m __ Out	3	0	0	0	0	21.1	36.1	0.1	F	NA	0	0	0	0	21.1
Old seeds with old ID, but with new datetime and new wind/gust measurements.																
2023-04-10 21:43:33	2023-04-10 21:43:32 __ 10.2 m __ Out	3	0	0	0	0	10.2	36.1	0.1	F	2023-04-10 21:43:32	0	0	0.21 + 0 = 0.21	2.43 + 0 = 2.43	10.2
2023-04-10 21:43:33	2023-04-10 21:43:32__ 10.2 m __ Out	3	0.1	0.3	-1	-0.7	13.2	36.1	0.1	T	**2023-04-10 21:43:33**	0.2	-2.23	0.2 + 0 = 0.2	0 - 2.23 = -2.33	13.2
2023-04-10 21:43:33	2023-04-10 21:43:32__ 10.2 m __ Out	3	0	0	0	0	17.4	36.1	0.1	F	2023-04-10 21:43:32	0	0	0 + 0.32 = 0.32	3.2 + 0 = 3.2	17.4
2023-04-10 21:43:33	2023-04-10 21:43:32__ 10.2 m __ Out	3	0	0	0	0	21.1	36.1	0.1	F	2023-04-10 21:43:32	0	0	0	3.6 + 0 = 3.6	21.1

Example: a seed moves into a new category

Datetime	Seed ID	Time interval (seconds)	Vertical wind speed	Vert. gust speed	Horizontal wind speed	Hor. gust speed	Sensor height = Original release height	Tree height	Vterm	Abscision	Time of abs.	New vert. distance	New hor. Distance	Sum vert. distance	Sum hor. distance	New release height
2023-04-10 21:50:30	2023-04-10 21:43:33 __ 10.2 m __ Out	3	0	0	0	0	10.2	36.1	0.1	F	2023-04-10 21:43:35	0	0	2.5	0	10.2

Datetime	Seed ID	Time interval (seconds)	Vertical wind speed	Vert. gust speed	Horizontal wind speed	Hor. gust speed	Sensor height = Original release height	Tree height	Vterm	Abscision	Time of abs.	New vert. distance	New hor. Distance	Sum vert. distance	Sum hor. distance	New release height
2023-04-10 21:50:33	2023-04-10 21:43:33 __ 10.2 m __ Out	3	1	2	0	0	10.2	36.1	0.1	F	2023-04-10 21:43:35	2.67	0	2.5 + 2.67 = 5.17	0	13.2

An upward dispersal of 5.17 m, in this case, exceeds the height of the next highest anemometer

The measurements of this anemometer are now used to calculate the further trajectory

The iterations continue until the last datetime in a data frame is reached, and then begin anew with a different terminal velocity. All seeds dispersed beyond the tree height or to the ground are stored in a separate dataframe. All seeds still unabscised or travelling within the tree column remain.

Dispersal outcomes

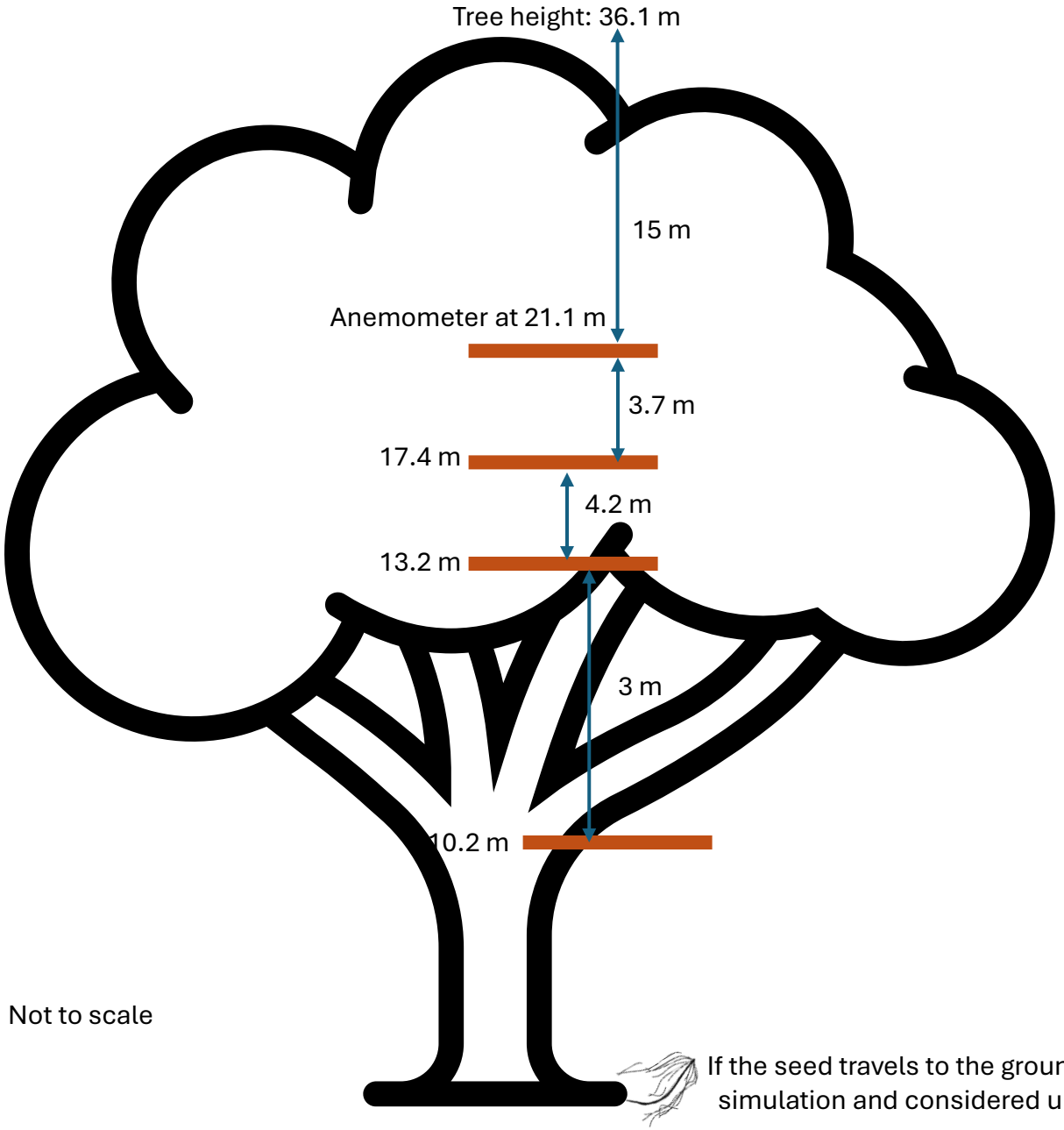

Not to scale

If the seed travels to the ground, it is removed from the simulation and considered unsuccesfully dispersed.

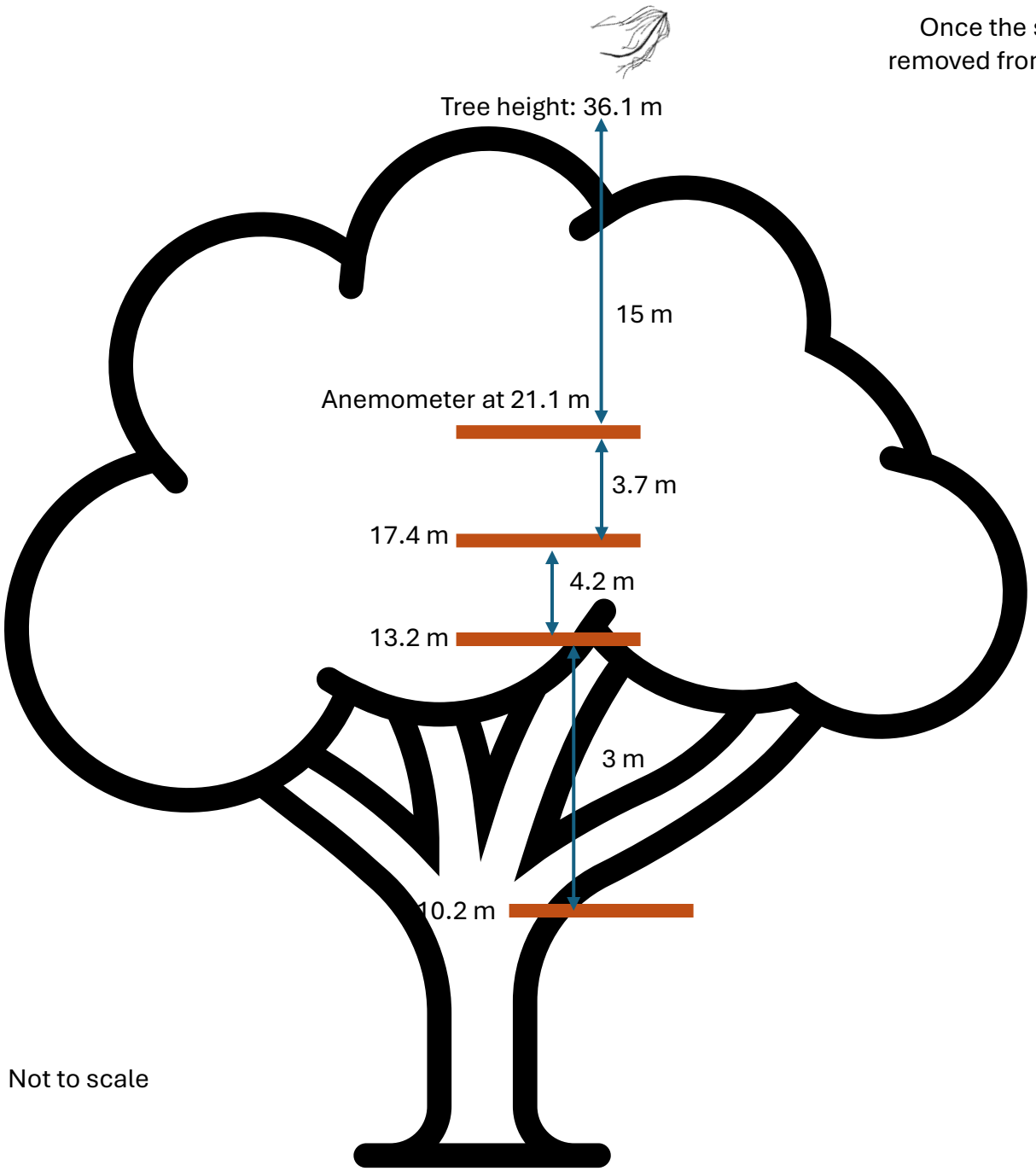

Not to scale

Once the seed has travelled beyond the tree height, it is removed from the simulation. *It now has the chance for long-distance dispersal.*

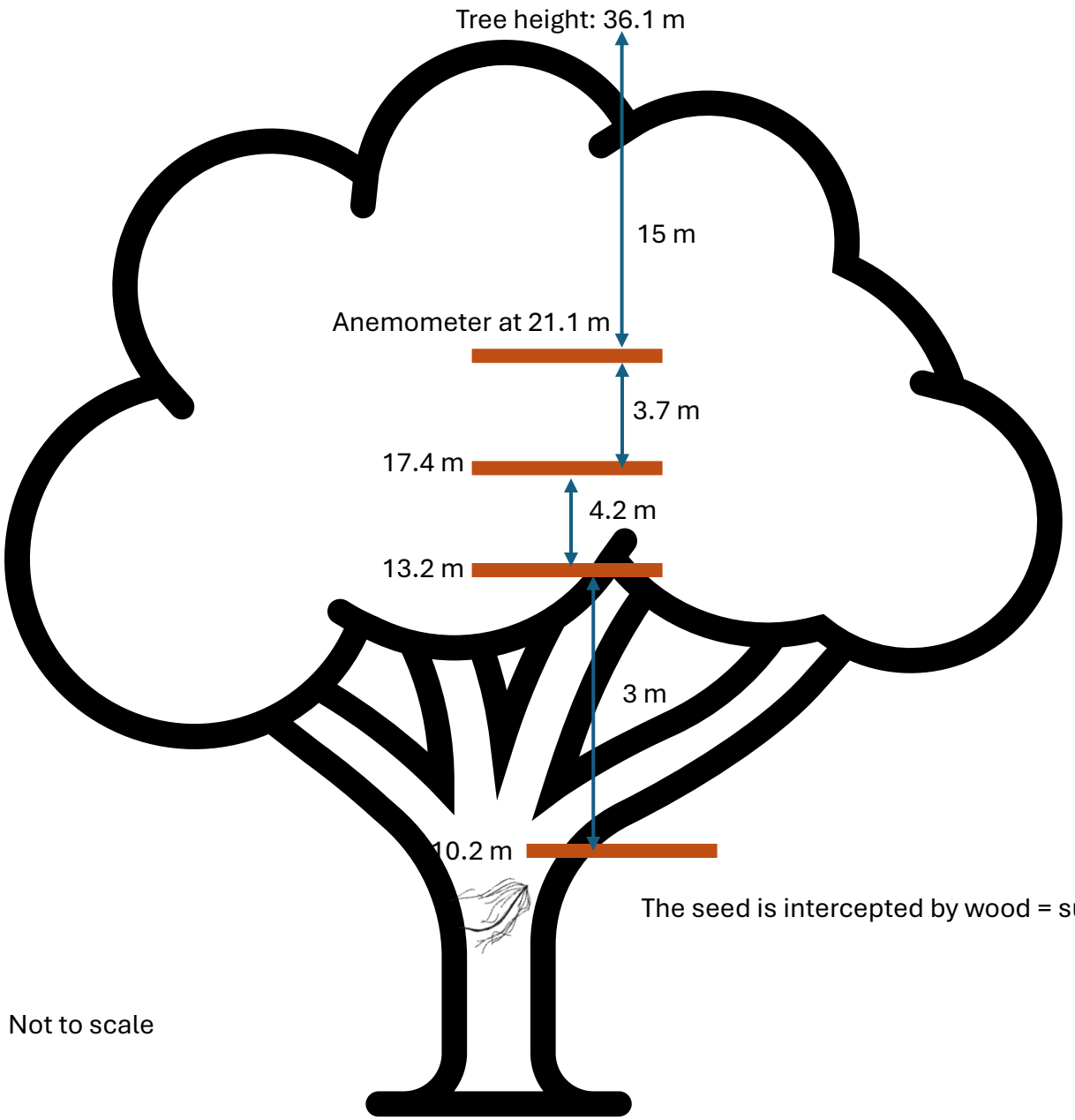

The seed is intercepted by wood = succesful dispersal

Not to scale

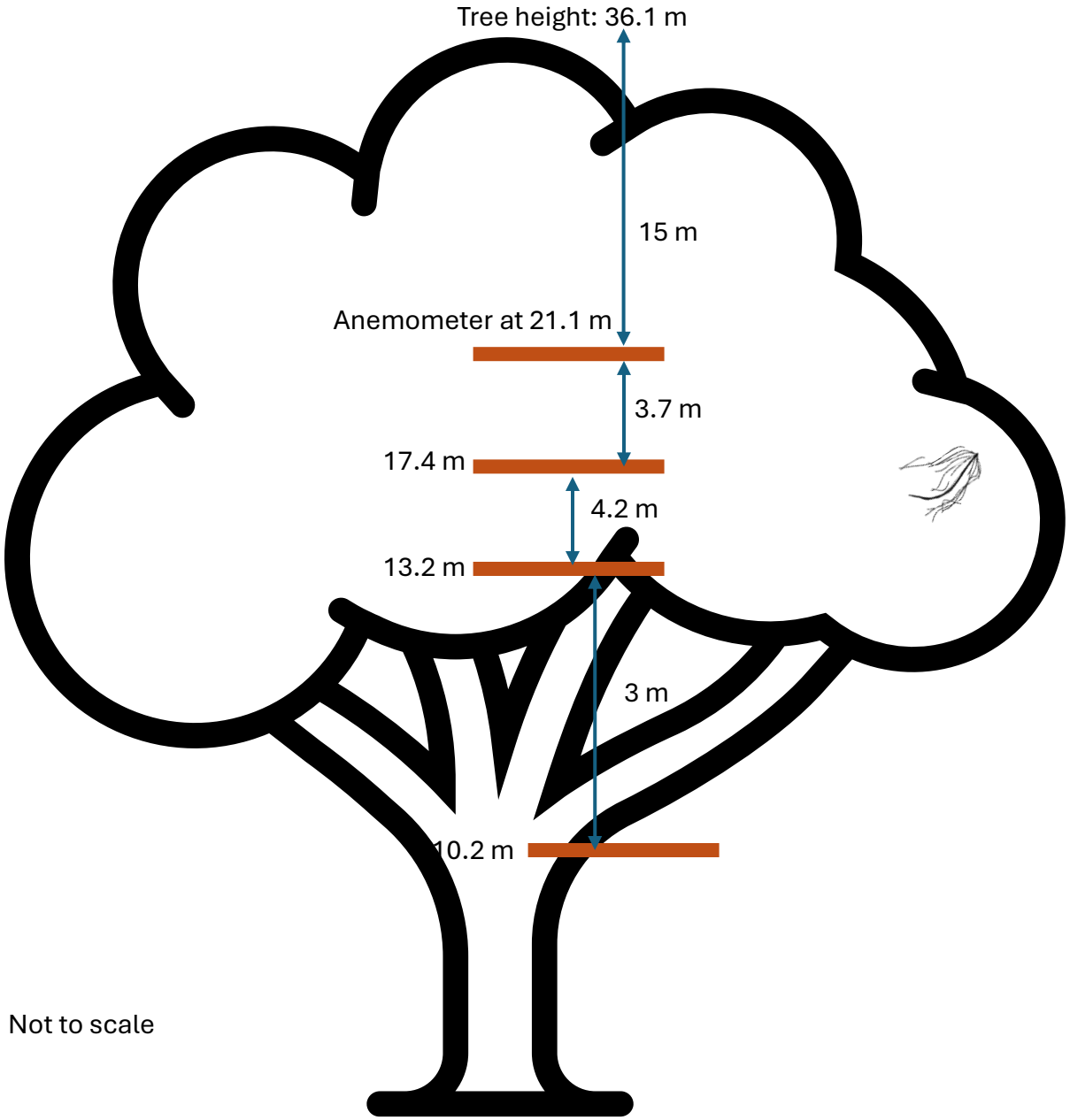

The seed is intercepted by a leaf = unsuccesful dispersal

Not to scale

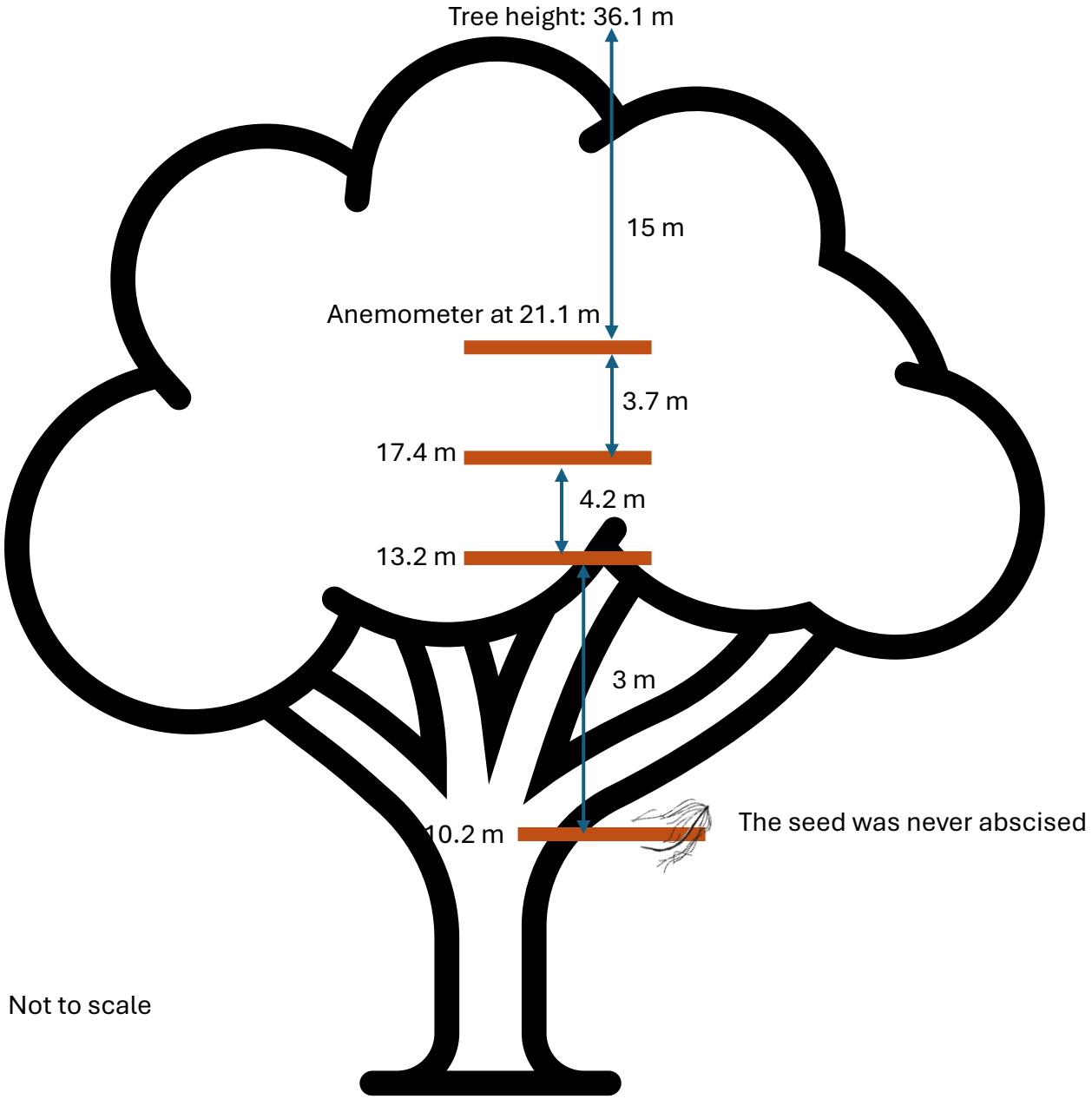
Tree height: 36.1 m
15 m
Anemometer at 21.1 m
3.7 m
17.4 m
4.2 m
13.2 m
3 m
10.2 m
The seed was never abscised

Not to scale

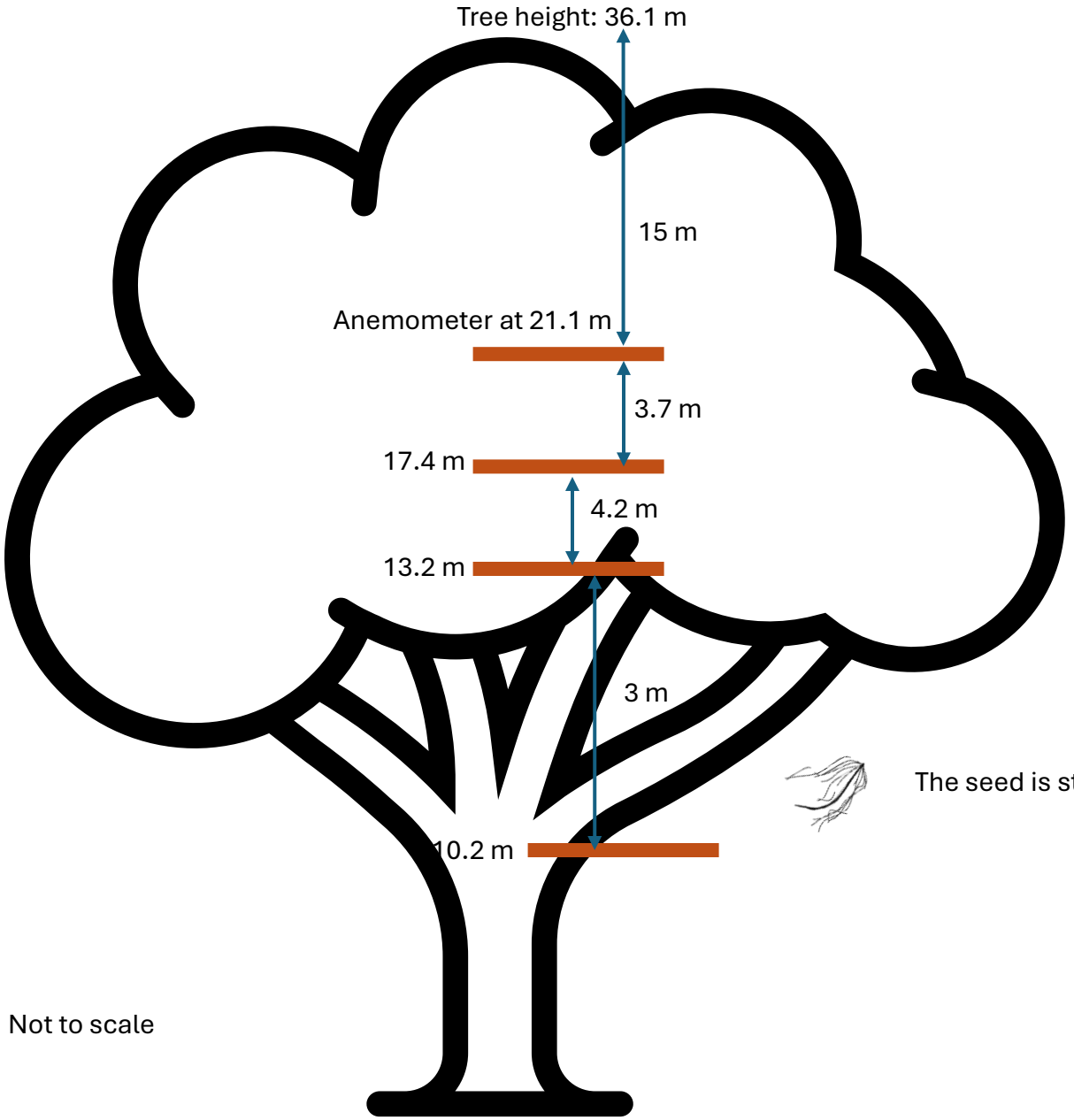

The seed is still «in dispersal» at the end of the simulation

Not to scale

Ecological Monographs

Appendix 4: Additional Results for:

Patterns of wind dispersal within a forest canopy: An epiphyte perspective

Marie Hoensbroech[1], Juliano Sarmento Cabral[2], Gerhard Zotz[1,3]

1: Institute of Biology and Environmental Sciences, Carl von Ossietzky Universität Oldenburg, Ammerländer Heerstr. 114–118, 26129 Oldenburg, Germany

2: Ecological Modelling, Bonner Institute for Organismal Biology — Department of Plant Biodiversity, Universität Bonn, Venusbergweg 22, 53115 Bonn, Germany

3: Smithsonian Tropical Research Institute, Box 0843-03092, Panama, Republic of Panama

Correspondence: Marie Hoensbroech; email: marie.hoensbroech@uni-oldenburg.de

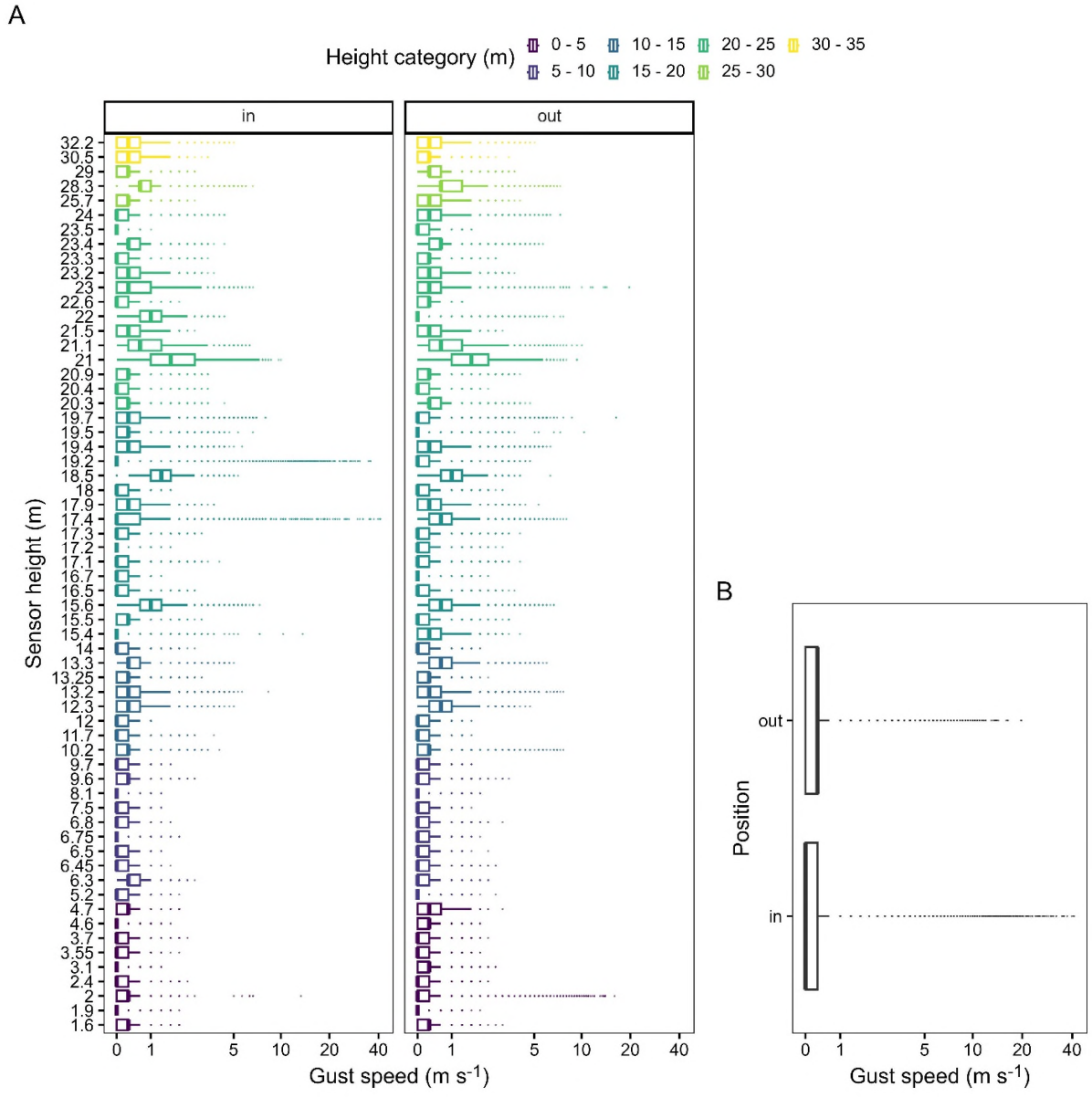

Figure S1. Variation in gust speed (all directions) across anemometer positions and measurement heights. **(A)** Differences in gust speed among replicates across height categories and anemometer positions (in = 0.35 m from the stem; out = 1.35 m from the stem). Boxplots show the median (vertical line), the interquartile range (box), values within 1.5 × the interquartile range (whiskers), and outliers (points). The x-axis is truncated at 1.5 to emphasize the denser range of

the data. **(B)** Differences in gust speed between the in and out anemometer positions, shown as standard boxplots. Although Dunn's test detected a significant difference between positions (compact letter display above the x-axis), the two distributions differ mainly in the frequency and extent of outliers.

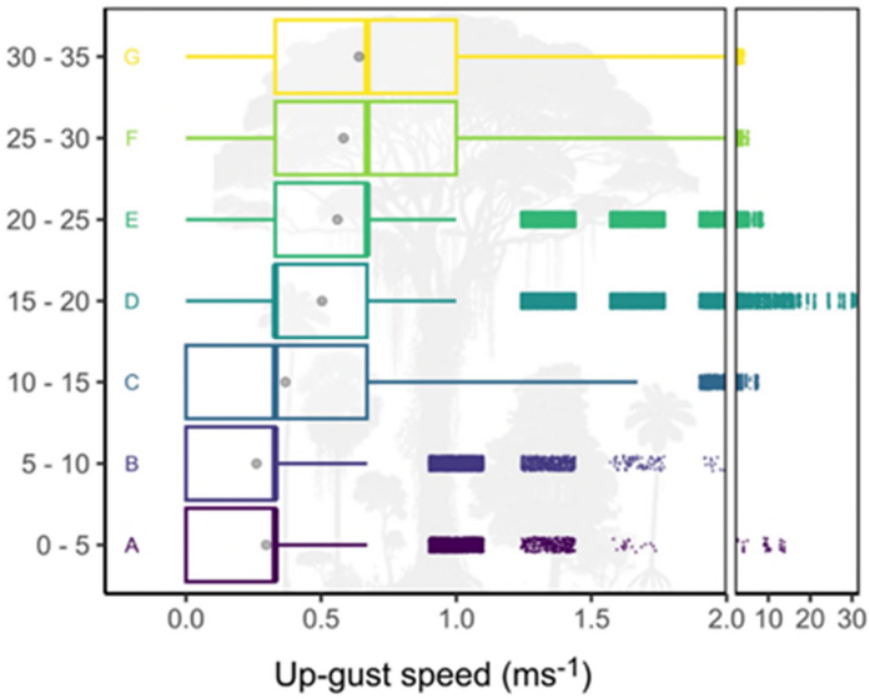

Figure S2. One-minute maximum up-gust speeds measured at different heights within the San Lorenzo forest. Note the axis-break at 2.0 ms^{-1} used to place focus of the denser data areas. Bars indicate medians, boxes the 0.25 and 0.75 quantiles, lines the 1.5 times interquartile range, and points outliers. Grey points inside the boxes show means. The silhouette in the mean panel illustrates forest structure and was adapted by MH from a graphic generated with Microsoft Copilot (Microsoft, 2024).

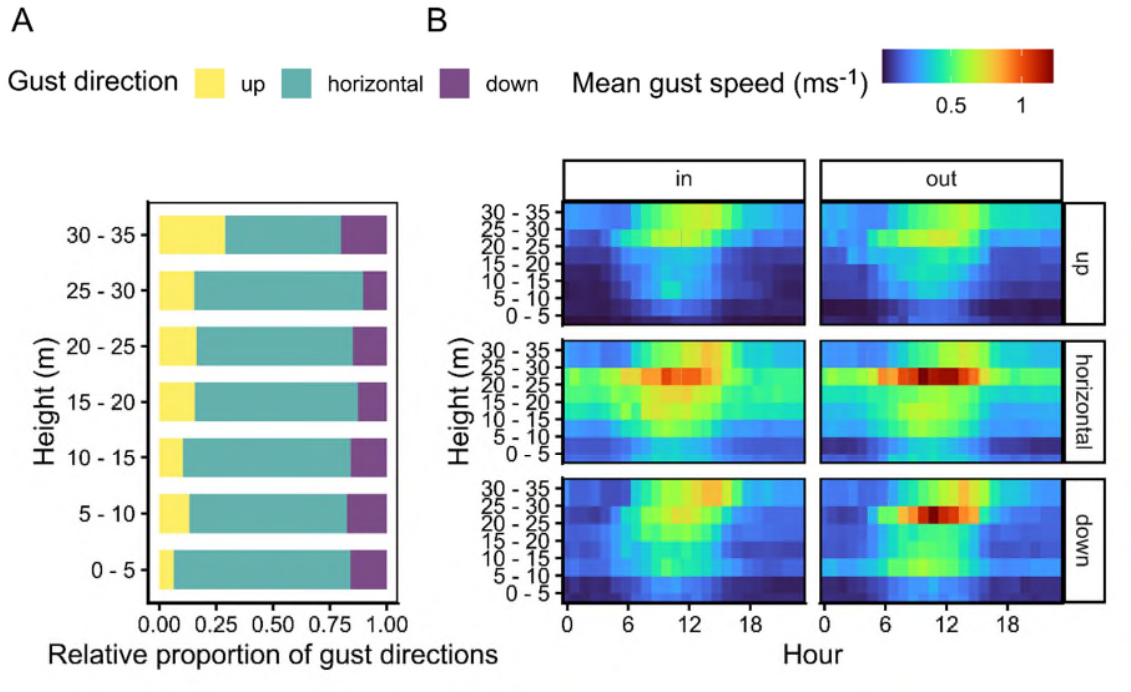

Figure S3. (A) Relative proportion of gust directions (gusts ≥ 0.33 ms^{-1}) per height category. **(B)** Mean gust speeds per hour of the day, based on their moduli (absolute values), separated by distance from stem (in = 0.35 cm, out = 1.35 cm) and gust direction.

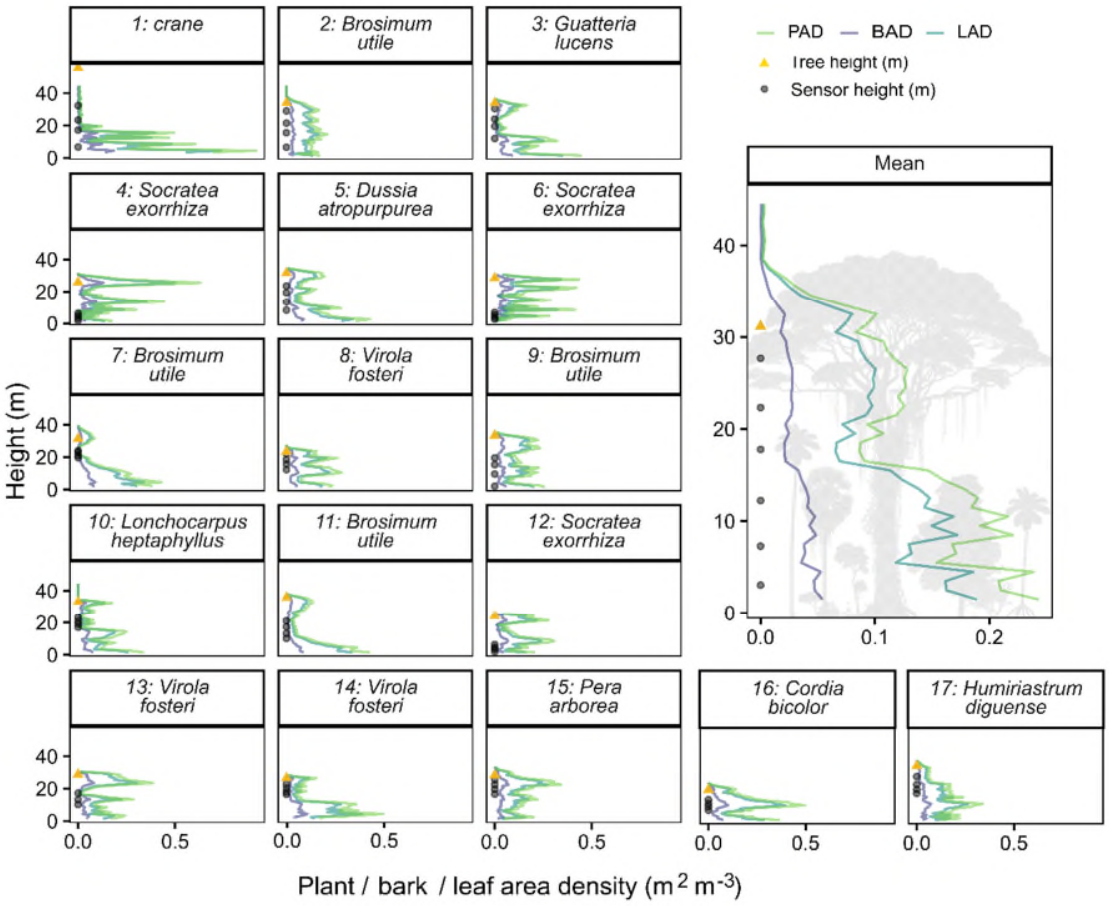

Figure S4. Bark area density (BAD), leaf area density (LAD), and their combination, the plant area density (PAD) along the individual vertical profiles and averaged across all, with the (mean) position of anemometers (grey dots) and tree tops (yellow triangle) shown. Refer to the Materials and Methods section in the main text for their derivation. The silhouette in the mean panel illustrates forest structure and was adapted by MH from a graphic generated with Microsoft Copilot (Microsoft, 2024). PAD was calculated from lidar data provided by Vasquez et al. (2024); the derivation of BAD and LAD leaned heavily on previous censuses at San Lorenzo (Janner & Fernández-Lucero, unpublished data; Ramos et al., 2024).

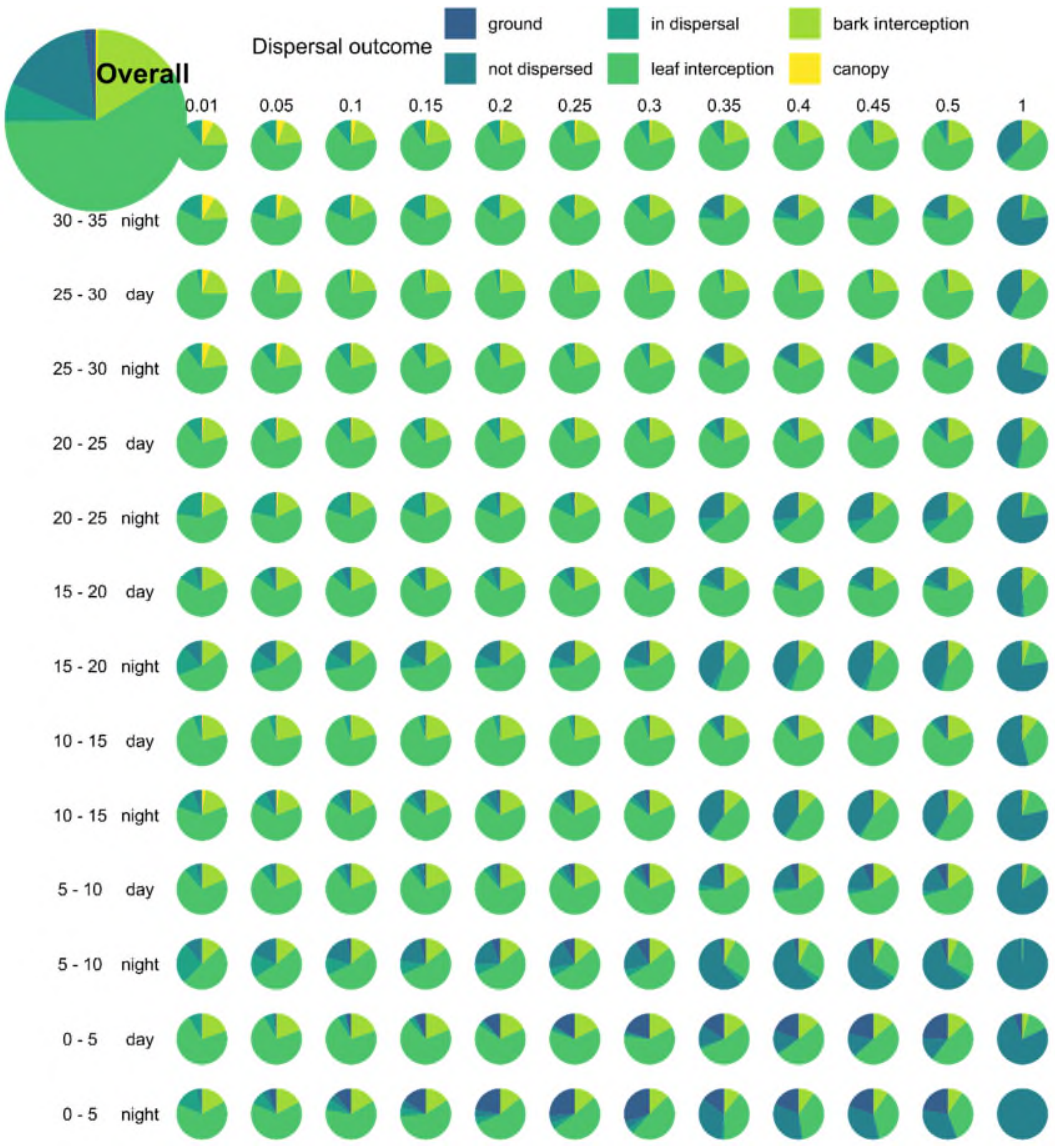

Figure S5. Relative proportion of dispersal outcomes of the hypothetical diaspores released by the trajectory model EpiDisp, separated by release height, time of day (rows), and terminal velocity ($V_{term,}$ columns) and overall proportion (inset). Ground = diaspore was dispersed to the ground; unabscised = diaspore was not abscised from the mother plant; dispersal = diaspore was still in the air at the end of the simulation period; leaf interception = diaspore intercepted a leaf

within the forest; bark interception = diaspore intercepted by bark within the forest; canopy = diaspore was dispersed above the canopy, where the simulation stopped.

Table S1. The number of simulated days per V_{term} and release height category, the absolute numbers of diaspores released (N_{total}), the absolute number and percentage (in parentheses) of diaspores per dispersal outcome. The last column reports diaspores that settled on bark after dispersing more than 5 m vertically (first number) or horizontally (second number), with their proportion of all successfully dispersed diaspores (bark interception) shown in parentheses.

V_{term}	Height	Days	N_{total}	Un-abscised	In dispersal	Ground	Leaf interception	Bark Interception	Above-canopy	>5m
0.01	**0 - 5**	3.4	30521	516 (1.7%)	3585 (11.7%)	68 (0.2%)	20731 (67.9%)	5621 (18.4%)	0	48 (<0.01%) / 1702 (0.3%)
	5 - 10	8.6	40808	2804 (6.9%)	6644 (16.3%)	7 (<0.01%)	24694 (60.5%)	6605 (16.2%)	54 (0.1%)	123 (<0.01%) / 1849 (0.3%)
	10 - 15	7.2	59345	1698 (2.9%)	5499 (9.3%)	76 (0.1%)	40175 (67.7%)	10985 (18.5%)	912 (1.5%)	357 (<0.01%) / 4006 (0.4%)
	15 - 20	13.7	104646	8690 (8.3%)	15598 (14.9%)	26 (<0.01%)	63007 (60.2%)	17106 (16.3%)	219 (0.2%)	907 (<0.01%) / 7851 (0.5%)
	20 - 25	11.9	90651	893 (1%)	13814 (15.2%)	0	58500 (64.5%)	15880 (17.5%)	1564 (1.7%)	871 (<0.01%) / 7133 (0.4%)
	25 - 30	3.8	20332	19 (<0.01%)	1360 (6.7%)	0	14095 (69.3%)	3809 (18.7%)	1049 (5.2%)	354 (<0.01%) / 2459 (0.6%)
	30 - 35	2.6	16784	2 (<0.01%)	2354 (14%)	0	10401 (62%)	2698 (16.1%)	1329 (7.9%)	615 (0.2%) / 1233 (0.5%)
0.1	**0 - 5**	3.4	30521	882 (2.9%)	1773 (5.8%)	2049 (6.7%)	20268 (66.4%)	5549 (18.2%)	0	3 (<0.01%) / 1665 (0.3%)
	5 - 10	8.6	38473	4073 (10.6%)	3047 (7.9%)	533 (1.4%)	24281 (63.1%)	6529 (17%)	10 (<0.01%)	167 (<0.01%) / 1754 (0.3%)
	10 - 15	7.1	57066	2247 (3.9%)	3012 (5.3%)	330 (0.6%)	40357 (70.7%)	10779 (18.9%)	341 (0.6%)	468 (<0.01%) / 3900 (0.4%)
	15 - 20	13.7	100256	10730 (10.7%)	9803 (9.8%)	83 (<0.01%)	62601 (62.4%)	16955 (16.9%)	84 (<0.01%)	1005 (<0.01%) / 7820 (0.5%)
	20 - 25	11.9	88450	1696 (1.9%)	11240 (12.7%)	5 (<0.01%)	58769 (66.4%)	15963 (18%)	777 (0.9%)	914 (<0.01%) / 7424 (0.5%)
	25 - 30	3.8	19787	80 (0.4%)	1191 (6%)	0	14218 (71.9%)	3925 (19.8%)	373 (1.9%)	236 (<0.01%) / 2518 (0.6%)
	30 - 35	2.6	16525	45 (0.3%)	2326 (14.1%)	0	10871 (65.8%)	2813 (17%)	470 (2.8%)	1005 (0.4%) / 1270 (0.5%)
0.3	**0 - 5**	3.4	30520	978 (3.2%)	855 (2.8%)	7543 (24.7%)	16550 (54.2%)	4594 (15.1%)	0	1 (<0.01%) / 1019 (0.2%)
	5 - 10	8.6	37043	4181 (11.3%)	1488 (4%)	2665 (7.2%)	22532 (60.8%)	6177 (16.7%)	0	576 (<0.01%) / 1347 (0.2%)
	10 - 15	7.1	54759	2338 (4.3%)	1850 (3.4%)	1099 (2%)	38765 (70.8%)	10690 (19.5%)	17 (<0.01%)	1175 (0.1%) / 3645 (0.3%)

	15 - 20	13.7	95489	10867 (11.4%)	6611 (6.9%)	1197 (1.3%)	60334 (63.2%)	16459 (17.2%)	21 (<0.01%)	2639 (0.2%) / 7139 (0.4%)
	20 - 25	11.9	81985	1896 (2.3%)	8473 (10.3%)	405 (0.5%)	55736 (68%)	15173 (18.5%)	302 (0.4%)	2408 (0.2%) / 6612 (0.4%)
	25 - 30	3.8	17430	100 (0.6%)	737 (4.2%)	1 (<0.01%)	12966 (74.4%)	3529 (20.2%)	97 (0.6%)	353 (0.1%) / 2197 (0.6%)
	30 - 35	2.6	15202	60 (0.4%)	1392 (9.2%)	0	10875 (71.5%)	2753 (18.1%)	122 (0.8%)	1595 (0.6%) / 1021 (0.4%)
0.5	**0 - 5**	3.3	30521	7220 (23.7%)	293 (1%)	7137 (23.4%)	12395 (40.6%)	3476 (11.4%)	0	6 (<0.01%) / 585 (0.2%)
	5 - 10	7.6	37732	13996 (37.1%)	1162 (3.1%)	2483 (6.6%)	15841 (42%)	4250 (11.3%)	0	482 (0.1%) / 999 (0.2%)
	10 - 15	6.6	56435	12473 (22.1%)	1145 (2%)	1431 (2.5%)	32301 (57.2%)	9074 (16.1%)	11 (<0.01%)	1309 (0.1%) / 3437 (0.4%)
	15 - 20	13.3	97532	26851 (27.5%)	4030 (4.1%)	1445 (1.5%)	51115 (52.4%)	14079 (14.4%)	12 (<0.01%)	2849 (0.2%) / 6657 (0.5%)
	20 - 25	11.7	81373	13296 (16.3%)	5954 (7.3%)	596 (0.7%)	48274 (59.3%)	13091 (16.1%)	162 (0.2%)	2763 (0.2%) / 5899 (0.5%)
	25 - 30	3.8	16771	1343 (8%)	505 (3%)	14 (<0.01%)	11619 (69.3%)	3224 (19.2%)	66 (0.4%)	637 (0.2%) / 1926 (0.6%)
	30 - 35	2.6	14641	1392 (9.5%)	813 (5.6%)	0	9802 (66.9%)	2591 (17.7%)	43 (0.3%)	1637 (0.6%) / 860 (0.3%)
1	**0 - 5**	3.1	30521	26847 (88%)	0	902 (3%)	2119 (6.9%)	653 (2.1%)	0	0 / 219 (0.3%)
	5 - 10	7.0	38740	35055 (90.5%)	109 (0.3%)	288 (0.7%)	2527 (6.5%)	761 (2%)	0	84 (0.1%) / 241 (0.3%)
	10 - 15	6.0	58314	37551 (64.4%)	240 (0.4%)	684 (1.2%)	15403 (26.4%)	4436 (7.6%)	0	753 (0.2%) / 2115 (0.5%)
	15 - 20	12.1	102579	63952 (62.3%)	1159 (1.1%)	837 (0.8%)	28403 (27.7%)	8223 (8%)	5 (<0.01%)	1865 (0.2%) / 4870 (0.6%)
	20 - 25	10.4	85380	51218 (60%)	1581 (1.9%)	376 (0.4%)	24858 (29.1%)	7309 (8.6%)	38 (<0.01%)	1675 (0.2%) / 4082 (0.6%)
	25 - 30	3.5	19835	10874 (54.8%)	182 (0.9%)	129 (0.7%)	6746 (34%)	1873 (9.4%)	31 (0.2%)	519 (0.3%) / 1494 (0.8%)
	30 - 35	2.3	15527	8796 (56.6%)	192 (1.2%)	0	5156 (33.2%)	1354 (8.7%)	29 (0.2%)	916 (0.7%) / 564 (0.4%)

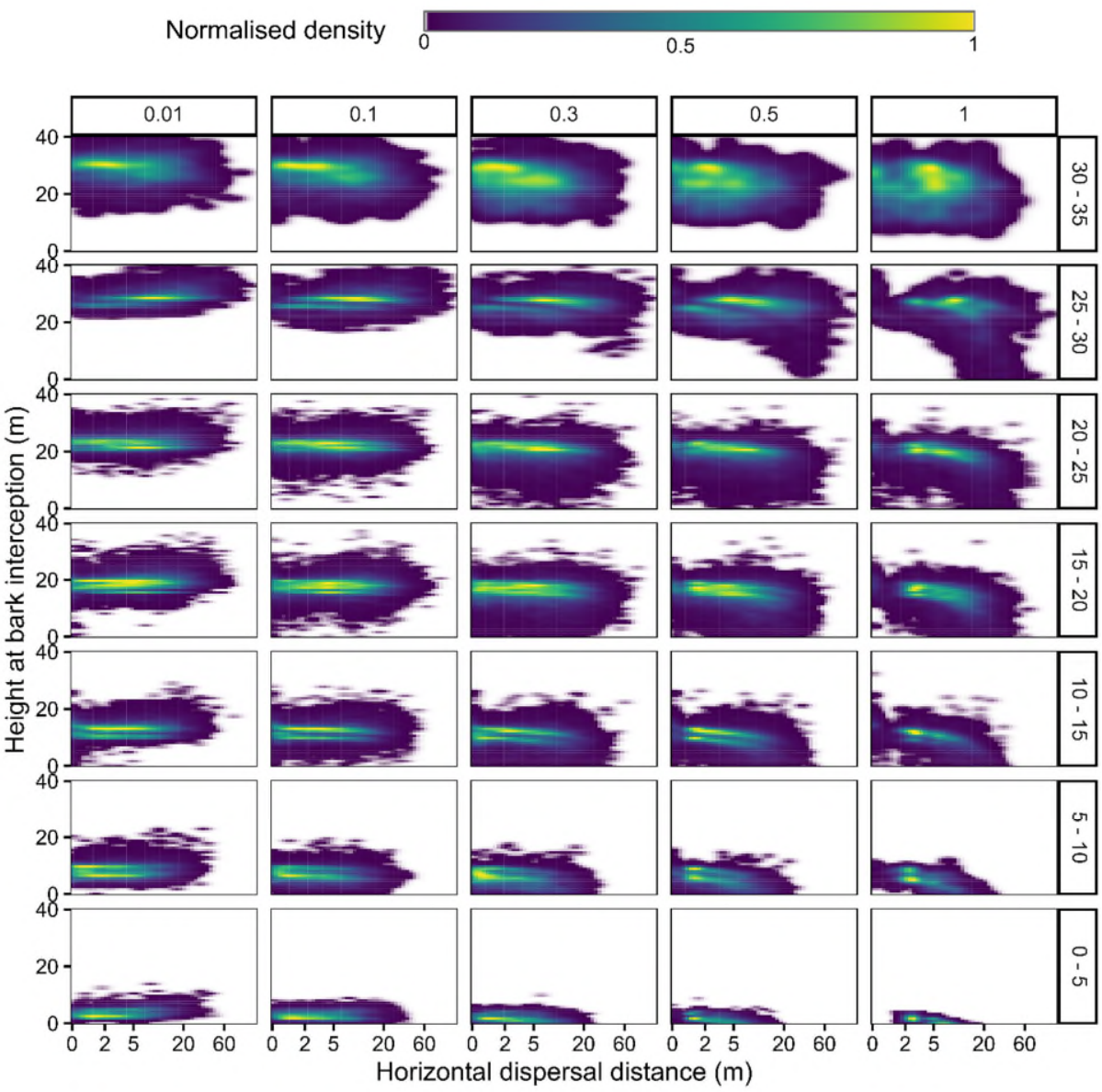

Figure S6. Density distribution of bark-intercepted diaspores. Normalized two-dimensional densities of successful dispersal outcomes within the forest, based on horizontal dispersal distance and height after bark interception, shown across terminal velocity classes (columns) and release-height classes (rows). Zero densities are shown as white gradient fill.

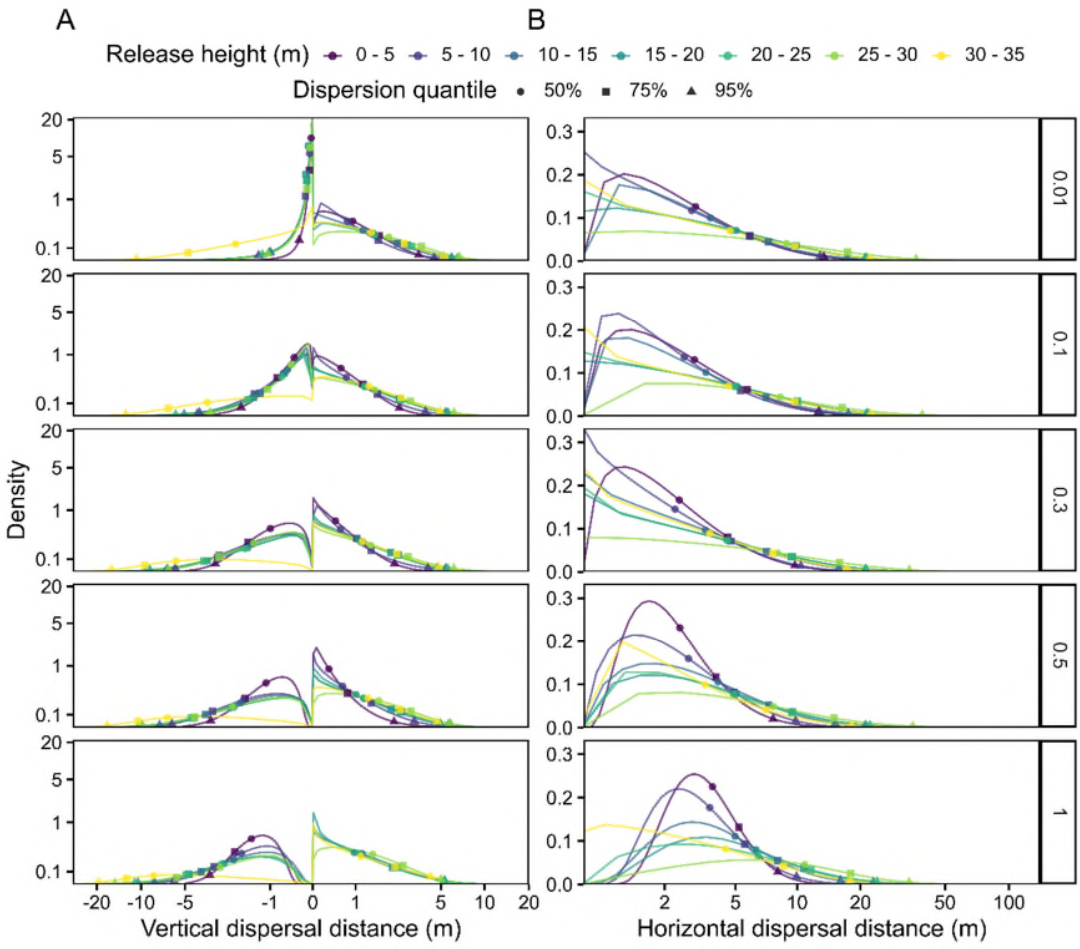

Figure S7. Fitted dispersal kernels for vertical **(A)** and horizontal **(B)** dispersal distances across release heights (colours) and terminal velocities (rows) for diaspores intercepted by bark. Markers show at which distance the cumulative dispersed population reaches a given percentage. The axes have been pseudo-log transformed; note the different scales.

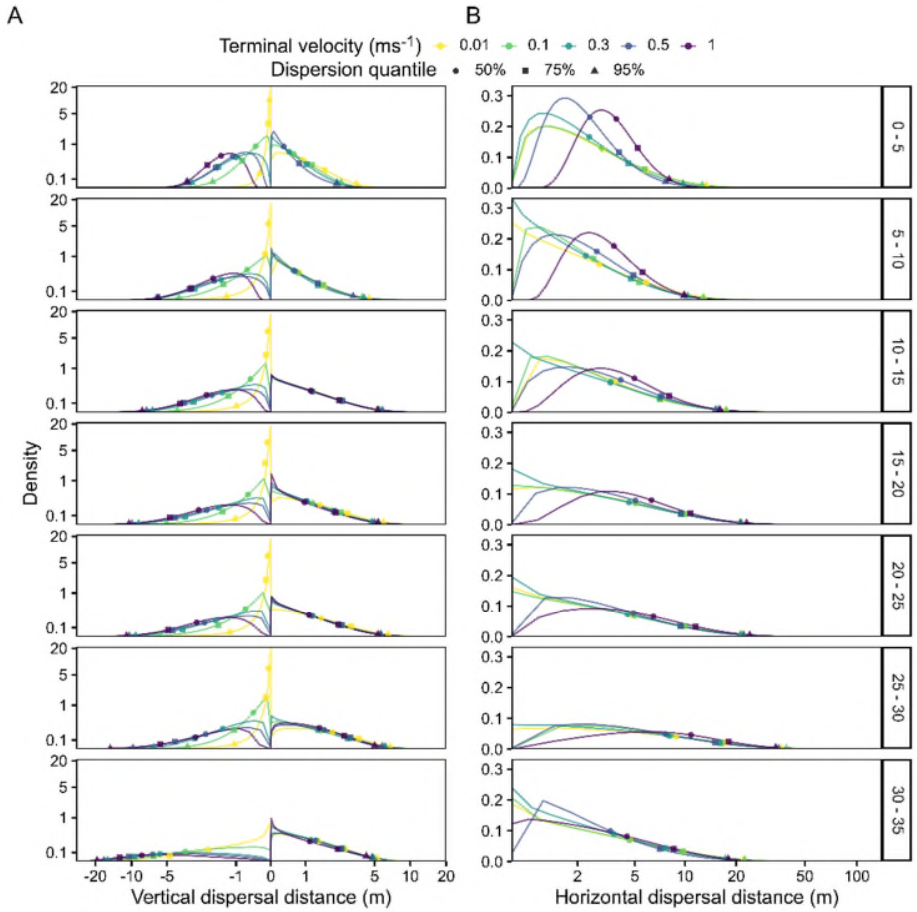

Figure S8. Fitted dispersal kernels for vertical **(A)** and horizontal **(B)** dispersal distances across terminal velocities (colours) and release height (rows) for diaspores intercepted by bark. Markers show at which distance the cumulative dispersed population reaches a given percentage. The axes have been pseudo-log transformed; note the different scales.

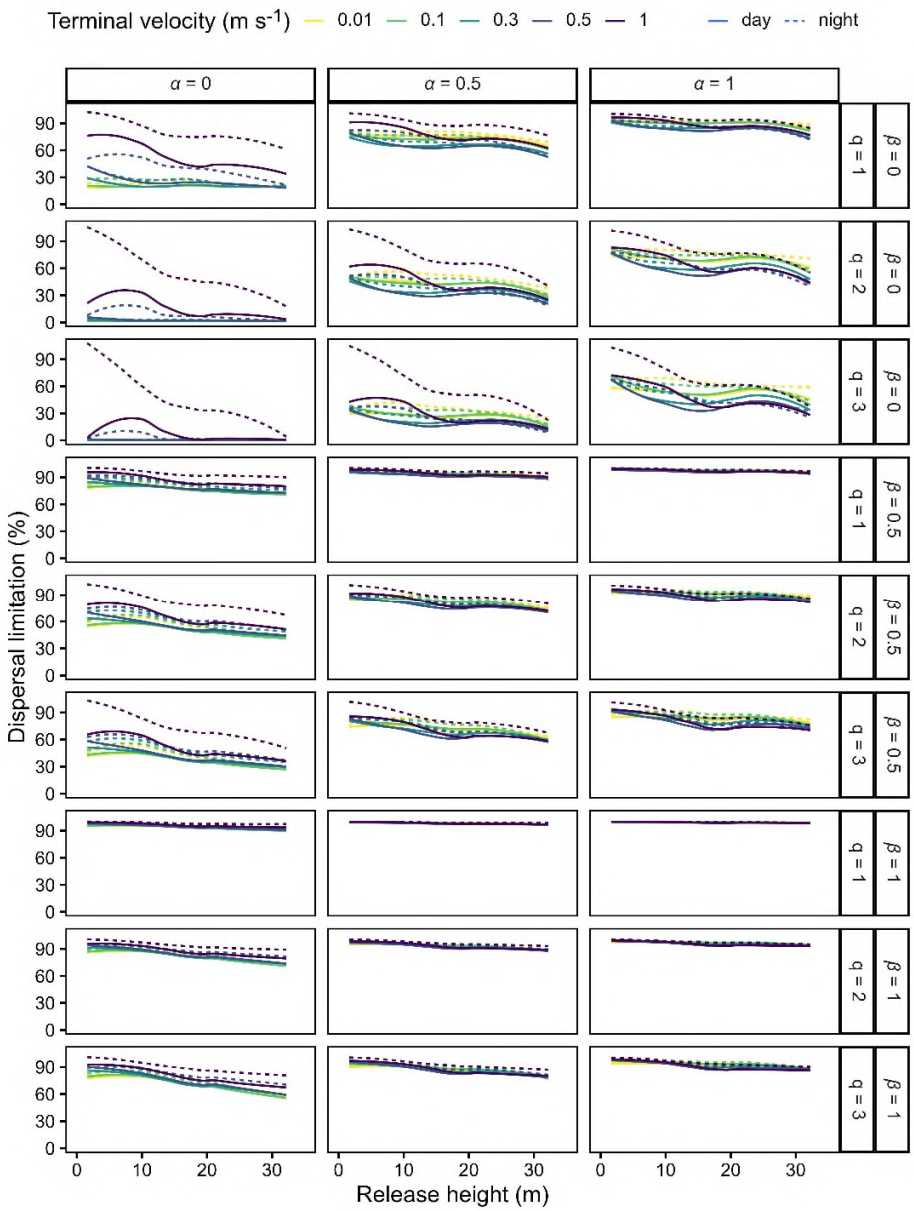

Figure S9. Sensitivity of dispersal limitation to vertical and horizontal weighting and aggregation of dispersal contributions. Dispersal limitation (%) is shown as a function of release height for combinations of vertical (α = 0, 0.5, 1) and horizontal (β = 0, 0.5, 1) weighting, and power-mean exponent (q = 1, 2, 3). Colours indicate terminal velocity (m s^{-1}), and solid versus dashed lines represent daytime and nighttime conditions, respectively.

References

Mendieta-Leiva, G., K. Wagner, and G. Zotz. 2021. “Vascular Epiphyte Census Data at the San Lorenzo Crane Plot [dataset].” *Zenodo.* https://doi.org/10.5281/zenodo.5645775.

Microsoft. 2024. "Microsoft 365 tools [software]". https://microsoft.com/microsoft-365.

Ramos, P., P. Villareal, and H. Muller-Landau. 2024. “Tree Height Allometry Data for 5109 Trees in Twenty-Four Small ForestGEO Plots in Panama, 2011–2020 [dataset].” *Smithsonian Tropical Research Institute.* https://doi.org/10.25573/data.24954204.v1.

Vasquez V., M. Garcia, M. Hernandez, ForestGEO Smithsonian, and H. Muller-Landau. 2024. “Smithsonian ForestGEO San Lorenzo and Panama Small Plots Aerial Photogrammetry Orthomosaics, Digital Surface Models, Point Clouds and Raw Images for 2015–2024.” *Smithsonian Research Data Repository*. https://doi.org/10.60635/C33W2K.

Ecological Monographs

Video S1 Metadata: Branch Sway for:

Patterns of wind dispersal within a forest canopy: An epiphyte perspective

Marie Hoensbroech[1], Juliano Sarmento Cabral[2], Gerhard Zotz[1,3]

1: Institute of Biology and Environmental Sciences, Carl von Ossietzky Universität Oldenburg, Ammerländer Heerstr. 114–118, 26129 Oldenburg, Germany

2: Ecological Modelling, Bonner Institute for Organismal Biology — Department of Plant Biodiversity, Universität Bonn, Venusbergweg 22, 53115 Bonn, Germany

3: Smithsonian Tropical Research Institute, Box 0843-03092, Panama, Republic of Panama

Correspondence: Marie Hoensbroech; email: marie.hoensbroech@uni-oldenburg.de

Video S1. Branch of *Dussia atropurpurea* gently swaying in the wind. Branch motion can be substantially more pronounced than shown here and may increase the apparent wind experienced by epiphytes relative to the actual wind. Even relatively weak branch sway can generate turbulence that may contribute to diaspore release, yet this remains a poorly investigated process. The video was taken by Marie Hoensbroech close to the canopy top of the San Lorenzo permanent forest plot (9.28°, -79.97°), approximately 30 m above ground.